STUDIES OF MOLTEN-SALT THERMOCELLS

by

Gail D. Ulrich

MASSACHUSETTS INSTITUTE OF TECHNOLOGY

SCHOOL OF ENGINEERING

CAMBRIDGE, MASSACHUSETTS

UNPUBLISHED PRELIMINARY DATA

SPONSORSHIP

National Aeronautics and Space Administration, NsG-496, M.I.T.
DSR-9845 Office of Naval Research, Nonr-1841(78), M.I.T. DSR-8848

February 1964

STUDIES OF MOLTEN-SALT THERMOCELLS

by

Gail D. Ulrich

MASSACHUSETTS INSTITUTE OF TECHNOLOGY

SCHOOL OF ENGINEERING

CAMBRIDGE, MASSACHUSETTS

SPONSORSHIP

National Aeronautics and Space Administration, NsG-496, M.I.T. DSR 9845

Office of Naval Research, Nonr 1841(78), M.I.T. DSR 8848

February 1964

ABSTRACT

STUDIES OF MOLTEN-SALT THERMOCELLS

by

Gail D. Ulrich

20641

This report is identical to a thesis submitted to the Department of Chemical Engineering, Massachusetts Institute of Technology, February, 1964, in partial fulfillment of the requirements for the degree of Doctor of Science.

The purpose of this thesis study was: first, to determine open-circuit voltages of several molten-salt thermocells which appeared to have promise for energy conversion; and second, to formulate an expression which satisfactorily described the effect of known variables on this voltage.

In line with these objectives, the open-circuit voltages of four thermocells were measured experimentally. All four had identical chlorine-on-graphite electrodes, but each contained a different electrolyte. The four pure molten salt electrolytes studied were lithium chloride, sodium chloride, potassium chloride and silver chloride. Open-circuit voltages were determined as a function of total pressure and of electrode temperatures, which ranged from near the melting points of the salts to 1300°C. Total pressures were varied from one atmosphere to a tenth of an atmosphere except in the lithium chloride-chlorine system which was studied at one atmosphere only. From the data, curves showing cell voltage as a function of electrode temperatures and total pressure were formulated.

The Seebeck coefficients of the four systems studied were found to vary. At high temperatures and low pressures in particular, there was a marked increase due to vapor pressure and dissociation effects.

An equation was derived which correlated the effects of a pressure change on cell voltage. It was found that the cell voltage could be predicted with accuracy once the voltage versus temperature characteristics of the system had been established at one pressure. The equation included the effects of salt vapor pressure and chlorine dissociation on voltage.

Calculations indicate that the maximum overall efficiency obtainable in any of the systems studied is around five per cent. This is the efficiency estimated for the silver chloride-chlorine thermocell operating at a total pressure of 0.4 atmospheres and cold and hot electrode temperatures of 500°C and 1300°C respectively. Voltages and efficiencies were estimated for the hypothetical lithium fluoride-fluorine thermocell. This system appears to have a maximum efficiency of around ten per cent which is thought to be the highest obtainable in any molten-salt system.

Author

ACKNOWLEDGEMENT

The author expresses his appreciation to his supervisor, Professor H. P. Meissner, for his help and advice during the course of the research and for his thorough analysis of this document. He also wishes to thank Professor D. L. White of the Electrical Engineering Department for his thoughts and suggestions.

The author acknowledges help received through discussions with Professor A. J. deBethune of Boston College, and Professor D. N. Hume and E. G. Larson of the M. I. T. Chemistry Department.

This research was made possible, in part, through support extended to the Massachusetts Institute of Technology by the Office of Naval Research under contract number Nonr 1841(78) and by the National Aeronautics and Space Administration under contract number NsG-496. Additional funds were supplied by the Atlantic Refining Company.

TABLE OF CONTENTS

TABLE OF CONTENTS (continued)

LIST OF TABLES

LIST OF FIGURES

LIST OF FIGURES (continued)

I. SUMMARY

A. Introduction

1. Thermoelectric Energy Conversion

During recent years, a great deal of research has been directed toward the development of new methods for converting heat and other forms of energy into electricity. Among these methods is thermoelectric energy conversion which depends on a principle first discovered by Seebeck who found that a voltage was generated when the junctions in an electric circuit composed of two different conductors were held at different temperatures. In honor of this discovery, the rate of change of voltage with temperature for such a system is called the Seebeck coefficient.

The most familiar application of Seebeck's discovery is in the bimetallic thermocouple. Although this is generally used to determine temperature from the measured voltage, it has also been recognized as a possible energy conversion device. The e.m.f. developed in such a system can be made to cause a current flow, thus producing energy. Under load, the thermocouple operates as a heat engine, receiving heat at the hot junction, rejecting heat at the cold junction and doing work. It is found, however, that the efficiency of the bimetallic thermocouple is extremely low.

The recent interest in thermoelectric energy conversion results from the develpment of solid-state thermoelectric generators which provide power at a much higher efficiency than was possible with bimetallic thermocouples. In fact, because of the advantage of no moving parts, these devices have already been produced commercially for a number of applications. They have the disadvantage, however, of deteriorating at high temperatures. Thus, for continuous operation, the solid-state thermoelectric device is limited to a relatively low temperature range and hence, a low maximum efficiency.

2. Efficiency of Thermoelectric Devices

Thermoelectric devices are judged in terms of their overall efficiency, which is defined as the fraction of the high temperature heat absorbed which is converted to useful work. The degree to which the efficiency of these devices falls short of the Carnot efficiency depends upon the relative magnitudes of the Seebeck coefficient and the thermal and electrical conductivities. Highest efficiencies require high Seebeck coefficients, high electrical conductivities, and low thermal conductivities. The influence of these three properties is formulated mathematically in standard texts(10,14) and is discussed in detail in the body of the thesis. High thermal conductivities coupled with low Seebeck coefficients have imposed definite restrictions on the efficiencies of bimetallic thermocouples. On the other hand, the development of solid-state materials with high Seebeck coefficients, relatively low thermal conductivities, and high electrical conductivities has made thermoelectric energy conversion possible at much higher efficiencies.

3. Thermocell Description

The thermoelectric effect is not limited to electronic conductors such as metals and semi-conductors but is also observed in molten salts, aqueous solutions, and ionic solids, which conduct electricity by ion migration. Thus, if two identical electrodes held at different temperatures are connected by an electrolyte having ions which can undergo reaction at the electrodes so that there is a reversible heat effect, a voltage is generated. Such a device is commonly called a thermocell.

The thermocell differs from the conventional thermocouple in that electrical conduction is accompanied by a transfer of material between electrodes due to ion migration. An example of a simple thermocell in which this occurs is shown in figure 1 where the silver chloride-silver system is illustrated. Note from the figure that it would be necessary

to recycle silver from the cold to the hot electrode if this system were to operate continuously as shown.

In the absence of extreme pressures, thermocells using aqueous solutions are limited to a small temperature range. Hence, they are not particularly attractive and will not be considered further. Cells containing solid ionic electrolytes are likewise not attractive today, since all known solid electrolytes show rather low electrical conductivities. On the other hand, electrical conductivities are high for many molten salts. In addition, the temperature range between their melting and boiling points is great allowing molten salt systems to operate above the maximum temperatures tolerated by conventional power generators. In light of these factors, the molten salt thermocell was chosen for study.

4. Selection of Molten Salt Systems to be Studied

The selection of the specific molten-salt thermocells to be studied was based on a consideration of the three factors affecting effiency. These are discussed below.

(a) Thermal Conductivity: Published data on thermal conductivity of molten salts are scanty. Recent work, however, (30,31) indicates that the major contribution to conduction in the electrolyte is by vibration of the ions making differences in thermal conductivity from melt to melt small (typical values range from 0.003 to 0.009 Watt/cm ^{o}C). Therefore, the choice of the molten salt electrolyte to be studied here was made without reference to thermal conductivity.

(b) Electrical Conductivity: In contrast to thermal conductivity, this property is profoundly influenced by the nature of the molten electrolyte. The metal fluorides have in general the highest electrical conductivities, but were not used because there is no suitable container at the present time. Four salts with slightly lower electrical conductivities are the

chlorides of lithium, sodium, potassium, and silver. Since suitable containers are available for them, these four electrolytes were selected for study.

(c) Seebeck Coefficient: It is possible for the electrode reactant to be a solid, a liquid, or a gas. It can be shown that due to the high entropy associated with gaseous molecules, thermocells having gas electrodes will in general have higher Seebeck coefficients. For example, the highest Seebeck coefficient yet reported for a molten-salt thermocell is that for the chlorine electrode in silver chloride(26). In addition, the Seebeck coefficient can be increased by reducing the pressure of the gas supplied to the electrode. On the basis of these facts, it was decided to use the chlorine electrode.

In the past, open-circuit voltages for silver chloride, sodium chloride, and potassium chloride thermocells with chlorine electrodes have been reported for a limited temperature range and at one atmosphere pressure(26,5). The data for the last two systems are considered by the author to be unreliable for reasons mentioned in the body of the thesis. The scope of this work included the study of these same systems over a larger range of temperature and pressure than that previously explored. It also included the study of the lithium chloride-chlorine cell at one atmosphere pressure.

The study of electrode kinetics was considered beyond the scope of this thesis. Hence, the proposed experimental work involved the measurement of open-circuit voltages only.

B. Theory

Based upon a thermodynamic analysis of the molten-salt thermocell using chlorine as the electrode reactant, the following expression for the voltage of one electrode at a temperature T_3 versus a reference electrode

at T_1 is proposed

$$E = \frac{1}{\mathcal{F}} \left[\int_{T_1}^{T_3} \Delta S^\circ dT + 1/2\ RT_1 \ln \pi - 1/2\ RT_3 \ln\left(\left[\frac{n-1}{n+1}\right]\pi'\right)\right] \qquad (28)$$

This equation allows for a significant salt vapor pressure and for chlorine dissociation at the temperature of the hot electrode, but these effects are assumed to be negligible at T_1. The various terms are defined as follows:

E is the voltage of the cell at open circuit.

$\mathcal{F}$ is the Faraday constant; 96,500 coulombs per gram equivalent.

ΔS° is the standard state entropy change $(1/2\ S^\circ_{Cl_2} + \bar{\bar{S}}_{e,g} - \bar{\bar{S}}_{Cl^-})$ for the following reaction:

$$Cl^- \longrightarrow 1/2\ Cl_2 + e^-$$

where $S^\circ_{Cl_2}$ is the entropy of chlorine gas at one atmosphere pressure, $\bar{\bar{S}}_{e,g}$ is the "transported entropy" of the electron in graphite, and $\bar{\bar{S}}_{Cl^-}$ is the transported entropy of the chloride ion in the pure molten salt (the transported entropy is defined as the sum of $\bar{S}$, the partial molal entropy and S^*, the "entropy of transfer").

R is the gas constant.

π is the total pressure and is equal to the chlorine pressure at the reference electrode. (At the reference temperature, the vapor pressure of the fused salt is negligible.)

π' is equal to the total pressure π minus the salt vapor pressure. (The salt vapor pressure may be significant at the temperature of the hot electrode.)

n is a function of the chlorine dissociation constant K and π', both evaluated at T_3. It is defined by the expression

$$n = \left(\frac{4\pi'}{K^2} + 1\right)^{1/2}$$

and is the parameter in equation (28) which accounts for dilution

of diatomic chlorine due to the dissociation reaction

$$Cl_2 \longrightarrow 2\ Cl$$

Note that the last two terms of equation (28) account for chlorine pressures different from unity. It is easily seen that at pressures less than one atmosphere the second term becomes negative and the last term becomes positive. It is clear also from inspection that the latter is always of the greater absolute magnitude. Hence, the net effect of a reduction in total pressure is an increase in voltage.

Inspection shows that all of the terms in equation (28) can be readily evaluated, except for ΔS° which is the entropy change for the ion discharge reaction and equals $(1/2\ S^\circ_{Cl_2} + \bar{S}_{e,g} + S^*_{e,g} - \bar{S}_{Cl^-} - S^*_{Cl^-})$. $S^\circ_{Cl_2}$ is, of course, readily available in the literature, as is $(\bar{S}_{e,g} + S^*_{e,g})$. Due to uncertainties in liquid state theory, however, it has not been possible in the past to calculate the partial molal entropy of a single ion in a molten salt. Recently, Pitzer(24) proposed an equation for the partial molal entropy which he considers to be valid for systems such as those explored here (simple 1-1 molten salts where the ions are not too greatly different in size), but so far, no method for experimentally confirming Pitzer's equation has been devised.

Another unknown in ΔS° is the quantity $S^*_{Cl^-}$. This term, the entropy of transfer, results from the migration of the ion through a non-isothermal electrolyte. Because of the uncertainties in $S^*_{Cl^-}$ and $\bar{S}_{Cl^-}$ as reflected in ΔS°, the voltage of a thermocell cannot be directly calculated from equation (28). Note, however, that once the open circuit voltage has been measured at a known pressure and electrode temperatures, the integrated quantity $\int_{T_1}^{T_3} \Delta S^\circ dT$ can be obtained. Further, since this quantity is presumably independent of pressure, the voltage of the same thermocell at the same electrode temperatures but at different pressures can now be cal

C. Experimentation

1. Apparatus

One of the first problems in the selection of an experimental system was that of finding a suitable container for the molten alkali chlorides. Previous workers had found that these melts attacked fused quartz*. Therefore, it was thought necessary to use other refractory materials which could not be formed into such complex shapes as the U-tubes used in previous thermocell studies. The cell design which resulted is shown in figure 5. The unit was constructed of standard refractory shapes.

The cell proper consisted of a large closed-end tube which held the molten salt. Inside was placed a smaller open-end tube which hung approximately one inch above the floor of the cell. The melt level was depressed in the small tube, and a graphite electrode and thermocouple were placed in the electrolyte at this point to form the cold junction of the device. The hot junction was formed by another graphite electrode placed just below the surface of the liquid in the annulus between the tubes. A thermocouple was also placed in the annulus adjacent to the hot electrode. The temperatures of these compartments were controlled independantly by devices which regulated the power input to the two zones of the tube furnace. Chlorine was supplied directly to the electrodes which were constructed so that only a small button of graphite adjacent to the thermocouple came into contact with the molten salt. All cell components were sealed together as a unit at the top of the large tube outside of the furnace. The seal was affected with a teflon plug-viton O-ring fitting which was gas tight at moderate vacuum.

---

* Note: It was found, however, that the melts themselves were not corrosive, but that corrosion resulted from contamination by moisture. If chlorine was bubbled through the salt for a few hours following melting as suggested by Maricle and Hume(20), corrosion of quartz was minimal. Bloom, et. al.(4) also found fused quartz suitable when the salt was pure.

2. Operating Procedure

The voltage versus temperature characteristics of a given cell at constant pressure were measured by holding the cold electrode at a given temperature while increasing the temperature of the hot electrode in steps of about 20°C. At a given temperature setting, the open-circuit voltage registered between electrodes and the e.m.f.'s of each thermocouple were determined. The temperature of the hot electrode was then increased and when steady-state was achieved, the readings were repeated. By this method, it was possible to determine cell voltage as a function of the temperature difference between the electrodes.

The geometry of the experimental cell prevented a temperature difference greater than 200°C. For that reason, when a string of data points had been determined at a steady cold junction temperature, the temperature of the cold electrode was increased by about 150°C. Then, while still at the same pressure, another string of data points were obtained starting with the hot electrode at the same temperature as the cold and again raising its temperature by 20°C steps. When the entire region of temperature had been explored at constant pressure in this manner, the pressure was changed and the process repeated. Then, by superimposing consecutive raw-data plots, it was possible to formulate a graph showing the voltage of the hot electrode at any temperature and pressure versus a cold electrode at a chosen reference temperature. The sample graph shown in Figure 10 is for the potassium chloride-chlorine system. Similar experimental curves were obtained for each of the other three systems studied at temperatures ranging from just above the melting point of the electrolyte to 1300°C. Pressures were varied from one atmosphere to as low as 0.1 atmosphere except for the lithium chloride-chlorine cell which was studied at atmospheric pressure only.

3. Experimental Results

The experimental results are shown in figures 12, 14, 15 and 16 for the four systems studied. The points shown represent voltages measured experimentally and formulated as described above. The lines on the figures are voltages calculated from equation (28). In brief, the calculation method was as follows:

First, the last two terms of equation (28) were evaluated for a given cell pressure and each of several hot electrode temperatures from data avialable in the literature (salt vapor pressures were taken from references(1) and(4), and dissociation data were taken from(8)). The cold electrode temperature used was equal to the reference temperature chosen for the particular cell. Second, these calculated quantities were subtracted from the corresponding experimental voltages to yield the value of $\int_{T_1}^{T_3} \Delta S^{o} dT$ as a function of temperature (shown as dotted lines in the figures). Then, voltages corresponding to different cell pressures at various temperatures were calculated from equation (28) using the known value of $\int_{T_1}^{T_3} \Delta S^{o} dT$. As shown in the figures, the cell voltages so calculated agree with those measured experimentally within the limits of experimental error.

The Seebeck coefficient, namely the slope of the E versus temperature curve, was not constant in these cells, but was found to vary significantly with temperature and pressure. Note in particular the upward curvature of the lines at high temperatures and low pressures which results from increasing salt vapor pressure and chlorine dissociation. This effect is not as pronounced in the silver chloride system where the melt has a comparatively low vapor pressure and a low melting point. In fact, for the silver chloride-chlorine thermocell, there is a noticeable decrease in Seebeck coefficient with temperature in the low temperature region. (The same trend can be observed in the dotted curves for all four systems.) This

behavior indicates a decreasing ΔS° with temperature due to a ΔC_p for the half cell reaction different from zero. For the silver chloride-chlorine cell, the measured ΔC_p is about -3.0 e.u. and is in striking agreement with the estimated value of -3.3. Similar agreement was found for the other systems also.

The average Seebeck coefficient for the silver chloride-chlorine cell between 500°C and 900°C and at one atmosphere pressure was found to be 0.655 mv/°C in agreement with the value of 0.664 ± 0.020 mv/°C reported by Senderoff and Bretz(26) for the same conditions. Detig and Archer(5) found the values 0.45 mv/°C and 0.40 mv/°C for the sodium chloride-chlorine and potassium chloride-chlorine thermocells respectively at about 850°C. These compare with 0.475 mv/C° found in this work for both cells under similar conditions.

D. Conclusions

1. Transported Entropies and Entropies of Transfer

From the data, the quantity $\bar{\bar{S}}_{Cl^-}$ was calculated and was found to be 19.72 e.u. in lithium chloride at 827°C, 21.61 e.u. in sodium chloride at 927°C, 21.73 e.u. in potassium chloride at 927°C and 17.09 e.u. in silver chloride at 727°C.

If the Pitzer equation(24) is correct, entropies of transfer are very nearly equal to zero in lithium chloride, sodium chloride and potassium chloride, but the value is -3.7 e.u. for the chloride ion in silver chloride. It must be recognized, however, that Pitzer's relationship does not necessarily hold with equal validity in all systems studied.

A more detailed discussion of the various entropy terms can be found in the body of the thesis.

2. Thermocell Efficiencies

The variation in Seebeck coefficient indicated by the curved lines in

expression derived for solid-state thermoelectric generators. Approximate thermocell efficiencies can, nevertheless, be estimated although the calculation is tedious.

At first glance, it would appear that maximum thermocell efficiencies will be obtained where the slope of the voltage versus temperature curve is steepest. However, under these conditions, the salt vapor exerts a large fraction of the total pressure in the hot electrode chamber. This means that, in operation, salt vapor will be carried along with the recirculating chlorine. Hence, heat will be absorbed at the hot electrode by vaporization and will be transported irreversibly to the cold electrode chamber. Therefore, when the salt vapor pressure becomes too large, this irreversible transfer of heat serves to reduce cell efficiency.

In calculating the maximum efficiency, it is necessary to balance the irreversible effects (ohmic loss, heat transferred by conduction, and heat transported by vaporization) against the rate of reversible heat absorption at the hot electrode. Such a calculation based on a cold junction temperature of 500°C was made for the silver chloride-chlorine thermocell with the results shown in table V. Note that the efficiency so calculated increases with reduced pressure and increased temperature in general until at 1300°C and 0.4 atm it reaches a maximum (4.5 per cent) and starts to decrease again. This phenomenon reflects the influence of the increasing salt vapor pressure. In fact at 1527°C and 1 atm pressure (20°C below the normal boiling point), the efficiency is only 2.7 per cent. Thus, it appears that the maximum efficiency for this particular system is in the neighborhood of 4.5 per cent at the conditions described above. The alkali chloride-chlorine thermocells because of high vapor pressures and shorter temperature ranges are even less efficient.

Also in table V are shown estimated efficiencies for two hypothetical thermocells, namely the lithium fluoride-fluorine cell which has an un-

usually high electrical conductivity and the boron oxide-oxygen cell which has a large temperature range and a low vapor pressure. The voltages to be expected from these systems were calculated from expressions analogous to equation (28). The half cell entropy changes were estimated using Pitzer's equation and assuming $S^{*}_{O^{-}}$ to be zero.

It is interesting to note that even though the boron oxide-oxygen system has a high Carnot efficiency due to a large temperature range, the actual efficiencies are low. This is due to the decrease in the number of moles reacting per electron transferred. The lithium fluoride-fluorine system on the other hand has an estimated efficiency of up to 11.4 per cent, the higher efficiency resulting mainly from the increased electrical conductivity of the electrolyte.

II. INTRODUCTION

During recent years, a great deal of research has been directed toward the development of better techniques for converting heat and chemical energy into electricity. This research has been motivated not only by the demand for lower cost domestic electricity but also by requests for efficient and compact electrical generators to be used in military and space applications.

One device resulting from this effort is the solid-state thermoelectric generator which is analogous to the familiar bimetallic thermocouple. The overall efficiencies of solid-state thermoelectric devices are, however, much higher than those achieved in the past using bimetallic thermocouples because of the high electrical conductivities, high Seebeck coefficients, and low thermal conductivities of the newly developed semi-conductors used in their construction. But, a serious problem with solid-state devices, at least as they are presently compounded, is that they tend to loose their favorable thermoelectric properties at high temperatures. Hence, they are limited to a temperature range in which the maximum theoretical (Carnot) efficiency is quite low.

A thermoelectric device analogous to the solid-state couple and known as the molten-salt thermocell has also been proposed as a possible electrical generator(28). Like semi-conductor thermoelectrics, simple thermocells consist of two dissimilar electrical conductors connected in series with the junctions at different temperatures. In the thermocell, however, at least one of the conductors is ionic rather than electronic, while both conductors are electronic in solid-state devices. Thus, in the thermocell, electrochemical half cell reactions occur at each of the junctions or electrodes. As an example, the silver chloride-silver thermocell is shown in figure 1. Here, the silver electrodes and wire

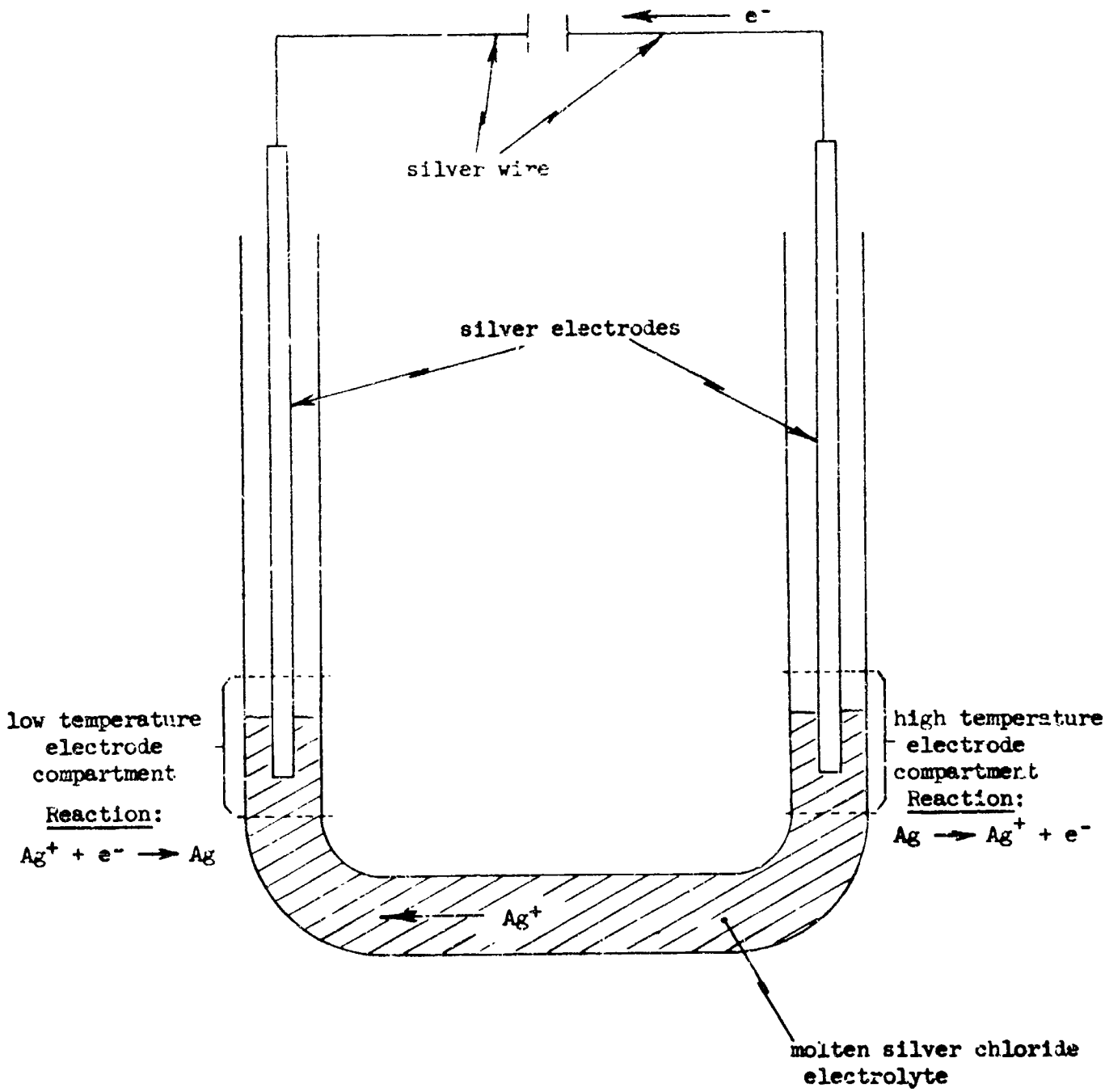

Figure 1. Schematic diagram of molten silver chloride-silver thermocell.

represent the electronic leg of the thermocell and the molten silver chloride represents the ionic leg. Notice that the two silver electrodes and the molten electrolyte surrounding them are at uniform but different temperatures with the temperature drop confined to the electrolyte connecting these electrode compartments. The silver wire connecting the two electrodes also passes through a thermal gradient. When this cell operates spontaneously, electrons and silver ions are produced by the half cell reaction at the "hot" electrode on the right as indicated, whereas, the reverse of this occurs at the "cold" electrode. Consequently, electrons flow through the silver wire and silver ions migrate through the melt, resulting in an accumulation of silver at the cold electrode.

It is not necessary in accordance with the basic definition given above that the electrolyte used in a thermocell be a molten salt. For example, aqueous solutions and some solids are also ionic conductors, but, because of the limited temperature range of aqueous solutions and the high electrical resistance of ionic solids, the efficiency of thermocells using these as electrolytes is low. Fused salt thermocells show greater promise for energy conversion because molten salts have a much lower electrical resistance than either of the other two ionic conductors. In addition, with the melting points of the electrolytes often between 400 to 1000°C (see table II) and with liquid ranges at atmospheric pressure of several hundred degrees, the molten-salt thermocell has potential, if other factors are favorable, as a "topping" device to extract electrical energy from high temperature heat while exhausting the unused heat at a lower temperature to a conventional generator.

Unlike semi-conductor thermocouples, the molten-salt thermocell does not have the problem of deterioration at the hot junction. On the other hand, because of corrosive attack, it is extremely difficult to

find suitable containers for molten salts at high temperatures.

A. Thermoelectric Effects in Thermocells

The thermocell develops a voltage because the reversible potential of a half cell reaction is a temperature function. This phenomenon is expressed quantitatively by the following equation:

$$\frac{dE}{dT} = \frac{\Delta S}{\mu \mathcal{F}} \qquad (1)$$

where E is the half-cell potential, ΔS is the half-cell entropy change, μ is the number of equivalents involved, and $\mathcal{F}$ is Faraday's constant; all in consistent units. The change of voltage with temperature in equation (1) is, of course, the Seebeck coefficient defined as usual. From equation (1), it can be shown that two identical electrodes at different temperatures when connected "back to back" through a common electrolyte will generate a net voltage, and the unit will function as a heat engine. Clearly, by the second law, the electrode reactions must occur in a direction such that heat is absorbed at the hot electrode if power is to be produced.

There is no general rule governing the polarity of the electrodes, that is, whether the half cell reaction at the hot electrode involves oxidation or reduction. This can be seen in table I which shows the change of voltage with temperature (Seebeck coefficients) for a few selected thermocells. According to these data, the hot electrode in a simple thermocell is generally negative for molten and solid salt systems. On the other hand, the opposite is true for cells containing aqueous electrolytes. Note, however, that there are exceptions to this generalization in both categories.

Of particular interest in table I is the large value of the Seebeck coefficient measured for the chlorine electrode in molten silver chloride. According to equation (1), this indicates a half cell electrode reaction

Table I

Seebeck Coefficients of Selected Thermocells

Electrolyte	Electrode Reactant	Temperature	Seebeck Coefficient (mv/°C)	Polarity of Hot Electrode	Reference
Molten Salts					
$AgNO_3$	Ag	500°K	0.329	negative	24
AgCl	Ag	800	0.403	"	24
AgBr	Ag	750	0.48	"	24
AgI	Ag	850	0.43	"	24
$ZnCl_2$	Zn	600	0.13	positive	24
AgCl	Cl_2 (b)	1000	0.664	negative	26
CuCl	Cu	800	0.437	"	22
Aqueous Solutions, one molal (a)					
H^+	H_2 (c)	298°K	0.871	positive	3
Cl^-	Cl_2 (b)	"	0.389	negative	3
Zn^{++}	Zn	"	0.962	positive	3
Cu^+	Cu	"	0.813	"	3
Ag^+	Ag	"	0.129	negative	3
Solid Ionic Salts					
AgCl	Ag	500°K	1.20	negative	24
AgBr	Ag	500	1.12	"	24
CuCl	Cu	500	0.93	"	24
PbI_2	Pb	550	0.39	positive	24

(a) Note that at infinite dilution in aqueous solutions, the counter ion has no influence on the entropy of the reacting ion. These values were obtained at infinite dilution and adjusted by calculation to the one molal reference state.

(b) These data are for chlorine at one atmosphere pressure reacting on graphite electrodes.

(c) This value is for the standard hydrogen electrode.

having a large entropy change. From the following definition of the entropy change for the chlorine electrode reaction,

$$\Delta S^{\circ} = 1/2\ S^{\circ}_{Cl_2} + \bar{S}_e - \bar{\bar{S}}_{Cl^-} \qquad (2)$$

it can be shown that the higher Seebeck coefficient for this cell results from the relatively large entropy of gaseous chlorine. It follows in general that whenever one of the reaction species is a gas, its contribution to the Seebeck coefficient will be large.

Observe that the chlorine pressure was one atmosphere in the silver chloride-chlorine thermocell discussed in table I. It was noted that the gaseous entropy $S^{\circ}_{Cl_2}$ can be increased even further by reducing the chlorine partial pressure. Thus, vacuum operation or dilution with an inert gas should in theory increase the Seebeck coefficient of this electrode.

It is to be recognized that the ionic and electronic entropies of equation (2) are not simply the partial molal entropies but are the "transported entropies". The transported entropy $\bar{\bar{S}}$ is defined as the sum of $\bar{S}$, the partial molal entropy, and S^*, the "entropy of transfer". (The nomenclature is that used by Pitzer(24) and some of the other authors writing in this field.) The term S^* relates to the transfer of a charged particle through a temperature gradient, and it will be discussed in detail in a later section.

B. Efficiency of Thermoelectric Devices

One of the most significant factors influencing the value of a device for energy conversion is the efficiency. The following equation derived in standard texts(10,14) for solid thermocouples also applies to molten-salt thermocells with constant Seebeck coefficients and with no convective heat transfer:

$$\epsilon = \left(\frac{T_H - T_C}{T_H}\right)\left(\frac{M - 1}{M + T_C/T_H}\right) \qquad (3)$$

where

ϵ = maximum possible efficiency; defined as the ratio of the useful work produced to the heat supplied to the hot junction.

T_H = absolute temperature of the hot junction; ^{o}K.

T_C = absolute temperature of the cold junction; ^{o}K.

and M is defined by the equation

$$M = [\ z\ (T_H + T_C)/2 \quad + \quad 1\ ]^{1/2} \tag{4}$$

The parameter z, generally used to characterize thermoelectric devices, is known as the figure of merit and is defined as follows:

$$z = \frac{\alpha^2}{[\ (k_1/\sigma_1)^{1/2} + (k_2/\sigma_2)^{1/2}\ ]^2} \tag{5}$$

where

α = Seebeck coefficient of the couple, dE/dT; volt/^{o}C.

k = thermal conductivity; Watt/cm ^{o}C.

σ = electrical conductivity; $ohm^{-1}\ cm^{-1}$.

Subscripts 1 and 2 refer to the properties of the two separate legs of the couple.

From these equations, it is apparent that the actual efficiency is the product of the Carnot efficiency and a factor involving the physical properties of the generator components. Notice that the maximum efficiency of the device approaches the Carnot limit as the figure of merit approaches infinity. This is compatible with the definition of z since high figures of merit characterize systems with high Seebeck coefficients (high potential per unit temperature difference), high electrical conductivities (low ohmic loss in the conductors), and low thermal conductivities (low energy degradation by thermal conduction).

The efficiency calculated from equation (3) is plotted versus temperature with z as a parameter in figure 2.

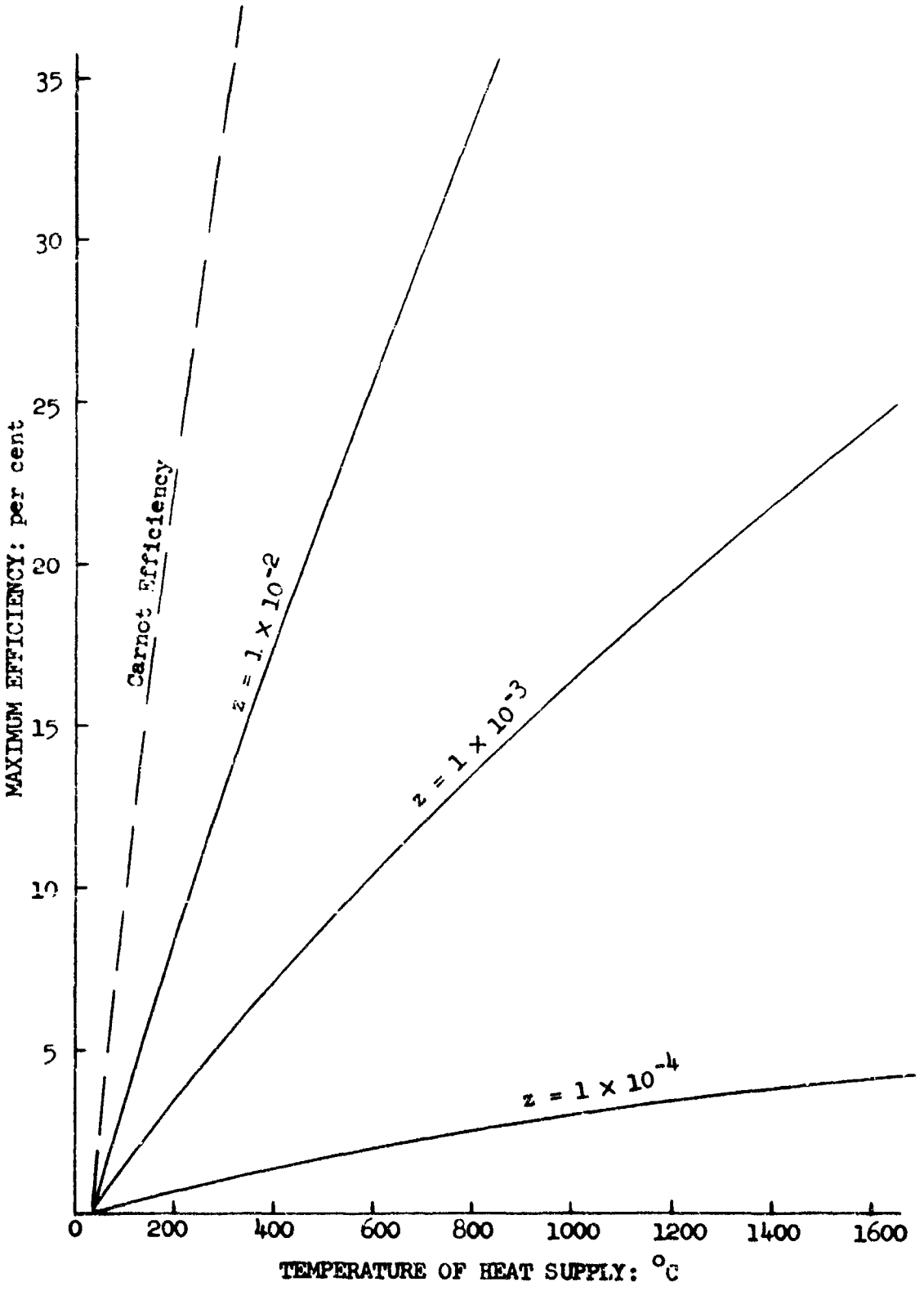

Figure 2. Maximum efficiency of a thermoelectric generator as a functio of temperature and figure of merit (based on a cold junction temperature of 30°C).

C. Selection of Experimental Systems

Sundheim(29) estimated a maximum figure of merit for molten-salt thermocells of 5.0×10^{-4}. He pointed out, however, the problem of transfer of the electrode reactant from one side of the cell to the other which makes recycling necessary. Since he apparently considered only cells involving solid electrode reactants, his conclusion was that these devices would be most useful in combination with a chemical process such as purification of the electrode material. Note, however, that use of the chlorine electrode avoids the necessity of mechanical recirculation. Also, as previously mentioned, the Seebeck coefficient of this electrode is unusually high, and theoretically, it can be increased even more by reducing the chlorine partial pressure. For these reasons, it was decided to study thermocells involving chlorine electrodes in several molten salts.

It is evident from equations(3), (4) and (5) that the molten salt used in a thermocell should have a low thermal conductivity and a high electrical conductivity. These properties are listed for a few selected molten salts in table II along with other properties of interest.

Even though thermal conductivity data are rather scant and unreliable for molten salts, the values shown indicate that this property does not vary signigicantly from salt to salt. (For further discussion of this, see references 29, 30 and 31.) For this reason, selection of the electrolytes to be studied was made on the basis of electrical conductivity.

From table II, it can be seen that the molten chlorides as a group have the highest electrical conductivities of the salts listed except for the fluorides which, because of their corrosive nature, are impractical to study at the present time. For this reason, four chloride salts were chosen for study; the chlorides of lithium, sodium, potassium, and silver. The silver chloride melt had additional value as a reference since results were already available on the silver chloride-chlorine thermocell in the

Table II

Thermal and Electrical Conductivities for a Few Selected Molten Salts

Molten Salt	Melting Point	Boiling point	Thermal Conductivity at Melting Point Watt/cm °C (a)	Electrical Conductivity ohm^{-1} cm^{-1} (b) At Melting Point	At 900°C
LiF	870°C	1670°C		8.3	8.5
NaF	980	1700		5.1	
KF	880	1500		3.7	3.8
LiCl	613	1353		5.7	7.0
NaCl	801	1413	(0.0083)	3.1	3.8
KCl	776	1420		2.2	2.5
LiBr	549	1265		4.7	
NaBr	745	1390		2.8	3.3
KBr	735	1380		1.6	2.0
LiI	465	1190		3.5	
NaI	659	1300		2.2	2.9
KI	723	1420			
RbCl	722	1390		1.5	2.0
RbBr	692	1340		1.1	1.5
RbI	647	1300		0.9	
CsCl	645	1290		1.1	1.8
Na_2CO_3	851			3.0	
$PbCl_2$	501	950		1.3	
KNO_3	334	d. 400	0.0043		
$AgNO_3$	212	d. 444	0.0038	0.7	
$ZnCl_2$	262	732	0.0031	0.1	
KCNS	173	d. 500	0.0028		
NH_4HSO_4	147		0.0036		
$KHSO_4$	210		0.0034		
$NaHSO_4$	180		0.0046		
AgCl	455	1500		4.3	5.1
AgBr	434	d. 700		3.0	
$NaNO_3$	307	d. 380	0.0056	0.9	
NaOH	318	1390	0.0092	2.1	
CuCl	422	1366		3.3	

(a) All thermal conductivities are taken from Turnbull(30,31).

(b) Electrical conductivities are taken from references 18,34,35 and 36.

It was hoped that the experimental results might suggest modifications which would increase the maximum figure of merit for molten-salt thermocells to a value higher than that estimated by Sundheim.

D. Review of Past Thermocell Research

The great majority of past work has involved aqueous thermocells. Eastman(7) initially derived the equations for these systems where thermal diffusion of the solute ions can also affect cell voltage. More recently, Tyrrell(32), deGroot(11) and others have analysed aqueous thermocells by non-equilibrium thermodynamics. All past work is discussed exhaustively in the reviews by deBethune, et. al.(2,3).

Following the pioneering work of Poincare(25) in 1890, the study of molten-salt thermocells lay dormant until the work of Holtan, et. al. (12,13,21), who studied a number of systems involving molten and solid-salt electrolytes. Since then, several other investigators have studied molten-salt thermocells(28,22,26,5). Most of these studies have involved the use of solid electrode reactants. Only recently, however, Senderoff and Bretz(26) reported results for the gaseous chlorine electrode in molten silver chloride, and Detig and Archer(5) published results for this same electrode in molten sodium chloride and molten potassium chloride. Both investigations involved chlorine at one atmosphere pressure. The former study appears to have been carefully done, and for this reason, the same system was investigated in this work so that experimental results could be compared. On the other hand, the results reported by Detig and Archer appear to be quite scattered, and for reasons discussed in section VII-B, can be seriously questioned. The author is not aware of any further work involving gaseous electrode reactants in molten-salt thermocells.

A possible weakness in some past studies is the questionable application of the equations derived for aqueous systems to molten-salt cells, giving

an expression dependant on the transference numbers of the ions in the melt. Nichols and Langford(22) and Senderoff and Bretz(26) recognized this and formulated their results accordingly. Pitzer(24) in his treatment of the subject also discussed this question as follows,".....and it is apparent that the transference number drops out of the equation for the pure salt cell. Indeed a transference number in a single component fused salt can only be defined in an arbitrary manner." His final statement is further substantiated by Van Artsdalen(33). The theoretical approach followed in this thesis and outlined in section III also yields a final expression for thermocell voltage independant of transference numbers.

E. Scope of This Work

The planned scope of this research encompassed two goals:

1. The execution of an experimental program in which the Seebeck coefficients of the chlorine-on-graphite electrode would be determined as a function of temperature and chlorine pressure in several selected molten salt electrolytes, and then, the formulation from these results of a generalized equation applicable to such systems.
2. The calculation of maximum efficiencies which can be expected from those molten-salt thermocells studied and estimation of efficiencies for other fused-salt systems yet unmeasured.

In fulfillment of the first goal, open-circuit voltages were successfully measured for the systems proposed over a temperature range extending from the melting point of the respective salt up to 1300°C; 300°C higher than previously reported for any thermocell. These measurements were made at chlorine pressures of one atmosphere and at various lower pressures for all systems except lithium chloride which was measured at one at-

mosphere only. These data are reported in section VI. In section III, a theoretical equation is developed which expresses the thermocell voltage as a function of the half-reaction standard entropy change, the electrode temperatures, and the partial pressure of the reacting species. This equation is an extension of equation (1) to conditions where the gas molecules, because of dissociation or dilution by the salt vapor, may have different fugacities at the two electrodes. The effect of having reduced chlorine partial pressures at both electrodes due to vacuum operation is also included in the expression, and the voltage represented is an integrated total voltage rather than the rate of change of voltage with respect to temperature given by equation (1); the expression commonly reported in the literature. The derived equation was compared with experimental data, and the agreement is discussed in section VII.

The second intended goal, that of calculating maximum thermocell efficiencies, was complicated by the fact that the Seebeck coefficient found under these experimental conditions was not a constant. Hence, equation (2) which was derived assuming constant α no longer holds, and a corrected equation becomes extremely complex due not only to variation of the Seebeck coefficient but also the need to allow for factors such as vaporization of the salt at the hot electrode into the gas stream followed by condensation in the return line. However, efficiencies can still be estimated, although the calculation is lengthy and tedious. Typical results of this calculation for the silver chloride-chlorine cell are shown in section VII-E.

In order to estimate efficiencies of cells which show promise for energy conversion and yet are difficult to investigate experimentally, it is necessary to know the transported entropy of the migrating ion. This quantity was evaluated experimentally for the chloride ion in the four molten salts studied, and in addition, an effort was made to estimate

its probable magnitude in other melts of interest. This transported entropy and its related quantities, the partial molal entropy and entropy of transfer are discussed in section VII-B. Based on the conclusions stated there, the efficiencies of the hypothetical boron oxide-oxygen and lithium fluoride-fluorine thermocells were estimated and are reported in section VII-E.

III. THEORY

The purpose of this section is to provide a quantitative theoretical tool for evaluation of the open-circuit voltages which were measured experimentally by the author. Therefore, the first stage of the following thermodynamic derivation is specific to molten-salt thermocells containing chlorine electrodes. Following the formulation of this specific expression, the result is generalized to include all similar molten-salt systems.

A. Description of Cell Model

Figure 3 shows a schematic diagram of the chlorine cell. The "cold" electrode is at an absolute temperature T_1 which is near the melting point of the salt. At this temperature, the vapor pressure of the melt and the amount of chlorine dissociation (diatomic to monotomic) are assumed to be negligible. The temperature at the hot electrode, T_3, is high enough so that either dissociation of chlorine or salt vaporization or both may occur in significant amounts. Zone 1 is designated as the cold electrode compartment and is considered isothermal at T_1. Zone 3, the hot electrode compartment, is isothermal at T_3. Zone 2 which includes both the melt and the graphite conductor is the non-isothermal region connecting zones 1 and 3. The entropy change for the chlorine half cell reaction is such that chloride ions migrate in the electrolyte from the cold to the hot side of zone 2, and electrons migrate through the graphite conductor in the opposite direction. Thus, the electrode reactions occur spontaneously as written in the figure.

B. Thermodynamic Analysis of Cell Model

The cell system chosen for analysis here contains the electrolyte, the wire and the two electrode chambers. As shown in figure 3, chlorine gas is permitted to cross the boundaries of this system.

Consider the passage of electricity through the cell in the direction

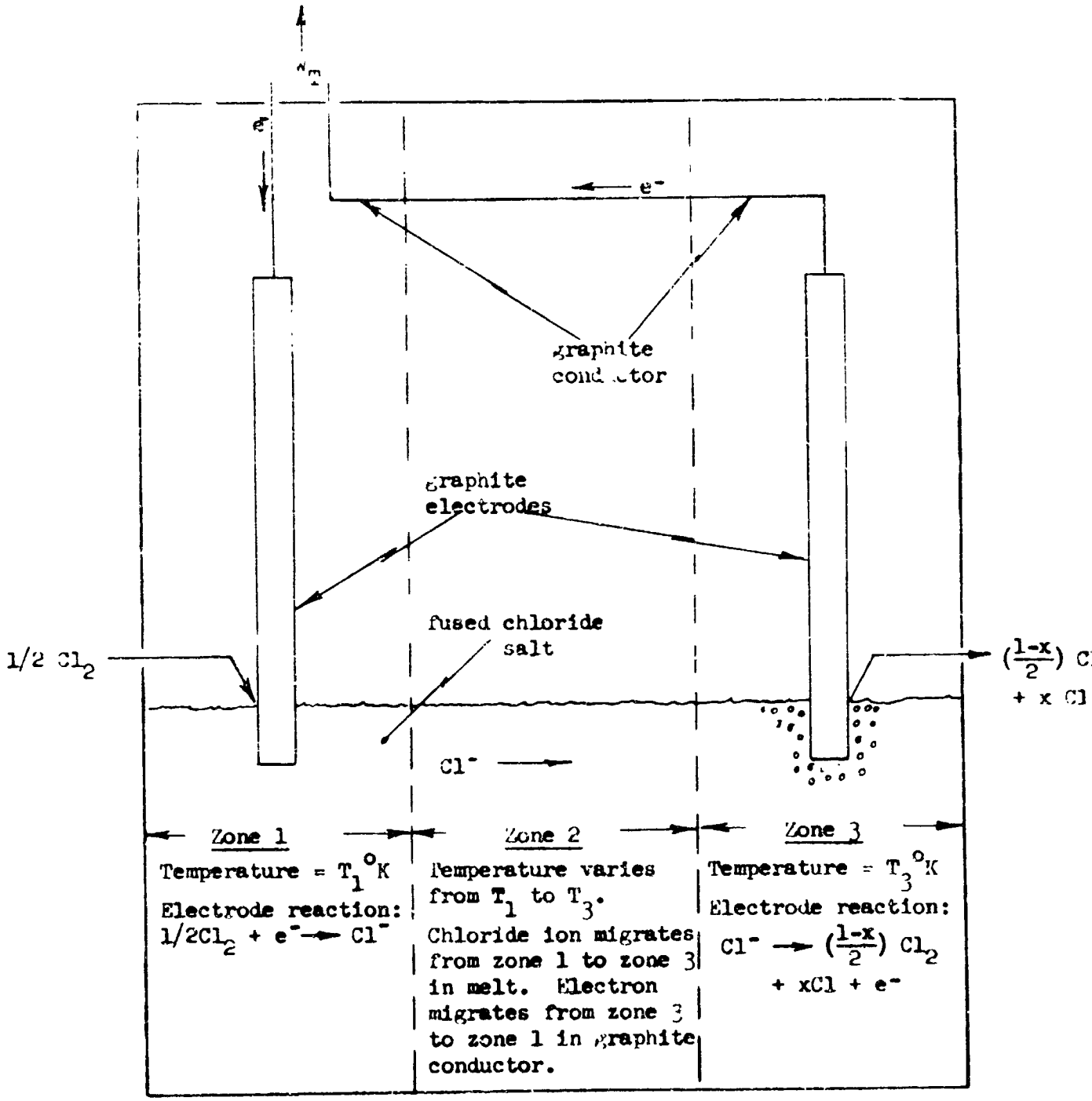

Figure 3. Schematic representation of molten-salt thermocell with chlorine (on graphite) electrodes.

indicated in figure 3. It is assumed that this passage occurs reversibly, meaning that the current is infinitesimal so that ohmic losses (I^2R losses in the conductors) and polarization effects are zero, and that the cell potential is equal to the open-circuit voltage. There is, of course, an irreversible phenomenon in this system due to the steady-state conduction of heat from the heat reservoir at T_3 to that at T_1. It is assumed, however, that the reversible phenomena can be analyzed independantly of this effect as though the irreversibility were not present. This is equivalent to assuming that the cell is divided into small segments, each isothermal but at a different temperature than its neighbor, and each connected to an appropriate heat reservoir. Matter can pass reversibly from segment to segment, but each is thermally insulated from the other. Heat can be conducted reversibly from each segment to its reservoir or visa versa as required. (These are the same assumptions made by Thomson (Lord Kelvin) in his formulation of the equations relating Peltier and Thomson heats to the voltage of a thermocouple. His results were later verified by experiment(10).)

For the system pictured in figure 3 and discussed above, the first law can be written as follows:

$$W_T = Q_T - \Delta H_T \tag{6}$$

where

W_T = total net work produced by the cell. This work is obviously all electrical work.

Q_T = total net heat added to the system. As mentioned above, this is the reversible heat only and it does not include that flowing in and out of the system due to steady-state thermal conduction.

ΔH_T = difference in enthalpies between the chlorine leaving and that entering the system.

It is possible further to separate the right side of equation (6) into corresponding terms for each of the three cell zones as shown below:

$$W_T = Q_1 - \Delta H_1 + Q_2 - \Delta H_2 + Q_3 - \Delta H_3 \qquad (7)$$

where the subscripts designate the zone to which the heat and enthalpy terms apply. Since the electrode processes of zones 1 and 3 occur reversibly and isothermally, Q_1 can be equated to $T_1 \Delta S_1$ where ΔS_1 is the entropy change for the process occuring in zone 1. By the same reasoning, Q_3 can be equated to $T_3 \Delta S_3$ where ΔS_3 is the entropy change for the process occuring in zone 3. With these substitutions, equation (7) can be rewritten as follows:

$$W_T = (T_1 \Delta S_1 - \Delta H_1) + (Q_2 - \Delta H_2) + (T_3 \Delta S_3 - \Delta H_3) \qquad (8)$$

Now, by recognizing that

$$T_1 \Delta S_1 - \Delta H_1 = -\Delta F_1 \qquad (9)$$

and

$$T_3 \Delta S_3 - \Delta H_3 = -\Delta F_3 \qquad (10)$$

equation (8) can be modified to

$$W_T = -\Delta F_1 - \Delta F_3 + (Q_2 - \Delta H_2) \qquad (11)$$

where ΔF_1 and ΔF_3 are the free energy changes for the electrode processes occuring in zones 1 and 3. For one equivalent of chlorine reacting, ΔF_1 is defined by

$$\Delta F_1 = \bar{F}_{Cl^-,T_1} - \bar{F}_{e,g,T_1} - 1/2\, \bar{F}_{Cl_2,T_1} \qquad (12)$$

where

$\bar{F}_{Cl^-,T_1}$ = partial molal free energy of chloride ion in the melt at T_1.

$\bar{F}_{e,g,T_1}$ = partial molal free energy of the electron in graphite at T_1.

$\bar{F}_{Cl_2,T_1}$ = partial molal free energy of chlorine gas at its partial pressure in zone 1 and at the temperature T_1.

Likewise, one can write for ΔF_3 in zone 3

$$\Delta F_3 = \left(\left[\frac{1-x}{2}\right] \bar{F}_{Cl_2,T_3} + x\, \bar{F}_{Cl,T_3} + \bar{F}_{e,g,T_3} - \bar{F}_{Cl^-,T_3}\right) \qquad (13)$$

where the partial molal free energies are for the indicated species at a temperature T_3. Note that equation (13) allows for dissociation of chlorine as mentioned above. Since, however, the dissociation reaction

$$Cl_2 \longrightarrow 2\ Cl$$

is in equilibrium,

$$2\ \bar{F}_{Cl,T_3} = \bar{F}_{Cl_2,T_3} \tag{14}$$

and equation (13) can be simplified to

$$\Delta F_3 = (\ 1/2\ \bar{F}_{Cl_2,T_3} + \bar{F}_{e,g,T_3} - \bar{F}_{Cl^-,T_3}) \tag{15}$$

For this analysis, the standard state for chloride ion is that in the pure melt and for the electron, that in graphite. Hence, they exist in the cell in their standard states. Then,

$$\bar{F}_{e,g,T_i} = F^{o}_{e,g,T_i}$$

and (16)

$$\bar{F}_{Cl^-,T_i} = F^{o}_{Cl^-,T_i}$$

where F^o designates the standard molal free energy. The standard state of chlorine gas is defined as the pure gas at one atmosphere pressure, and it is assumed that the fugacity is equal to the partial pressure. Hence, the partial molal free energies of chlorine at the electrodes can be expressed by

$$\bar{F}_{Cl_2,T_3} = F^{o}_{Cl_2,T_3} + RT_3 \ln p_{Cl_2,T_3}$$

and (17)

$$\bar{F}_{Cl_2,T_1} = F^{o}_{Cl_2,T_1} + RT_1 \ln p_{Cl_2,T_1}$$

Implied in these equations is the assumption that chlorine is an ideal gas--a reasonable assumption at fused-salt temperatures and low pressures.

The substitution of equations (12), (15), (16) and (17) into (11)

gives for the total work of the cell:

$$W_T = 1/2\ F^{\circ}_{Cl_2,T_1} - 1/2\ F^{\circ}_{Cl_2,T_3} + F^{\circ}_{e,g,T_1} - F^{\circ}_{e,g,T_3} + F^{\circ}_{Cl^-,T_3} - F^{\circ}_{Cl^-,T_1} + 1/2\ RT_1 \ln p_{Cl_2,T_1} - 1/2\ RT_3 \ln p_{Cl_2,T_3} + (Q_2 - \Delta H_2) \quad (18)$$

and since

$$F^{\circ}_{i,T_1} - F^{\circ}_{i,T_3} = \int_{T_1}^{T_3} S^{\circ}_i\, dT \quad (19)$$

equation (18) can be simplified further to

$$W_T = \int_{T_1}^{T_3} (1/2\ S^{\circ}_{Cl_2} + \bar{S}_{e,g} - \bar{S}_{Cl^-})\, dT + 1/2\ RT_1 \ln p_{Cl_2,T_1} - 1/2\ RT_3 \ln p_{Cl_2,T_3} + (Q_2 - \Delta H_2) \quad (20)$$

If the temperature at the hot electrode is high enough, the partial pressure of Cl_2 molecules is no longer equal to the total pressure because of dissociation to monatomic chlorine and also because of dilution by vaporized salt. Therefore, assuming that x moles of Cl_2 (on a one mole basis) dissociate to form 2x moles of Cl, leaving (1-x) moles of Cl_2, the equilibrium expression ($p_{Cl_2} = p^2_{Cl}/K^2$) can be written in terms of x as follows:

$$\left(\frac{1-x}{1+x}\right)\pi' = \frac{\left(\frac{2x}{1+x}\right)(\pi')^2}{K^2} \quad (21)$$

where K is the equilibrium constant for dissociation and π' is the total pressure of the mixed Cl_2 and Cl (π minus the vapor pressure of the salt). Equation (21) can be rearranged to

$$x = \frac{1}{[(4\pi'/K^2) + 1]^{1/2}} = \frac{1}{n} \quad (22)$$

where n can be evaluated from basic data, making it possible to calculate the pressure of diatomic chlorine from the material balance equation below:

$$p_{Cl_2} = \left(\frac{1-x}{1+x}\right)\pi' = \left(\frac{n-1}{n+1}\right)\pi' \quad (23)$$

Note that equation (23) would apply at the cold electrode also if the diatomic chlorine were appreciably dissociated or diluted by the salt vapor. In this case, however, n and π' would be evaluated at T_1. At the values of T_1 used in this thesis, salt vapor pressures and chlorine dissociation were negligible, thus, n was large and π' was insignificantly different from π making the chlorine pressure at the cold electrode equal to π.

Combining the four preceding equations, we now have

$$W_T = \int_{T_1}^{T_3} \Delta S \, dT + 1/2 \, RT_1 \ln \pi - 1/2 \, RT_3 \ln[(\tfrac{n-1}{n+1})\pi'] + (Q_2 - \Delta H_2) \tag{24}$$

where ΔS is the short-hand notation for the entropy change of the half cell reaction, i.e. $1/2 \, S^{\circ}_{Cl_2} + \bar{S}_{e,g} - \bar{S}_{Cl^-}$.

To clarify the significance of the term $(Q_2 - \Delta H_2)$, consider the system in figure 3 comprising the non-isothermal electrolyte. By the first law,

$$Q_{Cl^-} - W_{Cl^-} = \Delta H_{Cl^-} + Ne\psi + K.E. \tag{25}$$

where Q_{Cl^-} is the net heat added during the passage of one equivalent of chloride ions, W_{Cl^-} is the work performed, and ΔH_{Cl^-} is the enthalpy change. The potential difference due to a thermostatic field is ψ, N is Avagadro's number, e is the electronic charge and K.E. represents kinetic energy effects. It is obvious from the description of the system that no work crosses the boundaries. Likewise, the average velocity of the entering ions is the same as that of those leaving, hence, K.E. is zero. It is interesting to note that the potential energy term $Ne\psi$ would be zero if the migrating ion carried no charge, making $(Q_i - \Delta H_i)$ zero. On the other hand, when the species carries an electrical charge, $Q - \Delta H$ does not necessarily vanish, and there may be a voltage contribution

due to the non-isothermal transfer of charge through an electrostatic field. It should be observed that this contribution cannot, at the present time, be measured in isolation.

In accordance with past work in this area, equation (25) will be rewritten as follows:

$$Q_{Cl^-} - \Delta H_{Cl^-} = Ne\psi = -\int_{T_1}^{T_3} S^*_{Cl^-}\, dT \qquad (26)$$

where $S^*_{Cl^-}$ is the entropy of transfer of chloride ion in the molten electrolyte. The quantity S^* may be positive, negative or zero. (In section III-F, two alternate approaches are discussed which attempt to interpret the significance of the entropy of transfer.)

By an argument similar to that used above, an equation analogous to (26) can be written for the migration of an electron through the non-isothermal graphite wire. Combining this with equation (26) yields

$$Q_2 - \Delta H_2 = \int_{T_1}^{T_3} (S^*_{e,g} - S^*_{Cl^-})\, dT \qquad (27)$$

This equation substituted into (24) gives the following useful expression for the thermocell voltage:

$$E = \frac{1}{\mathcal{F}} \left[\int_{T_1}^{T_3} \Delta S^\circ\, dT + 1/2\, RT_1 \ln \pi - 1/2\, RT_3 \ln\left(\left[\frac{n-1}{n+1}\right]\pi'\right)\right] \qquad (28)$$

where ΔS° is equal to ΔS as defined in equation (24) plus the entropies of transfer of equation (27), i.e.,

$$\Delta S^\circ = 1/2\, S^\circ_{Cl_2} + \bar{S}_{e,g} - \bar{S}_{Cl^-}$$

The transported entropy $\bar{S}$, as mentioned before, is the sum $(\bar{S} + S^*)$. The relationship between reversible work and voltage ($W = \mu \mathcal{F} E$) was also used in the last step.

C. Analysis of Equation (28)

Equation (28) will now be discussed term by term. As mentioned

above, the quantity under the integral sign is the standard state entropy change (including entropies of transfer) for the half cell reaction written for the direction in which it proceeds spontaneously at the hot electrode. In accordance with the second law of thermodynamics, it is always positve. The second term is a correction accounting for chlorine partial pressures at the cold electrode different from one atmosphere. The third term of equation (28) shows the influence of chlorine partial pressures differing from unity at the hot electrode. Dilution of the diatomic chlorine by dissociation and by the presence of salt vapor is accounted for in this term. It should also be observed that the third term is always larger than the second under reduced pressure conditions. Thus, at pressures less than one atmosphere, the effect of terms two and three is to increase the voltage. Note that equation (28) simplifies to

$$E = \frac{1}{\mathcal{F}} \int_{T_1}^{T_3} (\Delta S^\circ - 1/2\ R \ln \pi)\ dT \qquad (29)$$

if T_3 is so low that chlorine dissociation and the vapor pressure of the salt are insignificant both at the hot and the cold electrodes. The term $1/2\ R \ln \pi$ is, of course, the standard ideal-gas entropy correction required to adjust the chlorine entropy, $1/2\ S^\circ_{Cl_2}$ to pressures different from one atmosphere. At a chlorine pressure of one atmosphere, equation (29) reduces to an expression of the form reported in the literature(26,24,22):

$$\frac{dE}{dT} = \frac{1}{\mathcal{F}} (1/2\ S^\circ_{Cl_2} + \bar{S}_{e,g} - \bar{S}_{Cl^-}) \qquad (30)$$

D. Formulation of a Generalized Expression for Thermocell Voltage

By a procedure analogous to that used in arriving at equation (28), the generalized equation (31) can be derived:

$$E = \frac{1}{\mu \mathcal{F}} \left[\int_{T_1}^{T_3} \Delta S^\circ\ dT + RT_1 \ln K_{T_1} - RT_3 \ln K_{T_3} \right] \qquad (31)$$

where ΔS° is the standard-state entropy change for any half cell reaction

written as it occurs at the hot electrode, and K_{T_1} and K_{T_3} are the activity ratios for this reaction evaluated at T_1 and T_3. For example, if the hot electrode reaction is

$$Cl^- \longrightarrow 1/2\ Cl_2 + e^-$$

then

$$K_{T_i} = \frac{[a_{Cl_2}]^{1/2}[a_e]}{[a_{Cl^-}]} \tag{32}$$

where the a's represent the actual activities of the respective species at the electrode temperature T_i. Clearly, a_e and a_{Cl^-} are both equal to unity and a_{Cl_2} is equal to the partial pressure of chlorine. With these substitutions, equation (31) reduces to (28) as originally derived. Observe also that the reaction involving the monotomic species occurs in the chlorine system as shown below:

$$Cl^- \longrightarrow Cl + e^-$$

It can be demonstrated by algebraic manipulation of thermodynamic identities that equation (31) written for this half cell reaction also reduces to equation (28). Note that equation (31) is not limited to cells with gas electrodes but applies in any case where the activities of the reacting species are known. For example, the activity ratio K_{T_i} for a reaction involving pure solid electrodes is unity and the last two terms in equation (31) vanish. Thus, the equation again reduces to the commonly used form:

$$\frac{dE}{dT} = \frac{\Delta S^\circ}{\mu \mathcal{F}} \tag{33}$$

E. Discussion of Ionic Entropies in Molten Salts

Notice that it is not possible to calculate a priori the voltage to be expected from a given cell. Even though it is true that the last two terms of equation (28) can be calculated from chlorine dissociation constants and vapor pressure data reported in the literature, the first term involves quantities about which little is known. As previously

mentioned, ΔS^{o} for the chlorine thermocells is defined as

$$\Delta S^{o} = 1/2\ S^{o}_{Cl_2} + \bar{\bar{S}}_{e,g} - \bar{\bar{S}}_{Cl^-}$$

where the entropy of chlorine gas at one atmosphere $S^{o}_{Cl_2}$ is well known and has been tabulated for a number of different temperatures(8). The transported entropy of the electron in graphite can also be evaluated (see Appendix, section C where it is estimated to be approximately 0.2 e.u.). On the other hand, the complicated ionic structure of the liquid electrolyte makes the quantitative estimation of $\bar{\bar{S}}_{Cl^-}$ difficult.

As defined previously, $\bar{\bar{S}}_{Cl^-}$ is equal to the sum of the partial molal entropy and the entropy of transfer neither of which can be calculated with confidence. Recently, however, Pitzer(24) proposed a method for the calculation of the partial molal entropy of ions in simple 1-1 molten salts. His expression is based on the assumption that the partition functions for both the cations and the anions in a pure melt will be approximately the same except for the mass contribution to translational entropy. This is expected to be true so long as the ions are not greatly different in size. Based on the mass correction term, $3/2\ R \ln M_2/M_1$, he proposed the following for the partial molal entropy of the positive ion in a pure melt:

$$\bar{S}_{M^+} = 1/2(S_{MX} + 3/2\ R \ln M_M/M_X) \qquad (34)$$

where

$\bar{S}_{M^+}$ = partial molal entropy of the positive ion.
S_{MX} = entropy of the pure molten salt.
R = the gas constant.
M_M = molecular weight of the positive ion.
M_X = molecular weight of the negative ion.

By difference, the corresponding expression for the anion entropy is

$$\bar{S}_{X^-} = 1/2(S_{MX} + 3/2\ R \ln M_X/M_M) \qquad (35)$$

Equations (34) and (35), if valid at all, should hold true for at least two of the salt systems studied here: the potassium chloride and sodium

chloride systems where the cations and anions are nearly the same size.

The partial molal entropies were calculated from equation (35) for chloride ions in the four pure melts studied. These were compared with the experimentally determined transported entropies for the same species. This comparison and its significance are discussed in section VII.

F. Interpretation of the Entropy of Transfer

In the past, the contribution to the cell voltage from the migration of charged particles through non-isothermal conductors has often been treated by the methods of non-equilibrium thermodynamics(32,11,4a). For example, following the treatment of Denbigh(4a), the equations relating the fluxes of heat and electricity to their driving forces can be written as follows for ion transfer in a molten electrolyte:

$$J_i = L_{ii} X_i + L_{iq} X_q \tag{36}$$

$$J_q = L_{qi} X_q + L_{qq} X_q \tag{37}$$

where

J_i = net flow of electrical current through the system.
J_q = net flow of heat through the system.
X_i = driving force for current flow.
X_q = driving force for heat flow.
L_{ii} = coefficient relating current flux to current driving force.
L_{qq} = coefficient relating heat flux to heat driving force.
L_{iq} = coefficient relating current flux to heat driving force.
L_{qi} = coefficient relating heat flux to current driving force.

It is to be noted that an equation similar to equation (36) applies for each migrating species in the electrolyte. But, the chloride ion is the only species which migrates in the systems studied, and since electrical neutrality requires that there be no net transfer of the cation, J_i applies to the transfer of current through the molten electrolyte as a result of chloride ion migration only. Under these conditions, the

forces can be defined as

$$X_q = -\frac{1}{T}\frac{dT}{dy} \tag{38}$$

$$X_i = -\left(\frac{d\bar{F}_{Cl^-}}{dy} - \frac{\bar{F}_{Cl^-}}{T}\frac{dT}{dy} + Ne\frac{d\psi}{dy}\right) \tag{39}$$

where $\bar{F}_{Cl^-}$ is the partial molal free energy (chemical potential) of the chloride ion, dT/dy is the derivative of temperature with respect to the direction of migration y, $\bar{N}$ is avagadro's number, e is the electronic charge, and $d\psi/dy$ is the derivative of electrical potential with respect to y. (For further details, see Denbigh, page 61.)

Since there is a temperature gradient in the electrolyte, the derivative of chemical potential with respect to y can be rewritten as shown below for a pure molten salt at constant pressure:

$$\frac{d\bar{F}_{Cl^-}}{dy} = \left(\frac{\partial\bar{F}_{Cl^-}}{\partial T}\right)\frac{dT}{dy} \tag{40}$$

This is changed further by the substitution of

$$\bar{F}_{Cl^-} = \bar{H}_{Cl^-} - T\bar{S}_{Cl^-} \tag{41}$$

into equation (40) to yield the expression

$$\frac{d\bar{F}_{Cl^-}}{dy} = -\bar{S}_{Cl^-}\frac{dT}{dy} \tag{42}$$

Also, from (41), it can be seen that

$$-\frac{\bar{F}_{Cl^-}}{T} = \bar{S}_{Cl^-} - \frac{\bar{H}_{Cl^-}}{T} \tag{43}$$

Substitution of (43) and (42) into (39) gives for the diffusion driving force:

$$X_i = \left(\frac{\bar{H}_{Cl^-}}{T}\frac{dT}{dy} - Ne\frac{d\psi}{dy}\right) \tag{44}$$

With the expressions (38) and (44) defining the forces X_i and X_q, equations (36) and (37) now become

$$J_i = L_{ii}\left(\frac{\bar{H}_{Cl^-}}{T}\frac{dT}{dy} - Ne\frac{d\psi}{dy}\right) - \frac{L_{iq}}{T}\frac{dT}{dy} \tag{45}$$

$$J_q = L_{qi}\left(\frac{\bar{H}_{Cl^-}}{T}\frac{dT}{dy} - Ne\frac{d\psi}{dy}\right) - \frac{L_{qq}}{T}\frac{dT}{dy} \tag{46}$$

Now, it is convenient to define a quantity Q_{Cl^-} called the energy of transport which is the total energy flow J_q divided by the ion diffusion flux at zero temperature gradient, i.e.

$$Q_{Cl^-} = \left(\frac{J_q}{J_i}\right)_{X_q = 0} \tag{47}$$

With the proper substitutions from equations (45) and (46) at $dT/dy = 0$, (47) becomes

$$Q_{Cl^-} = \frac{L_{qi}}{L_{ii}} \tag{48}$$

Now, consider the cell which has a thermal gradient as current approaches zero. In this case, J_i becomes zero and equation (45) can be rearranged to give the following expression for the gradient of electrical potential in the electrolyte:

$$\frac{d\psi}{dy} = \frac{1}{Ne}\left(\frac{\bar{H}_{Cl^-}}{T} - \frac{L_{iq}}{TL_{ii}}\right)\frac{dT}{dy} \tag{49}$$

Then, by using the Onsager reciprocal relationship $L_{iq} = L_{qi}$, the energy of transport can be substituted from (48) into (49) to give

$$d\psi = \frac{1}{Ne}\left(\frac{\bar{H}_{Cl^-} - Q_{Cl^-}}{T}\right)dT \tag{50}$$

which can be further simplified to

$$d\psi = -\frac{Q^*_{Cl^-}}{NeT}dT \tag{51}$$

where $Q^*_{Cl^-}$ is termed the heat of transport of the ion. Since the ratio $Q^*_{Cl^-}/T$ has the units of entropy, equation (51) is often written

$$d\psi = -\frac{S^*_{Cl^-}}{Ne}dT \tag{52}$$

where $S^*_{Cl^-}$ is the entropy of transfer of the chloride ion.

Equation (52) is also that derived by Tyrrell(32) where $d\psi$ is interpreted to be the contribution to the open-circuit thermocell potential which results from the transfer of the ion through a thermal gradient. One

of the problems of this derivation is the absence of a physical meaning for $S^{*}_{Cl^-}$. Since this quantity does relate to a real physical process, it was felt that another approach might be more satisfying. For this reason, the following derivation is proposed which relates the entropy of transfer to the entropy of activation of the ion species. This derivation uses a thermostatic approach and assumes that the reversible heat effect in this non-equilibrium system can be treated independantly of the irreversible thermal conduction effect. This was the same approach used by Thomson in his analysis of the thermocouple. (For further discussion, see de Groot(11), chapter 8.)

Suppose as a model for the migration of charge we consider the transfer of the chloride ion from one location in a pure melt to another location which is higher in temperature by the differential amount dT. One possible path, abc, is shown in figure 4 where the double-dagger superscript refers to the ion in its activated state.

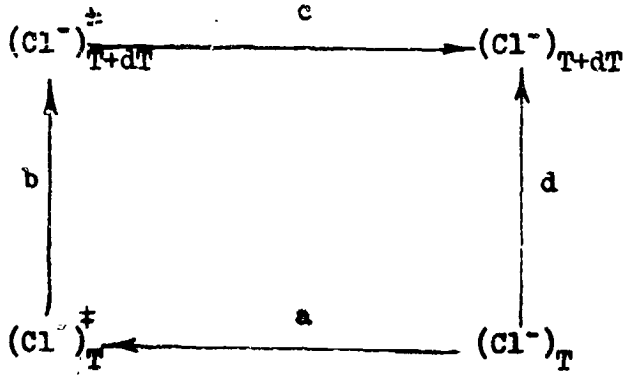

Figure 4. Diagram showing possible ion migration path.

For step a, the heat effect for reversible activation can be written as

$$\delta Q_a = T\,(S^{\ddagger}_{Cl^-} - S_{Cl^-})_T \qquad (53)$$

A similar expression holds for step c:

$$\delta Q_c = (T + dT)(S_{Cl^-} - S^{\ddagger}_{Cl^-})_{T+dT} \qquad (54)$$

Finally, for step b, the heat associated with the migration of the activated ion through a thermal gradient can be written as shown in equation (55):

$$\delta Q_b = C^{\ddagger}_{p,Cl^-}\,dT \qquad (55)$$

To evaluate the point function dH, the alternate path d can be

taken:

$$dH_d = C_{p,Cl^-}\, dT \tag{56}$$

and now, all of these terms can be summed to give the expression:

$$\sum_{i=a}^{c} \delta Q_i - dH_d = T\,(S^{\ddagger}_{Cl^-} - \bar{S}_{Cl^-})_T + (T + dT)(\bar{S}_{Cl^-} - S^{\ddagger}_{Cl^-})_{T+dT} + (C^{\ddagger}_{p,Cl^-} - C_{p,Cl^-})\, dT \tag{57}$$

By recognizing that

$$(S^{\ddagger}_{Cl^-} - \bar{S}_{Cl^-})_{T+dT} + (\bar{S}_{Cl^-} - S^{\ddagger}_{Cl^-})_T = (C^{\ddagger}_{p,Cl^-} - C_{p,Cl^-})\,\frac{dT}{T} \tag{58}$$

equation (57) can be further simplified to the following:

$$\sum_{i=a}^{c} \delta Q_i - dH_d = (\bar{S}_{Cl^-} - S^{\ddagger}_{Cl^-})\, dT \tag{59}$$

Note carefully that this result depends on the path chosen to evaluate the heat terms. If the path d had been chosen instead of abc, then δQ_d is equal to dH_d and the left side of equation (59) is zero. It is logical to suspect that the ion activation does not actually occur isothermally, but in a thermal gradient so that the real path is somewhere between the extremes of path abc and that of d. In this case, the right side of equation (57) must be multiplied by a factor (designated by λ) which is less than unity. It seems reasonable that most of the ion migration will occur in the activated state and the actual path will be similar to path abc of figure 4 when the non-migrating ion is relatively large. In this case, λ will approach unity. On the other hand, if the neutral ion is small, the path should more closely resemble d in figure 4, and λ will be more nearly equal to zero. At any rate, equation (59) can be modified to equation (60) below by the inclusion of λ as a multiplier:

$$\delta Q - dH = \lambda(\bar{S}_{Cl^-} - S^{\ddagger}_{Cl^-})\, dT \tag{60}$$

It is apparent that this equation represents the contribution to the total work of the cell arising from migration of the chloride ion through the temperature difference dT. By comparison with the thermocell analysis

of Tyrrell (reference 32, page 60), it can be seen that the quantity (δQ - dH) in equation (60) is the same as $d\Psi$ in equation (52). Thus, the right side of equation (60) can be equated to the right side of equation (52) to give the following expression relating the entropy of transfer to the entropy of activation:

$$S^{*}_{Cl^-} = \lambda \left(S^{\ddagger}_{Cl^-} - \bar{S}_{Cl^-}\right) \qquad (61)$$

where, as mentioned above, λ can be any number between one and zero.

IV. APPARATUS

With the exception of the work of Poincare, all molten-salt thermocell work known to this author has been done in U-type apparatus. Poincare (25) used a saucer-like dish which was not amenable to careful temperature control. In the U-type apparatus, the temperature of each leg of the tube is controlled separately either by submerging the whole apparatus in a high temperature bath and electrically heating one leg independently (28), by insulating and heating each leg independently (12, 26, 5), or by placing the cell inside a muffle furnace having an imposed temperature gradient (22). Because of the corrosive nature of the melts to be studied here and the desire to operate under reduced pressure, it was decided to design a different type of cell. First, it had to be of simple geometric form in order to utilize some of the refractory materials which cannot be easily or inexpensively formed into complex shapes. Second, the salt container had to be removable from the furnace so that container replacement would not be too difficult, and third, the cell had to have two temperature zones capable of careful control.

A. The Cell

With these criteria in mind, the cell shown in figure 5 and described in more detail in section A of the Appendix was conceived.* The outside containing tube, 2-1/4" O.D. x 2" I.D. and 24" long was closed at one end. Inside this was another tube 1-1/8" O.D. x 7/8 " I.D. x 24" long open at both ends. The smaller tube was secured with a combination "teflon" plug-"viton" O-ring fitting so that it hung about two inches above the floor of the larger tube. Electrodes, thermocouples, and vent tubes secured by the same fitting were also placed in the cell. The unit when assembled was gas

---

*Note: In a conversation with R. I. Bretz of Union Carbide Corporation, the author was told that they had used a similar design to study an alkali chlorides eutectic thermocell. The conversation took place in April, 1963. Further details are unknown.

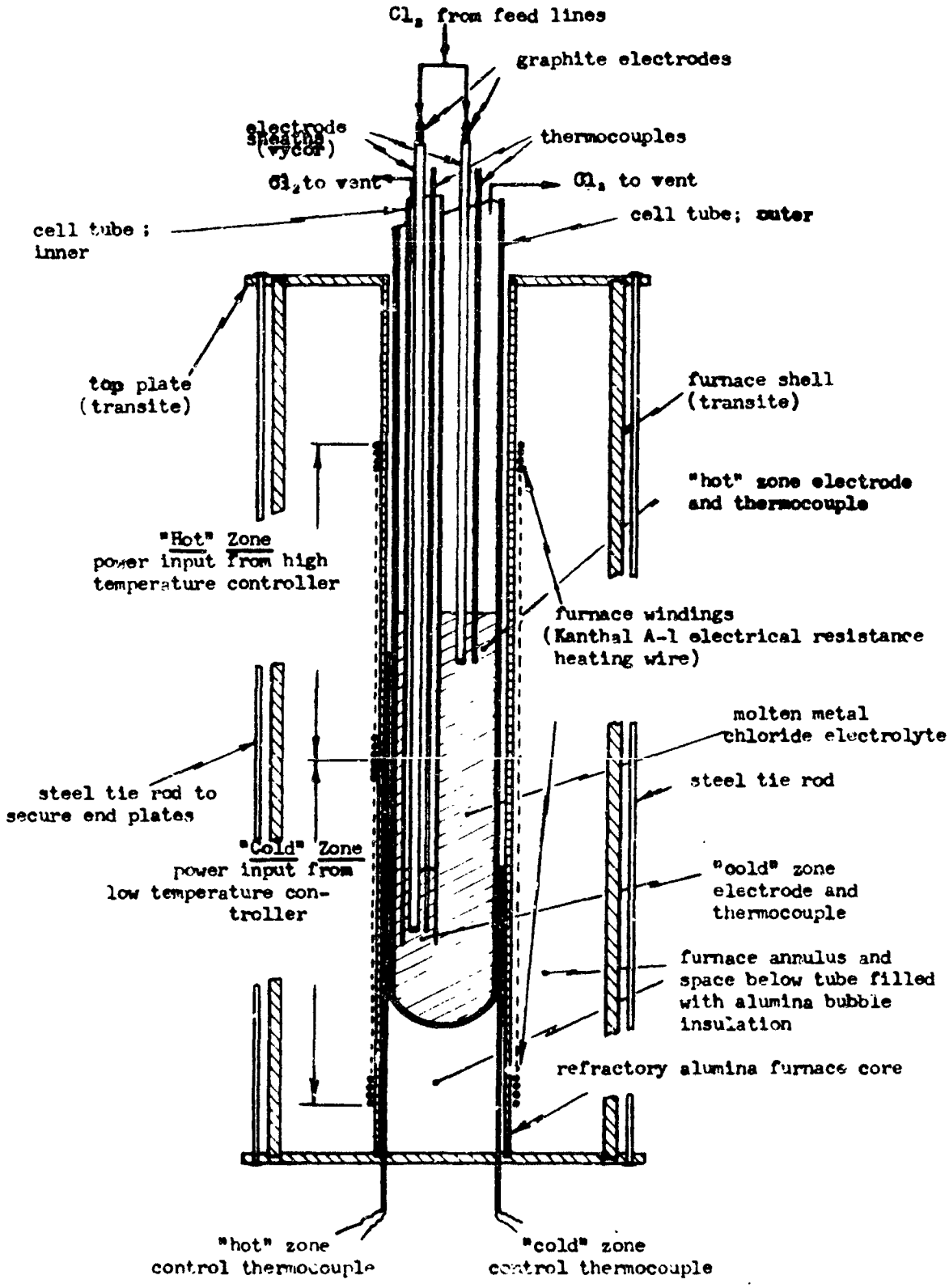

Figure 5. Configuration of experimental thermocell-furnace unit.

tight and proved to be entirely satisfactory for operation under moderate vacuum.

B. [illegible] Furnace

The [illegible] was placed in an upright tube furnace wound with Kanthal A-1 resistance heating wire. The furnace winding was done so as to form two zones which could be heated independently. Thermocouples located in each furnace zone supplied the control input to two separate Barber-Colman indicating controllers, which in turn regulated the silicon control rectifiers supplying power to the furnace.

When the cell was placed in the furnace, the bottom of the inner tube was opposite the center of one furnace zone. A graphite electrode and a thermocouple were located inside the inner tube in contact with the molten salt at this point. Similarly an electrode and thermocouple were placed in the annulus between the tubes at an elevation approximately six inches higher, just opposite the second heating zone. Then, by varying the settings on the power input controllers, it was possible to vary the individual temperatures of the electrodes and their surroundings.

C. Electrodes

The electrodes were constructed of graphite rod (National Carbon grade AGSX) and sheathed with 9mm "vycor" tubing so that only a small "button" 1/8" thick by 5/16" O.D. was exposed to the melt. Liquid was prevented from rising in the annulus between the electrode and its sheath by a downward flow of chlorine through this space. The chlorine subsequently bubbled to the surface and left the compartments via the vent system. The chlorine (Matheson 99.5 per cent pure) coming directly from the cylinder through a reducing valve passed through a glass drying column packed with anhydrous magnesium perchlorate. It then separated into two streams and passed through teflon needle

valves and flow meters to the electrodes.

D. Thermocouples

The thermocouples used were made from pure platinum and 90 per cent platinum- 10 per cent rhodium wires. They were calibrated with a National Bureau of Standards calibrated thermocouple and were found to deviate less than a degree from the standard tables.

E. Reduced Pressure System

For operation at atmospheric pressure, the gas from the external vent system was expelled at the hood outlet. For reduced pressure operation, the exit gases were throttled through a teflon needle valve before passing to the water aspirator. With this setup, steady pressures of less than 0.1 atmosphere were obtained.

F. Container Materials and Melt Purification

Reports of previous investigators (17) indicated severe corrosion of fused silica by the alkali chloride melts. It was thought that these salts catalyzed the low temperature reversion of the thermodynamically unstable glass state to the crystalline form of quartz (devitrification occurs naturally at a measurable rate in the absence of a catalyst at temperatures in excess of about 1200°C). With this information in mind, the experimental unit was designed to accomodate a variety of different refractory tubes. At first, the tubes used were of "Mullite", manufactured by McDanel Refractory Procelain Company. They were satisfactory for about one week's operation, but for longer times the stress due to thermal gradients imposed by the two-zone furnace caused leakage in the outer tube. (This material was entirely satisfactory, however, for the inside tube.) McDanel "Zirco", ZM30 tubes were also tried with the same results.

In order to overcome the problem of thermal cracking, fused-silica was considered because of its exceedingly low coefficient of thermal expan-

sion. The results of other workers (1) using this material indicated that the corrosion problem may have resulted from impurities present. Water is especially troublesome. Not only is it difficult to exclude moisture from these salts, but upon melting, the corrosive hydroxyl ion is formed by the following reaction between water and chloride ions

$$H_2O + Cl^- \longrightarrow OH^- + HCL\uparrow$$

In this work, it was found that corrosion of silica was minimal if the salt was pure. In fact, the silica container survived for more than thirty days at a time at temperatures up to 1300° C and when examined showed only minimal devitrification on the surface which contacted the melt. At first, the purification method recommended by Laitimen, Ferguson, and Osteryoung (16) was tried, but the method proposed by Maricle and Hume (17) of bubbling chlorine through the fused salt was also found to be satisfactory and was much easier. Even though Maricle and Hume did not predict good results with salts other than the low melting lithium chloride-potassium chloride eutectic, it was found in the case of each salt studied here that tube attack was negligible when chlorine was passed through the melt for 12 hours at a temperature just slightly above the melting point.

V. OPERATING PROCEDURE

The following discussion explains the experimental procedure used in these investigations. It was essentially the same for each of the four melts studied.

A. Melt Preparation

The required amount (an amount equivalent to about 23 cu. in. of fused salt) of reagent grade metal chloride was placed in the outer cell tube and vacuum dried for several days to remove as much excess moisture as possible. It was heated gradually to the melting point under vacuum over the period of a day and was then melted, also under vacuum. Chlorine was immediately admitted to the cell and bubbled through the molten salt for 12 hours. Next, the inside tube, electrodes, thermocouples, and vent tubes were secured. Connections with the external vent system were fastened and the difference in height between the melt in the inside of the small tube and that in the annulus was adjusted by the CCl_4 level in the external bubbler (See section A-4 of the Appendix). This completed the cell preparation.

B. Observation Method

To determine a single data point, the low temperature control unit was set so as to maintain this zone of the furnace at a temperature just above the melting point of the salt, and the temperature of the other furnace zone was increased by steps of about 20°C. When the cell voltage became steady following each temperature change, the thermocouple e.m.f.'s and the e.m.f. registered between the electrodes were recorded. Thermocouple e.m.f.'s were read with a Rubicon catalogue no. 2731 potentiometer to a precision of 1°C. The open-circuit cell voltage was read with a Sergeant Model MR recorder to a precision of 0.1 millivolts. The recorder was standardized periodically and checked with the potentiometer. Open circuit cell voltages were plotted ver

the measured ΔT's yielding a curve such as that shown in Figure 6. The maximum ΔT obtainable by this cell was about 150 to 200°C because of conduction of heat from the hot to the cold zone through the melt. In other words, with a ΔT of this magnitude, all of the power supplied to the furnace came through the high temperature control unit, and any further increase in this control temperature served only to raise both the hot and the cold electrode temperatures without increasing ΔT appreciably. Therefore, after the first string of runs were made to a ΔT of 150 to 200°C, the cold electrode temperature was raised about 100°C, the hot electrode dropped to the same temperature, and another string of runs made by heating the hot electrode in 20°C steps until ΔT was again 150 to 200°C. By this method, a number of curves similar to figure 6 were obtained, each corresponding to a different cold junction temperature, but "overlapping" by about 50°C.

C. Reduced Pressure Runs

When measurements over the complete temperature range from just above the melting point to about 1300°C were made at atmospheric pressure, the procedure was repeated at various degrees of vacuum. Reduced pressure was affected by expelling the chlorine from the gas exit system through a water aspirator. Excellent pressure control was obtained by throttling the electrode feed streams and the gas to the aspirator through teflon needle valves. For vacuum data, the cell pressure was initially reduced to a -5 inches of mercury and held there for a series of runs covering the temperature range from the melting point up to nearly 1300°C. Then the pressure was reduced to a -10 inches of mercury and the procedure repeated. This was done in turn for pressures of -15, -20, -25, and in two sytems, -27 inches of mercury. Pressures were determined to within $\pm$ 0.1 inch of mercury by a vacuum gage placed in the vent line from the cold electrode. The gage was calibrated with a mercury monometer. Vacuum readings were converted to abso-

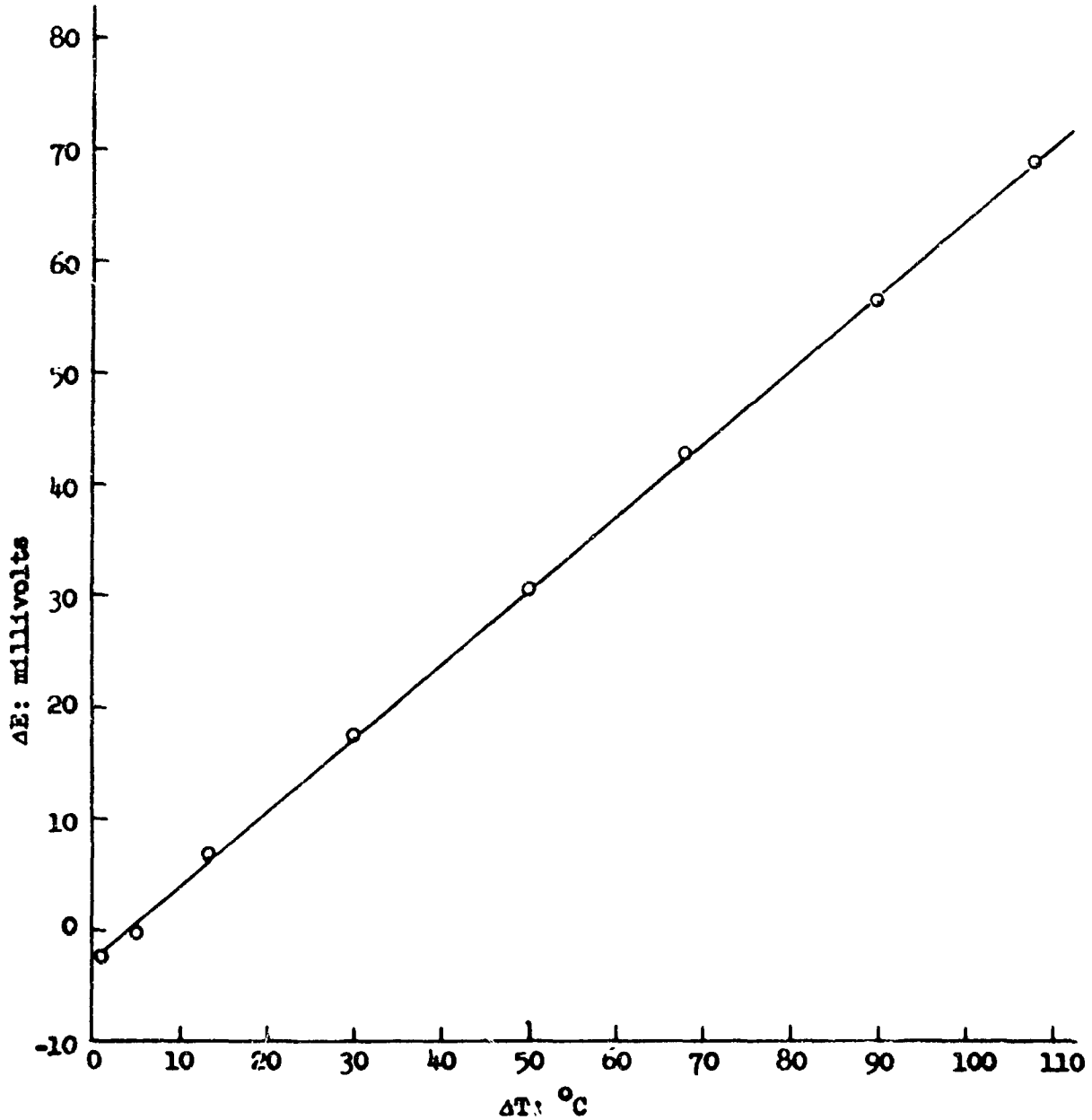

Figure 6. Plot of experimental voltage versus thermocouple temperature difference for the silver chloride-chlorine thermocell (cold electrode held at approximately 630°C).

lute pressures by subtracting the vacuum reading from the prevailing atmospheric pressure and then correcting for the small pressure difference between the hot and the cold chambers of the cell. These corrections were relatively small except at the lowest pressures. At low pressures, the maximum cell temperature was less than 1300°C owing to the softening of the quartz which occurs at high temperatures.

D. Dilution of Chlorine Feed Gas

It was considered desirable to measure the effect of diluting the chlorine feed to the electrodes with an inert gas. In this case, pure argon and chlorine were throttled through similar flow meters at variable rates. After passing through the flow meters, the two gases entered a single line, passed through a drying column, entered the separate electrode feed lines, passed through needle valves and then through flow meters to the electrodes. Flow rates in terms of moles per minute of the pure gas were calculated from equations recommended by the meter manufacturer.

E. Cell Behavior

The voltage readings were generally steady to within ± 0.1 millivolts when the gas feed rate to the electrode was held in the range of 2 x 10^{-4} gram moles/ min (a flowmeter reading of about 3 at atmospheric pressure). Higher flow rates tended to cause too much convective mixing at the electrodes which produced e.m.f. fluctuations corresponding to the temperature fluctuations of these disturbances. Otherwise, large changes in flow rate did not influence cell voltage. In general, the cell behavior was excellent. Disturbances in cell voltage were usually traceable to temperature fluctuations caused by high electrode-gas flow rates or by vent line restrictions resulting from condensed salt "dust" carried out of the cell by the gas. When these flaws were corrected, the system became stable and voltage fluctuations disappeared.

VI. RESULTS

A. Discussion of Raw Data

The first step in treating the experimental results was to formulate them in a series of graphs similar to figure 7 which shows raw data for the silver chloride-chlorine cell at one atmosphere pressure. Here, the measured voltage in millivolts is plotted versus the temperature difference between electrodes indicated by the thermocouples. Each curve represents an experimental run during which the cold electrode was held steady at a given temperature level whole the temperature of the hot electrode was increased stepwise. For each cell system, this process was repeated at one atmosphere pressure until adequate data were obtained covering the temperature span from just above the salt melting point to 1300°C. Then, the cell pressure was reduced and the entire temperature span explored again. This was repeated for a number of pressures from one atmosphere to less than a tenth of an atmosphere. The procedure was the same for each of the separate cells investigated except for the one containing lithium chloride which was studied at one atmosphere pressure only.

Measurements of cell voltage were occasionally repeated under identical conditions to see if there was any drift of e.m.f. with time. Data taken on occasions differing by several weeks were in excellent agreement. Electrodes were also changed from time to time with no noticeable effect on the results. The voltage versus ΔT curves were also found to be the same whether the hot electrode temperature was increased or decreased so long as the total pressure and the cold electrode temperature remained unchanged.

As shown in figure 7, each curve does not go through the origin as expected but shows a residual voltage at zero ΔT. Sundheim and Rosenstreich(28) observed similar behavior in their cell. Several possible reasons for this discrepancy exist, and they are discussed in detail in

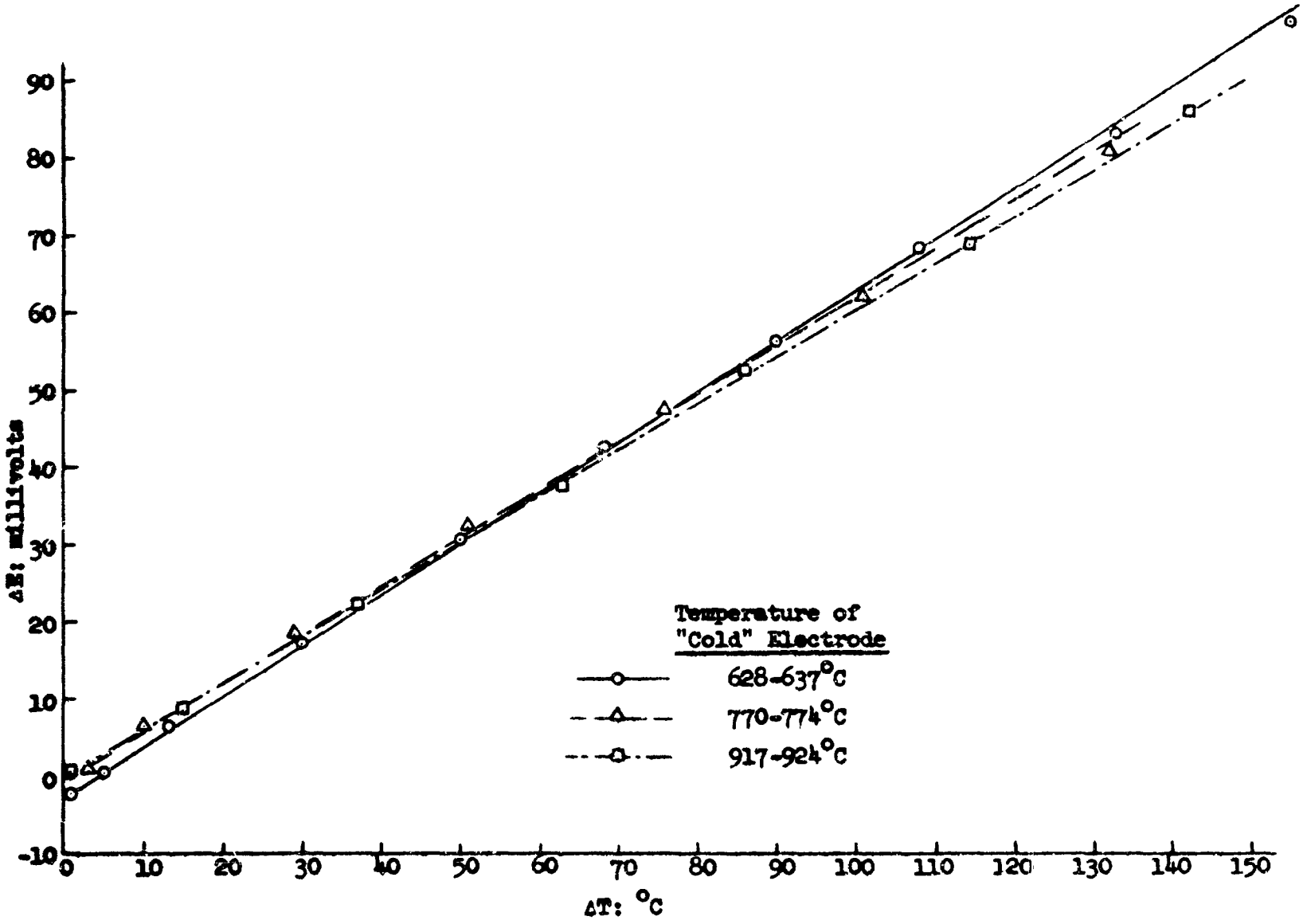

Figure 7. Plot of experimental voltage versus thermocouple temperature difference for the silver chloride-chlorine thermocell at several base temperatures.

the Appendix, section IX-E, which deals with experimental errors. On the basis of strong evidence supplied there, it is concluded that the residual did not vary with ΔT. Thus, it can be subtracted from each data point thereby forcing the curves on the raw data plots to pass through the origin. With this correction, these curves can then be superimposed by the method explained in subsection B below.

B. Formulation of the Final Voltage Versus Temperature Graphs

It can be seen from equation (28) that E for a given cell system is a single-valued function of temperature and pressure once a reference temperature has been selected. Therefore, it was thought desirable to formulate a chart for each cell system showing voltage as a function of these variables over the entire regions of temperature and pressure explored. However, since the largest ΔT obtainable in the experimental cell was less than 200°C, it was necessary to combine the results from many runs in order to obtain such a chart.

To illustrate, let us consider the silver chloride-chlorine thermocell. The reference temperature chosen for this system was 500°C. The raw data points for the run in which the cold electrode was at this temperature were first corrected for the residual voltage. They are represented by the circles in figure 8. (Cell pressure was one atmosphere.) Next, the voltages observed with a cold electrode at 654°C and a cell pressure of one atmosphere were corrected for the residual. These were then added to the e.m.f. observed during the previous run which corresponded to a hot electrode temperature of 654°C. For example, the voltage of the cell was 95.9 mv when the hot electrode was at 800°C and the cold electrode was at 654°C. The voltage of a hypothetical cell having a hot electrode at 800°C and a reference electrode at 500°C is therefore equal to the sum of 95.9 mv and 103.0 mv (which corresponds to 654°C) or 198.9 mv. This step was repeated for every point in each set of raw data to give

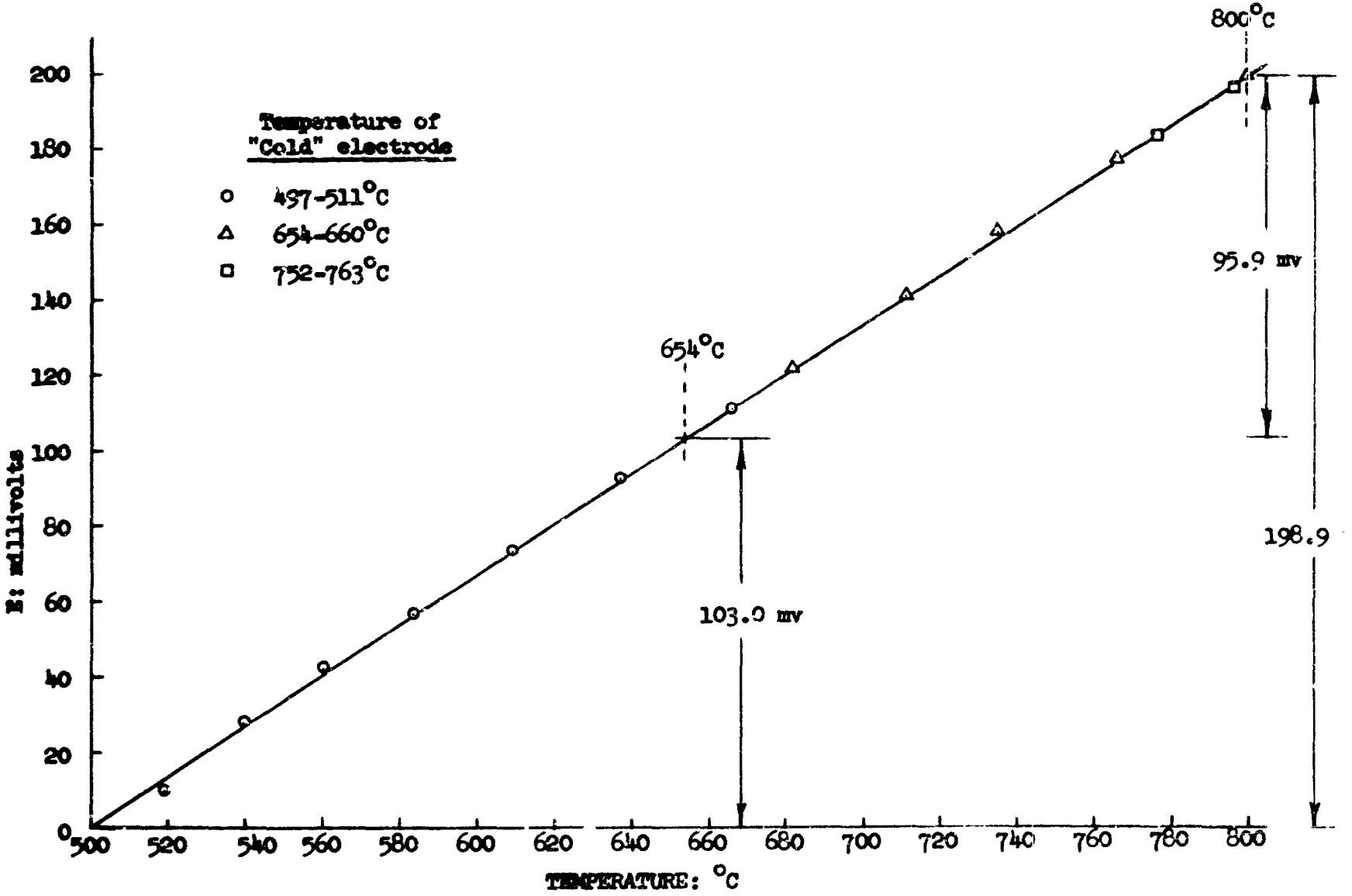

Figure 8. Illustration of method used to synthesize E versus temperature curves from ΔE versus ΔT data.

the total voltage versus temperature curve shown in figure 9. The entire cycle was repeated for each cell pressure, and these results are also shown in figure 9. Similar curves describing the voltages of thermocells containing other melts are given as figures 10 (potassium chloride), 11 (sodium chloride) and 12 (lithium chloride). These figures include reduced pressure data for all systems except the lithium chloride-chlorine cell which was studied at one atmosphere only.

The method of superimposing curves discussed above can be justified by looking at equation (31). If we write for the voltage between electrodes at T_1 and T_2,

$$E_{1-2} = \frac{1}{\mu \mathcal{F}} \left[\int_{T_1}^{T_2} \Delta S^\circ dT + RT_1 \ln K_{T_1} - RT_2 \ln K_{T_2} \right] \qquad (62)$$

and for E_{2-3} between T_2 and T_3,

$$E_{2-3} = \frac{1}{\mu \mathcal{F}} \left[\int_{T_2}^{T_3} \Delta S^\circ dT + RT_2 \ln K_{T_2} - RT_3 \ln K_{T_3} \right] \qquad (63)$$

then E_{1-3}, the voltage for a reference electrode at T_1 and a hot electrode at T_3, is clearly the sum

$$E_{1-3} = E_{1-2} + E_{2-3} \qquad (64)$$

It is admitted that the method of curve summation discussed in this section may lead to an accumulation of small errors, but this disadvantage is far outweighed by the convenience of a total voltage versus temperature diagram.

C. Calculation of the Reaction Entropy

In order to evaluated the transported entropies in the systems studied, it was necessary to isolate the first term of equation (28), $\frac{1}{\mathcal{F}} \int_{T_1}^{T_3} \Delta S^\circ dT$. This was done by calculating the last two terms of the equation and subtracting them from the experimental voltage E. The resultant value, the integrated reaction entropy, is shown as a dotted line in figures 9

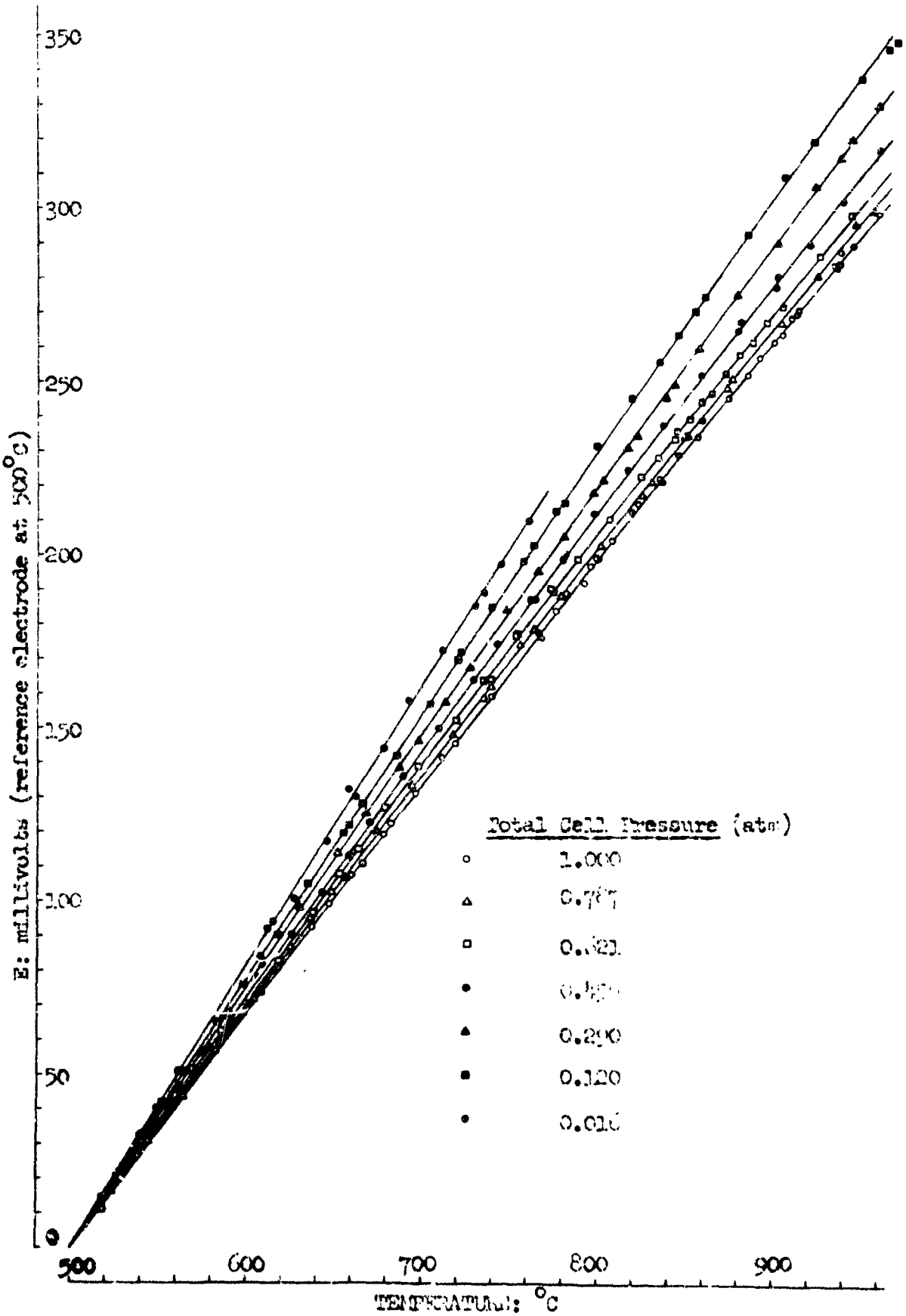

Figure 9. Measured voltage versus temperature for the silver chloride-chlorine

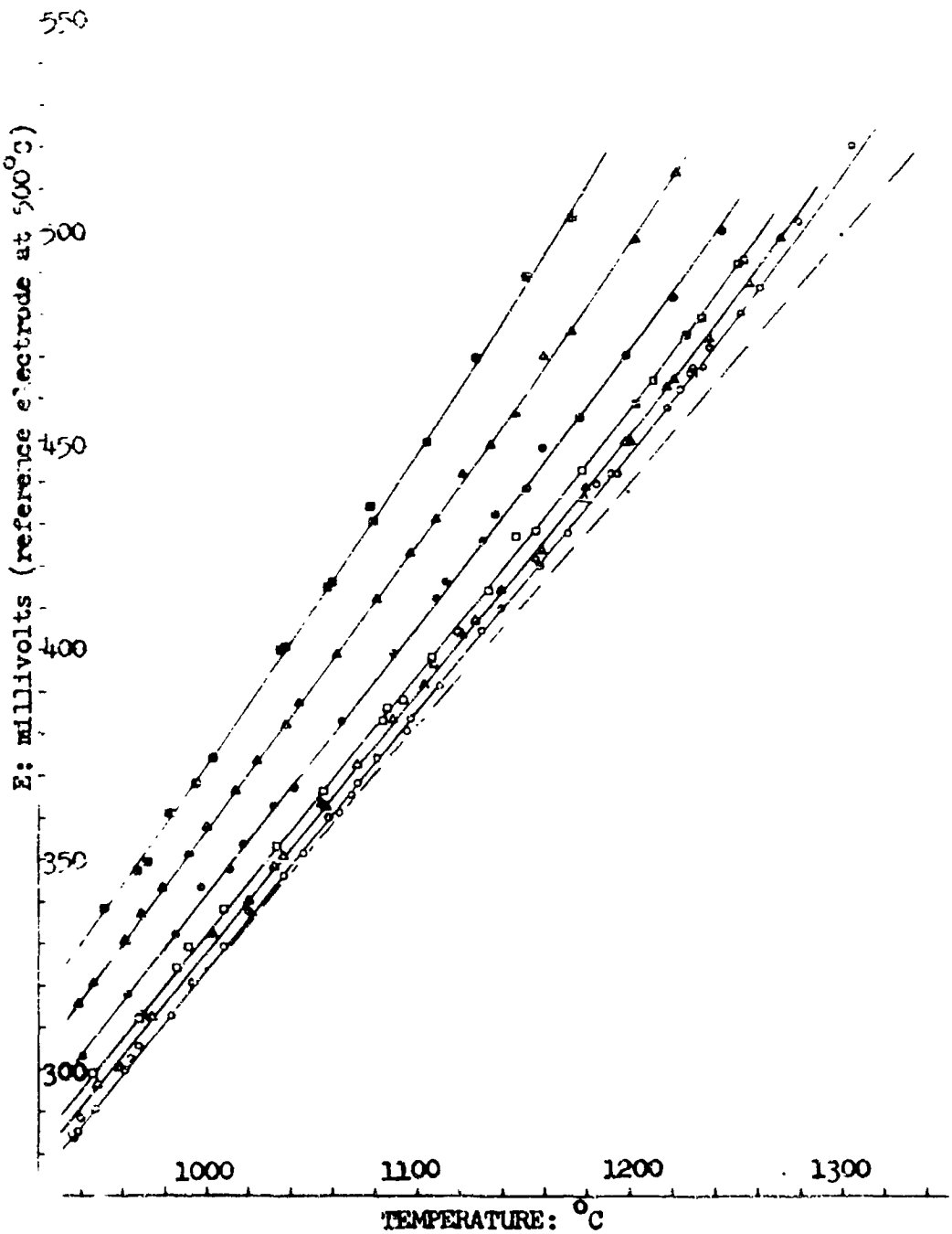
550
500
450
400
350
300
E: millivolts (reference electrode at 500°C)
1000
1100
1200
1300
TEMPERATURE: °C

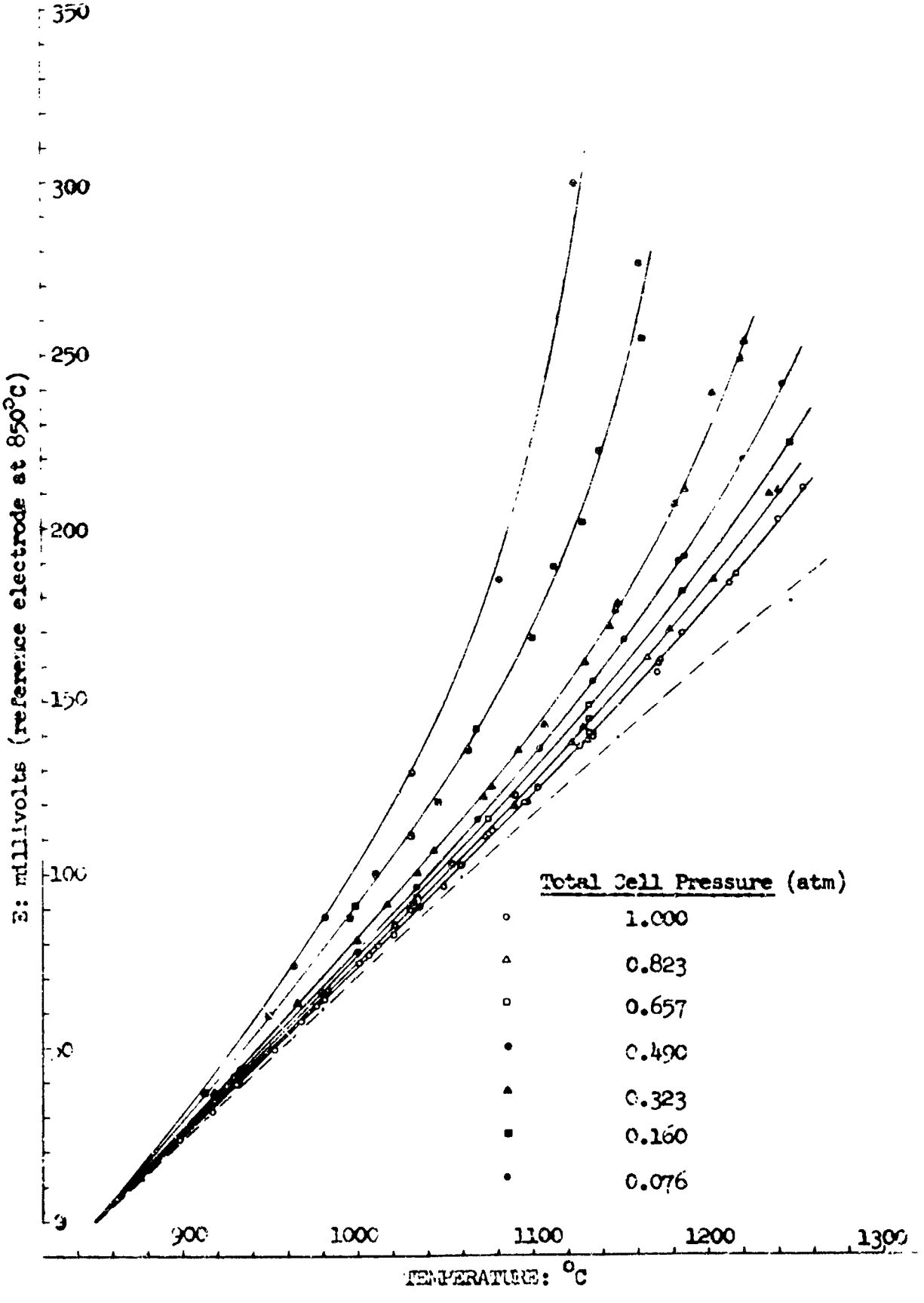
E: millivolts (reference electrode at 850°C)
350
300
250
200
150
100
50
0
900
1000
1100
1200
1300
TEMPERATURE: °C
Total Cell Pressure (atm)
1.000
0.823
0.657
0.490
0.323
0.160
0.076

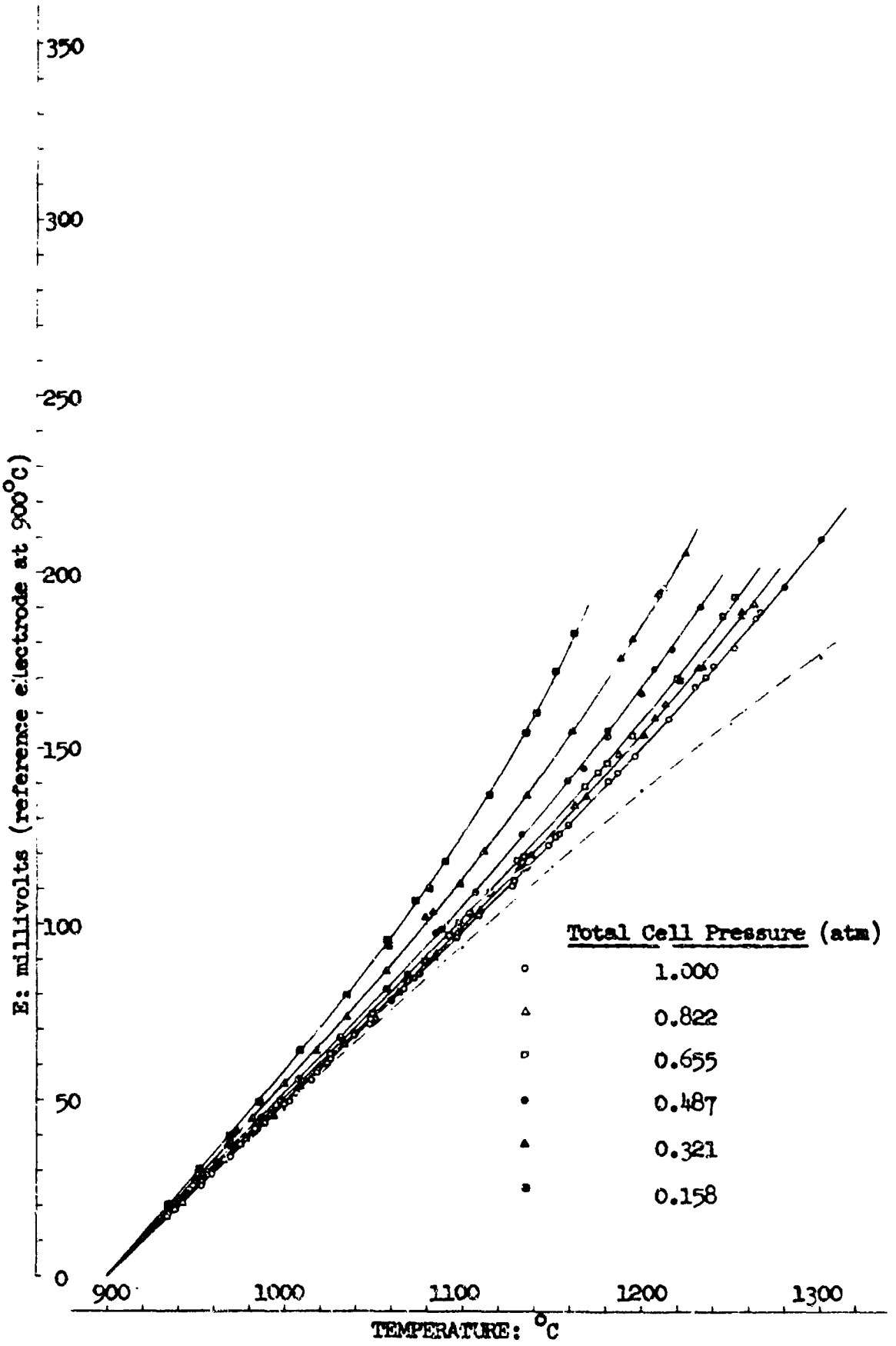

versus temperature for the sodium

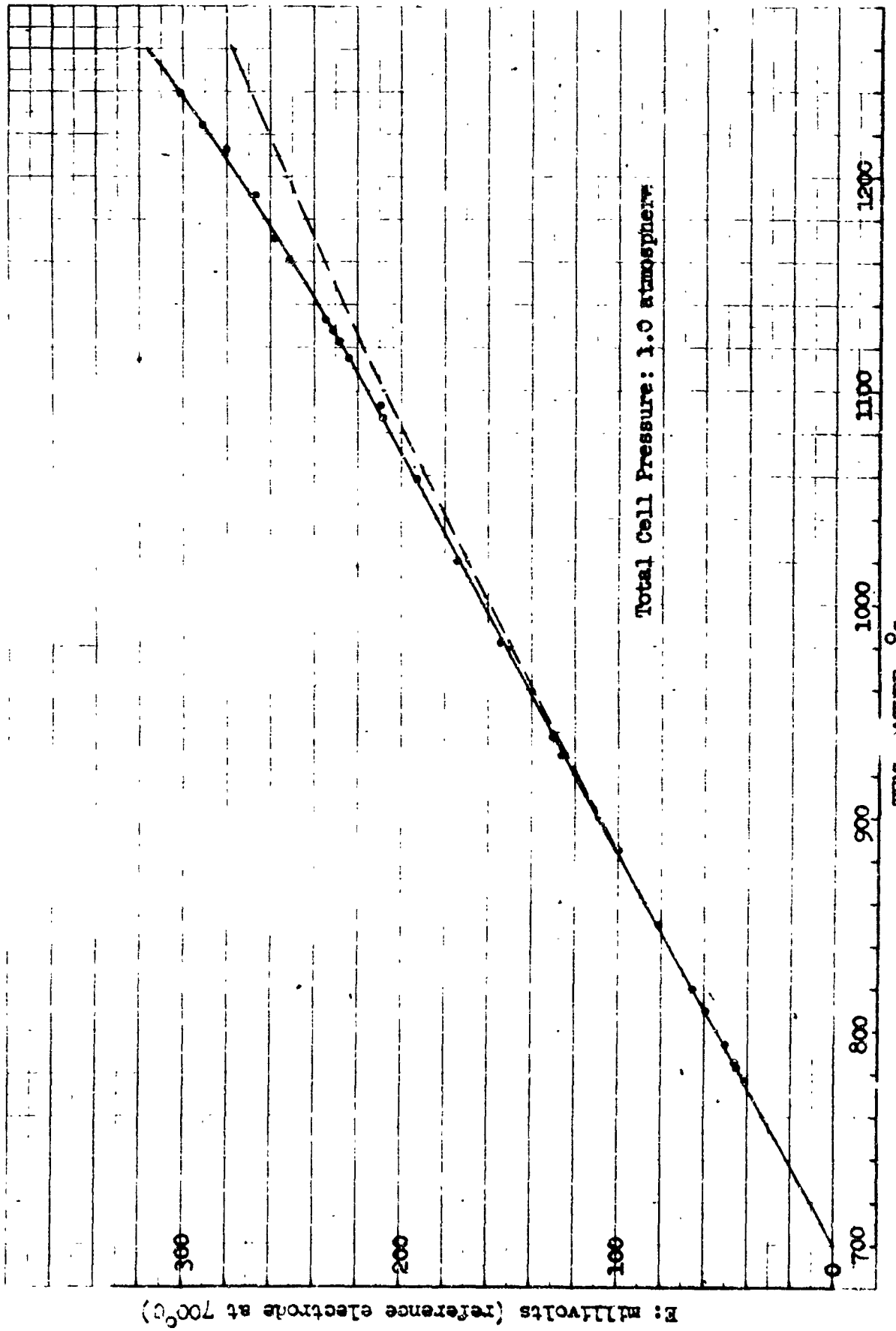

Figure 12. Measured voltage versus temperature for the lithium chloride-chlorine thermocell.

through 12. The detailed calculation is discussed in the Appendix, section IX-B.

D. Dilution of Electrode Feed Gas

A few runs were made with feed gas mixtures of chlorine and argon. These data were all taken with the silver chloride melt at a temperature level where chlorine dissociation and melt vapor pressure are unimportant. The results are summarized in Table III below.

Table III

Summary of Data Obtained with Mixed Chlorine-Argon Feed Gas and Molten Silver Chloride Electrolyte

Average Temperature: 700°C

Total Cell Pressure: 1 atm.

Flow Rates (millimoles/min)		Partial Pressure of Chlorine	Seebeck Coefficient (mv/°C)	
Chlorine	Argon	(atmospheres)	Experimental	Calculated
0.145	0.104	0.582	0.682	0.688
0.087	0.168	0.341	0.708	0.711
0.060	0.155	0.278	0.730	0.720
0.002	0.191	0.010	0.795	0.885

The calculated Seebeck coefficients in the table were determined from the differential of equation (28) which is

$$\left(\frac{dE}{dT}\right)_p = \frac{1}{\mathcal{F}}\left(\Delta S^\circ - \frac{R}{2} \ln p_{Cl_2}\right) \qquad (65)$$

where ΔS° was determined from the slope of the voltage versus temperature curve for the thermocell at 700°C using pure chlorine at one atmosphere pressure.

The Seebeck coefficients measured while using a diluted chlorine feed are in good agreement with those calculated from equation (65) except for the data at high dilution which were taken with the chlorine flow meter operating in a questionable calibration range. As expected, they show

that addition of a diluent has the same effect as a reduction in the chlorine partial pressure brought about by another method, namely that of lowering total pressure.

E. Operation Under Load

In designing a thermocell for energy conversion, it is necessary to know the voltage not only at open circuit but also with current passing through the cell. Even though it was not intended to make a detailed study of these voltage-current characteristics, some preliminary data were taken. They are shown in figure 13, where voltage is plotted versus current for several cell pressures and at constant electrode temperatures. The data were obtained using the potassium chloride-chlorine thermocell at an average temperature of 975°C. The results were normalized by the addition or subtraction of a correction term to each data point in order to give the same open-circuit voltage for each pressure condition (this involved only a small correction since all of the open-circuit voltages differed by only a few millivolts from that shown).

The initial slope of the voltage versus current line of figure 13 is presumably due to the electrical resistance of the melt (the slope corresponds to a resistance of 1.3 ohms which is logical for the geometry of the system). At higher currents, a change in the slope of the line is evident, indicating a slowly increasing overpotential. Since this overvoltage is independent of chlorine partial pressure for all but one run, it appears to be an activation over-potential. At a chlorine pressure of 0.33 atmospheres, the electrode suddenly becomes concentration controlled indicating that polarization is due to a diffusion process. In all cases except at the lowest chlorine pressure, the extent of polarization is small compared to the ohmic losses. Based on the findings of Murgulescu, et. al.(19), who report no polarization at all for the chlorine discharge reaction in the same system at current densities of up to 2 amps/sq. cm., it appears

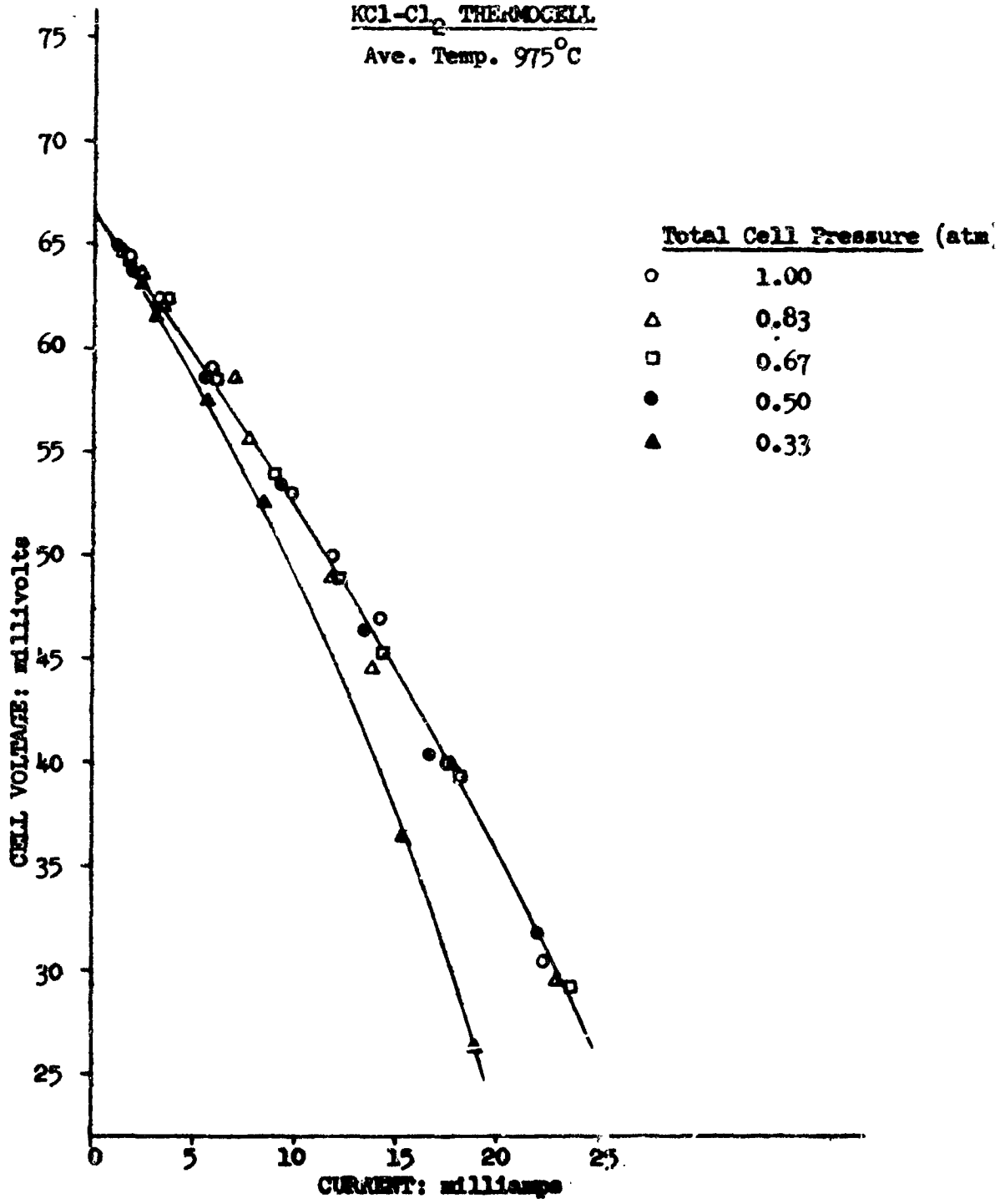

Figure 13. Voltage-current characteristics for the potassium chloride-chlorine thermocell at various pressures. The gas supplied to the cell was undiluted chlorine.

that the polarization observed here occurs entirely at the low temperature (reduction) electrode.

Since this part of the thesis investigation was exploratory, any further evaluation of electrode mechanisms is considered beyond the limits of this study.

VII. DISCUSSION OF RESULTS

A. Comparison of Equation (28) with Experimental Data

It is not possible to predict the voltage of a proposed thermocell from equation (28) alone owing to the unknown magnitude of its first term $\int_{T_1}^{T_3} \Delta S^\circ \, dT$. As cited previously, ΔS° is defined by the following equation

$$\Delta S^\circ = 1/2\, S^\circ_{Cl_2} + \bar{S}_{e,g} - \bar{S}_{Cl^-}$$

The term $S^\circ_{Cl_2}$ is, of course, the entropy of diatomic chlorine at the one atmosphere reference state. Its magnitude is tabulated in the literature for the temperatures of interest(8). Transported entropies of the electron are also available from literature data (see the Appendix, section C). On the other hand, there is no accepted method for calculating $\bar{S}_{Cl^-}$, but this term can only be found from experimental thermocell measurements themselves.

Even though the magnitude of the entropy term is unknown, equation (28) can be used to calculate the effects of total pressure, vapor pressure, and dissociation on cell voltage. For example, it is possible with the aid of available physical and thermodynamic data to calculate the last two quantities in equation (28), and by subtracting these quantities from the experimentally measured cell voltage, the entropy term can be determined. Then, since $\int_{T_1}^{T_3} \Delta S^\circ \, dT$ is presumably uninfluenced by pressure (except when complex ions are present--see subsection F), the same value of the integrated entropy can be used again and again to calculate voltages which correspond to other cell pressures. That the voltages calculated by this technique agree with those measured is shown in figures 14 through 16 where the points, taken directly from figures 9 through 11, represent experimental data and the solid curves represent the calculated values. A detailed discussion of the calculation is given in the Appendix, section

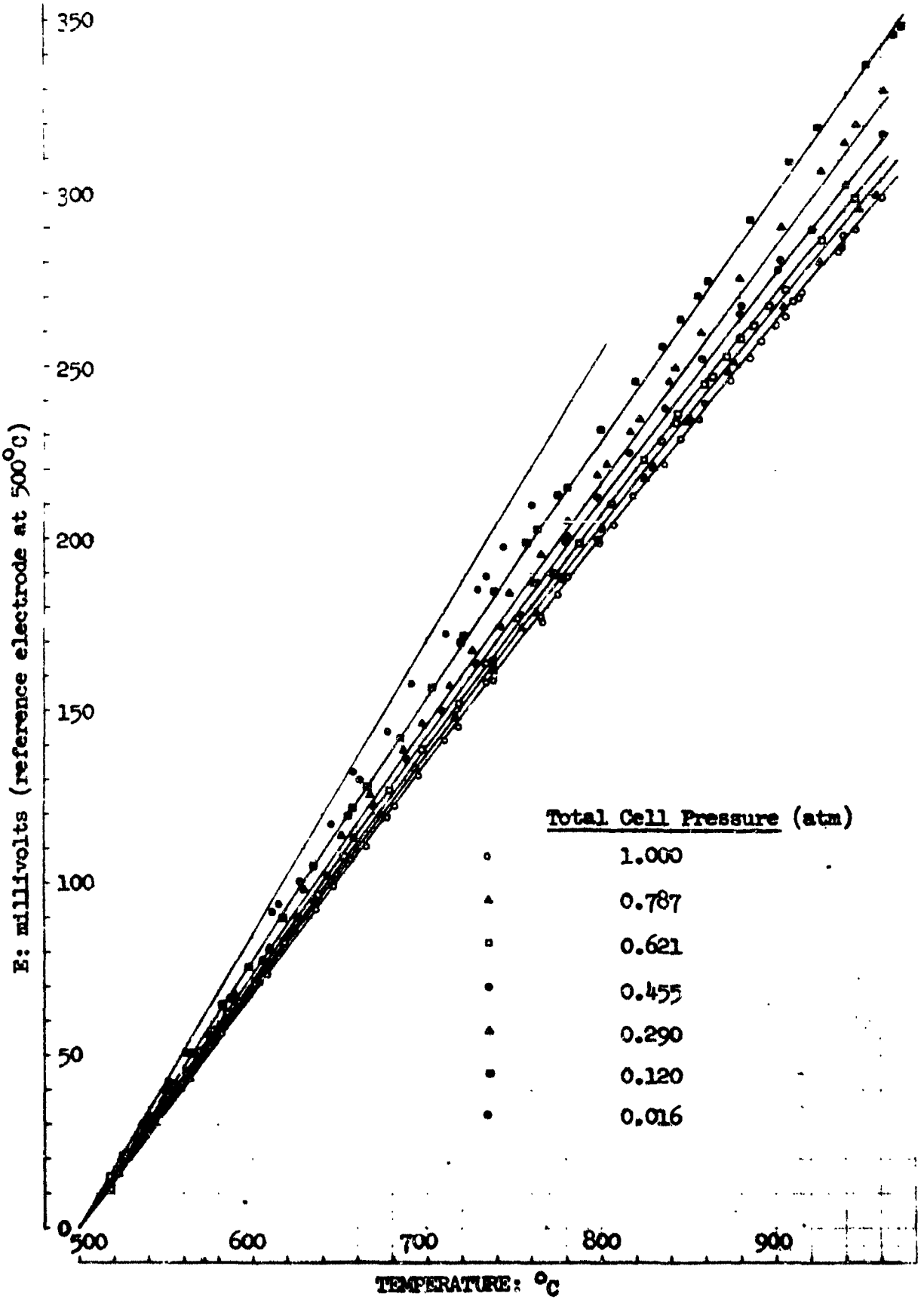

silver chloride-chlorine

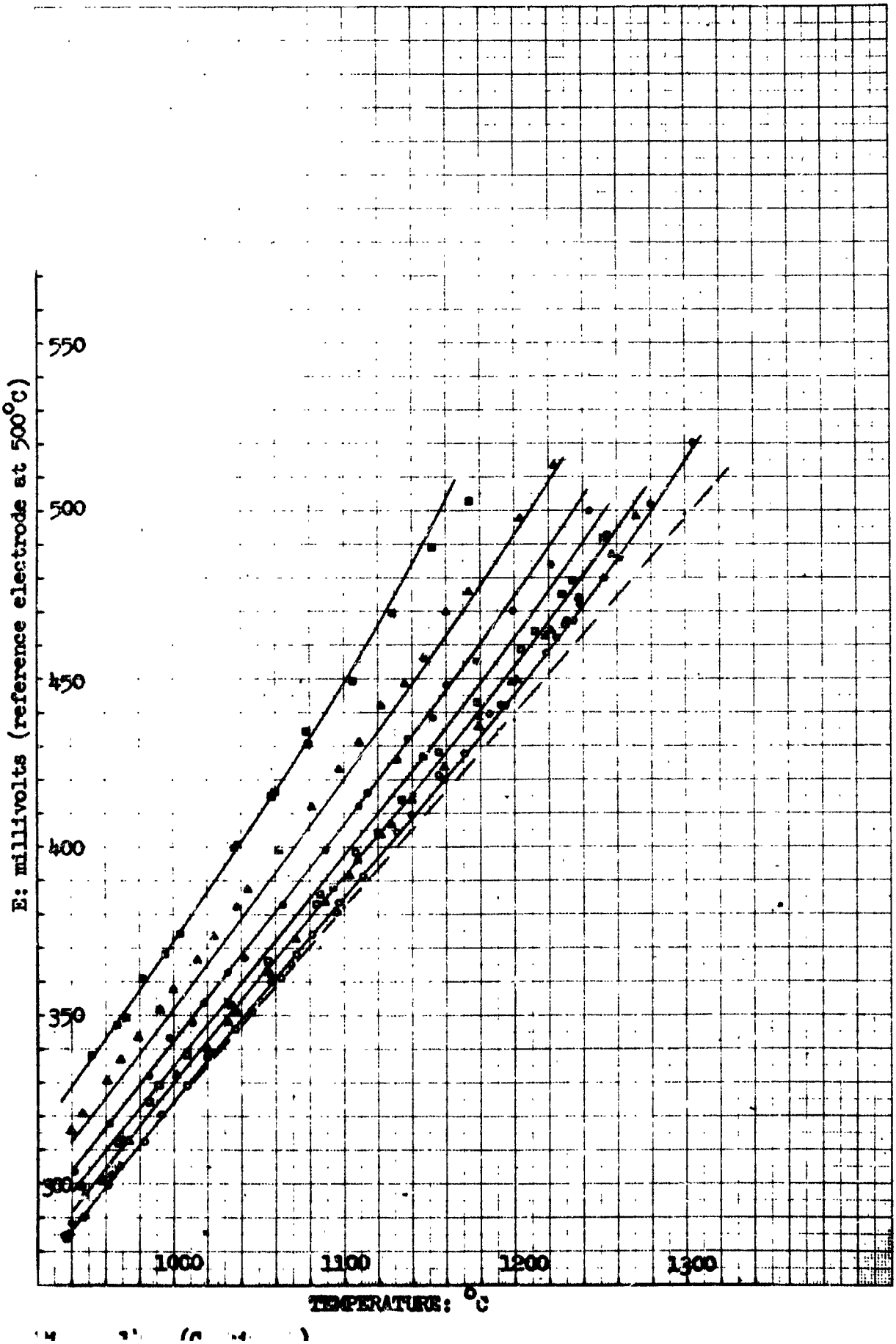
E: millivolts (reference electrode at 500°C)
550
500
450
400
350
300
1000
1100
1200
1300
TEMPERATURE: °C

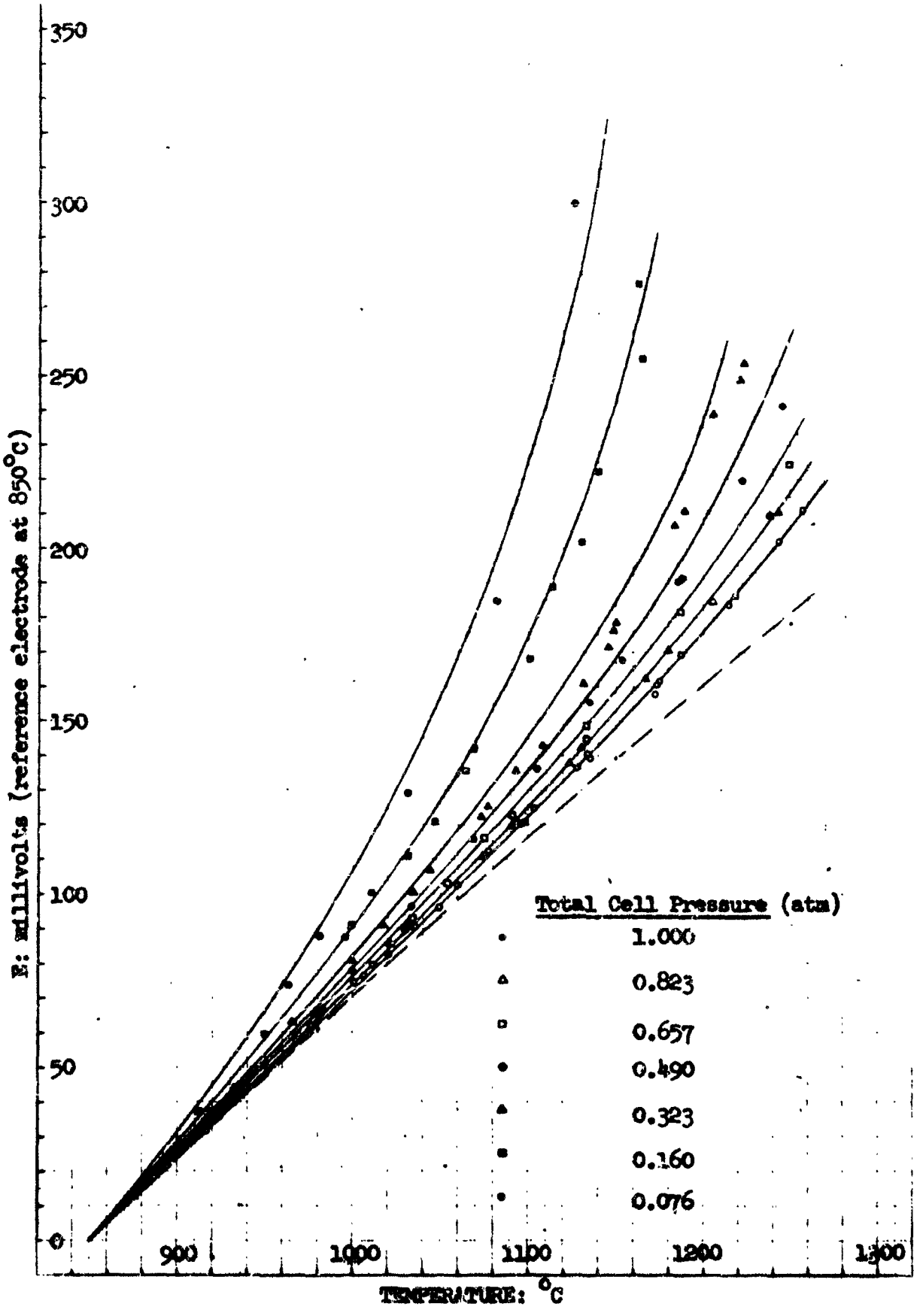

Figure 15. Voltage versus temperature for the potassium chloride-chlorine

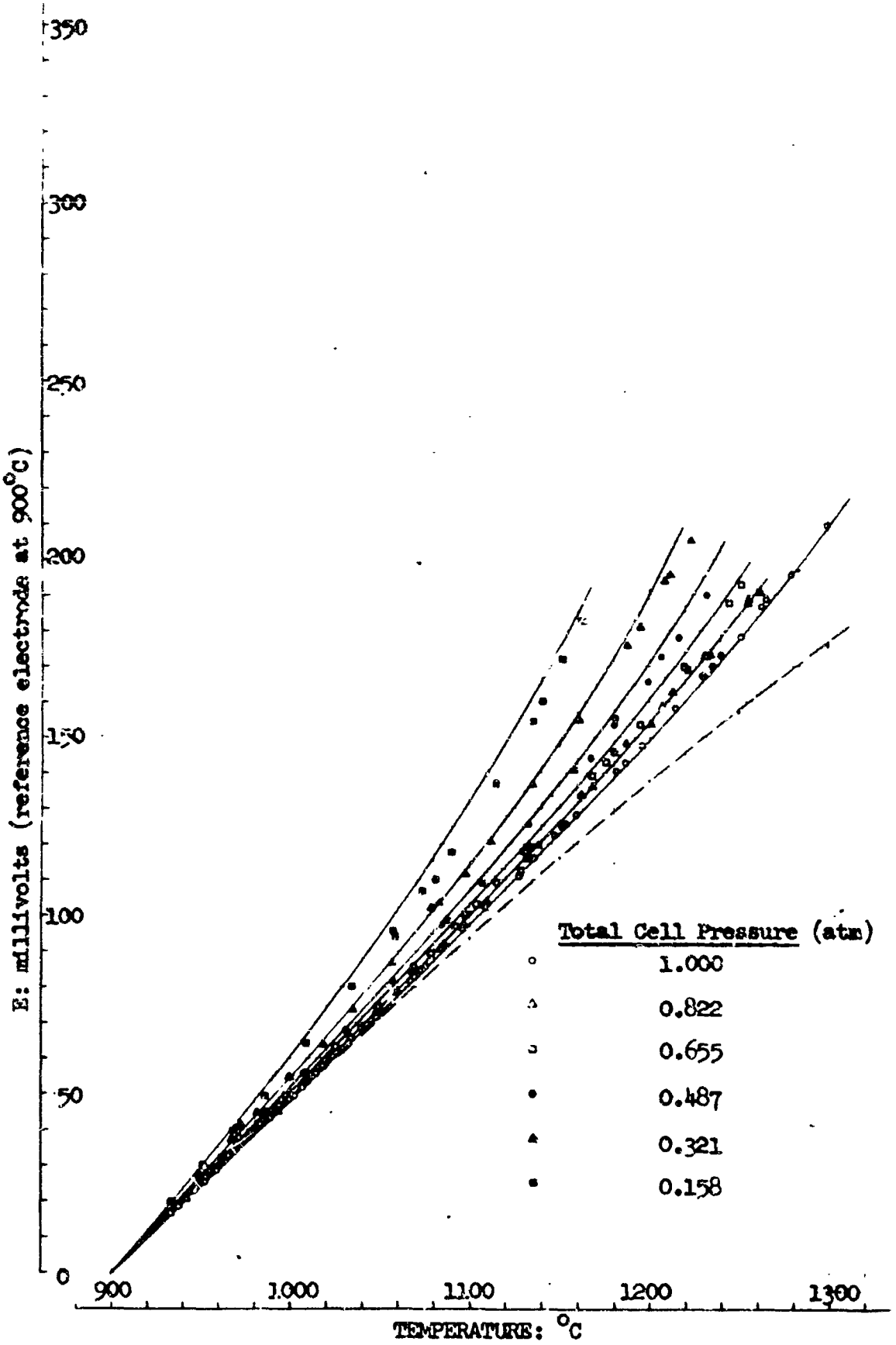

Figure 16. Voltage versus temperature for the sodium chloride-chlorine

First, the last two terms of equation (28) were evaluated at a selected cell pressure and at each of several hot electrode temperatures from vapor pressure and dissociation data available in the literature(1,4,8,27). Second, these calculated quantities were subtracted from the corresponding experimental voltages, yielding $\int_{T_1}^{T_3} \Delta S^\circ \, dT$ at several different temperatures (shown by the dotted lines in the figures). Then, voltages at different cell pressures and temperatures were calculated directly from equation (28) using the known value of $\int_{T_1}^{T_3} \Delta S^\circ \, dT$. As mentioned above, these calculated results are compared with experimental data in figures 14 through 16 (there was no such comparison for the lithium chloride-chlorine system since data were available at only one pressure in this case). Inspection shows that the theoretical curves are in excellent agreement with the experimental points. In fact, any deviations of the points from the curves are thought to be within experimental error. (Note that discrepancies at very low cell pressures can be attributed to slight uncertainties in the pressure measurements. Drifting of the points from the curves at high temperatures is probably due to small errors accumulating during the synthesis of the experimental curves from raw data.)

B. Consideration of Ionic Entropies in Molten Salts

As discussed earlier, the transported entropy $\bar{S}_{Cl^-}$ is the sum of two terms, the partial molal entropy $\bar{S}_{Cl^-}$ and the entropy of transfer $S^*_{Cl^-}$. Neither of these quantities can be calculated with confidence. Recently, Pitzer(24) proposed a quasi-theoretical equation from which $\bar{S}$ in simple 1-1 molten salts can presumably be calculated. So far, however, no experimental technique has been found for obtaining $\bar{S}$ as an isolated quantity. Hence, Pitzer's equation cannot be confirmed by experiment.

Even though ΔS°, due to the uncertainty in $\bar{S}_{Cl^-}$, cannot be calculated directly, it is interesting to compare an estimated ΔS° with

that measured experimentally. For this purpose, table IV was prepared. In the table, ΔS° which was taken from the slopes of the dotted curves in figures 9 through 12 is compared with $\Delta S'$, the calculated entropy change. The procedure for determining $\Delta S'$ (described in detail in the Appendix, section C) was as follows:

The partial molal entropy of the ion was calculated from Pitzer's equation (see equation (35), section III) using the data of Kelly(15) for the entropy of the pure molten salt. The entropy of chlorine at one atmosphere pressure was taken from Evans, et. al.(8), and the transported entropy of the electron in graphite was estimated from the work of Temkin and Khoroshin as reported by Tyrrell(32). $\Delta S'$ thus determined is the entropy of chlorine gas plus that of the electron minus the partial molal entropy of the chloride ion and does not include the entropy of transfer of the chloride ion $S^{*}_{Cl^-}$. Therefore, the estimated value of $S^{*}_{Cl^-}$ is equal to the difference between $\Delta S'$ and ΔS°. All of these quantities; ΔS°, $\Delta S'$ and $S^{*}_{Cl^-}$ are tabulated in table IV.

Observe that the resultant values of $S^{*}_{Cl^-}$ for the chloride ions in the alkali chlorides are almost zero while the same quantity in silver chloride is approximately -3.7 e.u. (The last figure compares with -3.4 e.u. as estimated by Senderoff and Bretz(26) by this technique and for the same system.) All of these values appear to support the hypothesis expressed in equation (61) that the absolute value of the entropy of transfer should be less than the entropy of activation*. It appears,

* Note: Activation entropies estimated from conductivity measurements by Van Artsdalen and Yaffe(34,35) are about -6 to -7 e.u. for the alkali chlorides. Senderoff and Bretz estimated a value nearer unity for silver chloride. Note, however, that activation entropies calculated from conductivity measurements are not strictly applicable since conduction in the latter measurements is by both ion species rather than just the chloride ion as is the case with the molten salt thermocell.

Table IV

Comparative Tabulation of $\Delta S'$, ΔS° and S^{*} for the Chlorine Half Cell Reaction

(For a more complete tabulation of intermediate quantities, see table VIII in section C of the Appendix.)

Electrolyte	Temperature	$\Delta S'$	ΔS°	$S^{*}_{Cl^-}$
AgCl	527°C	11.95	15.6	-3.65
"	627	11.53	15.46	-3.93
"	727	11.15	14.78	-3.63
NaCl	927°C	10.78	11.08	-0.30
"	1027	10.50	10.83	-0.33
"	1127	10.25	10.50	-0.25
"	1227	10.00	9.58	0.42
KCl	927°C	10.57	10.96	-0.39
"	1027	10.29	10.83	-0.54
"	1127	10.04	10.03	0.01
"	1227	9.80	9.70	0.10
LiCl	827	12.15	12.58	-0.43

at first, that the absolute magnitude of the entropy of transfer is small for thermocell systems where the moving ion is larger than or of approximately the same size as the "stationary" ion; the alkali chlorides for example. It might appear, in addition, that the entropy of transfer is more nearly equal to the activation entropy when the stationary ion is large; take for example the migrating chloride ion in molten silver chloride. In this latter case, it can be argued that the moving ion is in the activated state during the major part of each migration jump, similar to path abc of figure 4. Hence, there is a large entropy of transfer. But, when the stationary ion is relatively small, it can be reasoned that only a small amount of the total migration process occurs with the ion in the activated state, and the path is similar to path d in figure 4. Consequently, the heat absorbed by the migrating ion is nearly equal to its enthalpy change and the difference, which is related to the entropy of transfer is small (see equation (26)).

On the other hand, it could be argued that Pitzer's equation, equation (35), does not hold for molten silver chloride where the difference in ion sizes is extreme and where other forces not included by Pitzer may be signigicant. It is helpful in this connection to cite some past work which was done using silver electrodes in molten silver chloride(26)and copper electrodes in molten cuperous chloride(22). Using Pitzer's equation to calculate the partial molal entropies of the silver and copper ions, it is found from the data cited that the resulting entropy of transfer for silver ion is 3.4 e.u. and that for cuperous ion, 3.6 e.u. Obviously, these values are both relatively large, and further, both are for systems where the migrating ion is considerably larger than the stationary ion. Hence, these results do not agree with the supposed variance of S^* with the size of the stationary ion as discussed previously. On the other hand, if a correction of 3.4 e.u. is added to the partial molal entropy of silver ion

as calculated from Pitzer's equation, the resulting entropy of transfer of this ion is zero. Then, a consequent correction of the same magnitude but of opposite sign applied to the partial molal entropy of chloride ion in silver chloride changes the entropy of transfer of this ion from -3.7 e.u. to -0.3 e.u. This value is similar to those found for the three alkali chlorides.

C. Qualitative Discussion of the Experimental Data

A close look at figures 9 through 12 reveals two effects which have not been mentioned in the work of previous investigators. These are first, a noticeable increase in the slopes of all of the constant pressure curves at high temperatures and second, a slightly decreasing slope with temperature at the low temperature ends of the isobaric curves. The latter effect is particularly noticeable for the silver chloride-chlorine cell (voltages shown in figure 9) at low temperature conditions and also for the dotted lines in figures 9 through 12 which represent the integrated entropy term $\int_{T_1}^{T_3} \Delta S^\circ \, dT$ of equation (28).

The first effect, the increasing slope or Seebeck coefficient at high temperatures and low pressures can be attributed to the influence of high molten salt vapor pressures and chlorine dissociation which occur at these conditions. These factors were considered in the derivation of equation (28) and the quantitative agreement of the experimental results with this equation is discussed in section A. Previous investigators using gas electrodes worked at temperatures and pressures corresponding to the lower part of figure 9 where curvature due to dilution of chlorine is not apparent. (Of course, for systems involving solid electrode reactants, vapor pressure has no influence on cell voltage and no dissociation of reaction partners occurs to affect the voltage.) This explains why the phenomenon observed here at high temperatures and low pressures was not

reported previously.

The second effect, a decreasing Seebeck coefficient with temperature especially noticeable in the lower portion of figure 9 and also seen in the dotted lines of figures 9 through 12, is experimental evidence that ΔS° varies significantly with temperature.

It is well known from basic thermodynamics that the reaction entropy change at a given temperature ΔS°_T is equal to that at a reference temperature $\Delta S^\circ_{T_o}$ plus the expression

$$\int_{T_o}^{T} \frac{\Delta C_p}{T}\, dT \tag{66}$$

where ΔC_p is the change in the specific heat (products minus reactants) for the reaction defining ΔS°. For the cell of interest here, ΔC_p is

$$\Delta C_p = 1/2\ C_{p,Cl_2} + C_{p,e,g} - C_{p,Cl^-} \tag{67}$$

assuming that $(dS^*_{Cl^-}/dt)_p$ and $(dS^*_{e,g}/dT)_p$ are negligible or zero.

Since the specific heats of chlorine and the electron are available from standard references, ΔC_p can be calculated if the specific heat of chloride ion is known. The latter quantity can be estimated by combining the definition of specific heat:

$$C_{p,Cl^-} = T(d\bar{S}_{Cl^-}/dT)_p \tag{68}$$

with Pitzer's expression, equation (35), for the partial molal entropy of the chloride ion. The resulting value is given below as equation (69).

$$C_{p,Cl^-} = \frac{T(dS_{MCl}/dT)_p}{2} = 1/2\ C_{p,MCl} \tag{69}$$

Now, as an example, consider the silver chloride-chlorine system. At 1000°C, the specific heat of silver chloride is 16.0(6), that of chlorine is 9.0(23), and that of the electron in graphite is approximately 0.2*. Therefore, we obtain for ΔC_p the value of -3.3 e.u. calculated

*Note: This value was approximated from comparable values for the electron in platinum and in copper determined from equations on page 71 of Tyrrell(1

as follows:

$$\Delta C_p = \frac{9.0}{2} + 0.2 - \frac{16.0}{2} = -3.3$$

As shown above, ΔC_p is equal to $(d\Delta S^\circ/dT)_p$, and from equation (28), ΔC_p is further equal to $(d^2E/dT^2)_p$ or is the second derivative of the voltage versus temperature curve. Obviously, it is difficult to obtain the second derivative with precision from the experimental curves. Nevertheless, the approximate experimental value of -3.0 ± 0.5 e.u. obtained from the silver chloride-chlorine results at 1000°C is in agreement with the value -3.3 e.u. calculated above. Similar agreement was found for the other three molten-salt systems.

D. Comparison with the Work of Other Investigators

Prior to this work, Senderoff and Bretz(26) studied the silver chloride-chlorine thermocell at temperatures ranging from 475 to 900°C. Their work was the first reported for molten-salt thermocells using the chlorine electrode, and this author derived many helpful ideas therefrom.

In their published results, they plotted E versus ΔT at various base temperatures and noted no significant change in the slope with temperature. Since their data points were not given except in a small graph, it is difficult to check the results closely. However, it appears that the limits of precision in their cell may have prevented them from observing the trend of ΔS° with temperature discussed above. At any rate, they were able to draw a straight line through their points with a slope of 0.664 ± 0.020 mv/°C. In comparison, the Seebeck coefficient at one atmosphere pressure measured in this study was found to vary with temperature (see figure 9) from 0.685 mv/°C at 500°C to 0.625 mv/°C at 900°C yielding an average value of 0.655 mv/°C in good agreement with the result of Senderoff and Bretz. Of course, at the maximum temperature of 900°C

achieved in their work, dilution of chlorine by salt vapor and dissociated gas was not sufficient to affect cell voltage. Such effects were not observed in our study of the same system until a temperature of 1000°C had been reached.

During the past year, Detig and Archer(5) reported Seebeck coefficients for two of the thermocells studied here; sodium chloride-chlorine and potassium chloride-chlorine. They measured E for a constant ΔT of about 25°C at various temperature levels. Their measured Seebeck coefficients (0.45 mv/°C for the sodium chloride-chlorine cell and 0.40 mv/°C for the potassium chloride-chlorine cell) agree somewhat with the values of about 0.475 for both cells as found here. However, they estimate a random error of up to 8 per cent, and if there were any residual voltages in their cell, a consistent error is introduced which cannot be detected from their data. They mention the variation of voltage with the dilution of chlorine in their cell but are unable to explain the phenomenon. They also use a questionable equation for the Seebeck coefficient which is based on transference numbers. On the basis of these facts, the validity of their results is questioned.

So far as the author knows, no other work has been done for the specific systems studied here.

E. The Molten-Salt Thermocell for Energy Conversion

1. Applications

There a number of factors influencing the possible application of fused-salt thermocells to thermoelectric energy conversion. Not only must the theoretical efficiency be reasonably high, but radiative and convective heat transfer must be avoided. To prevent the latter, the cell should not be subject to vibration or other disturbances. These considerations, plus the additional complications of auxiliary equipment necessary for control of internal gas pressure suggest that any practical use of

thermocells is limited to large power installation. On the other hand, these cells have the positive advantage of functioning with no moving parts which permits operation at higher temperatures than would be possible otherwise.

A possible thermocell design for energy conversion is shown in figure 17 where only a single unit is shown. To minimize radiation from the hot to the cold end of the cell and also, to minimize convection, the electrolyte is contained in a matrix such as a porous insoluble refractory. Alternatively, the electrolyte could be mixed with a refractory powder to make a paste. To reduce radial heat losses, it would be necessary to place a number of the cell units together in a bank as illustrated in figure 18. (The configuration and number of cells shown is arbitrary and is given only for purposes of illustration.) Additional electrical energy could be extracted by conventional low-temperature converters from the heat given off at the exterior of the bank.

The actual efficiency of a molten-salt thermocell of this design in such a power generating bank would closely approach that derived for a cell having no internal convection or radiation and no extraneous heat losses.

2. Ideal Cell Efficiency

The calculation of an ideal efficiency for the type of thermocell investigated here is complicated by two factors. First, the assumption of a constant Seebeck coefficient used in the derivation of the efficiency expression, equation (3), is not valid. Second, at high temperatures, salt vaporization absorbs large quantities of heat which is subsequently transferred irreversibly to the cold junction. These complications make the task of deriving a simple exact equation for the efficiency of such a cell formidable. However, it is possible to introduce some reasonable

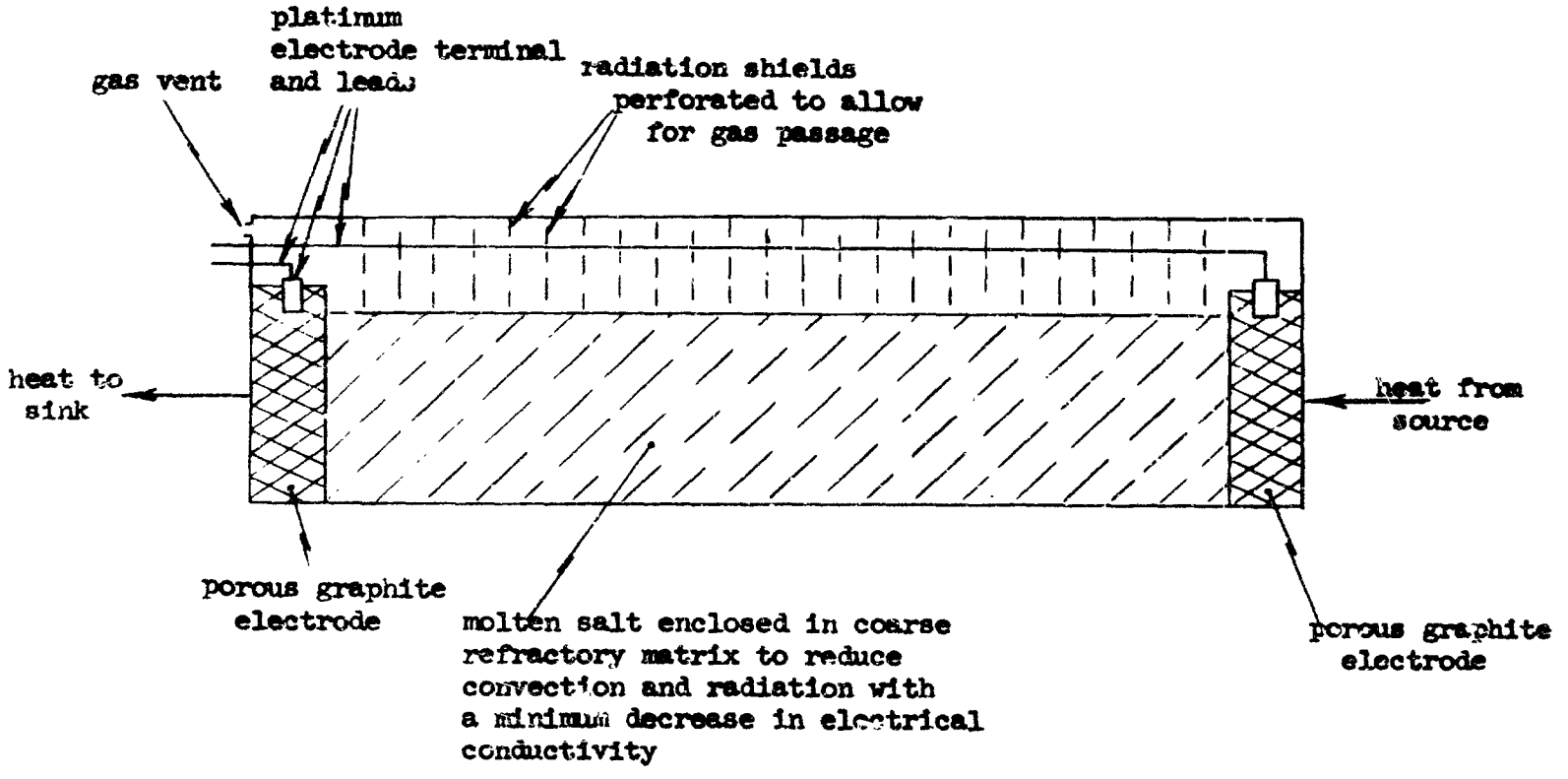

Figure 17. Example of possible thermocell design.

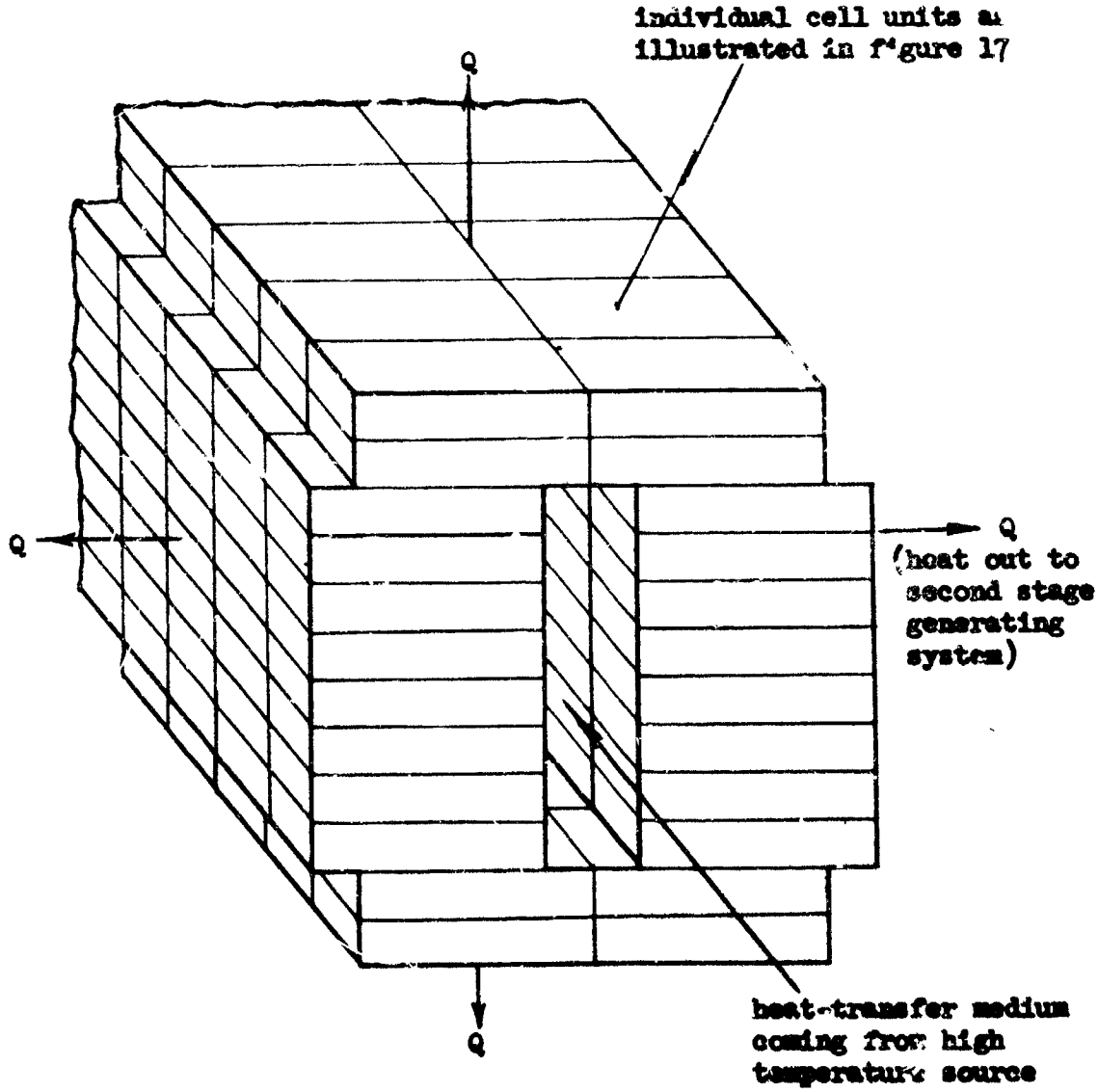

Figure 18. Sample cell arrangement for the first stage of an energy conversion system.

simplifications, permitting overall cell efficiency to be estimated.

In the first place, the thermoelectric effect in the solid conductor connecting the electrodes is negligible in comparison to that of the electrolyte. Likewise, the ratio of thermal to electrical conductivity for the solid is less than five per cent of that same ratio for the melt. Thus, the effect of heat degradation by conduction and ohmic loss can be closely approximated by considering the melt alone. (Of course, the system could be complicated by the addition of a second thermocell in which the charge flows in the opposite direction from that considered, thus replacing the solid conductor, but for purposes of simplification, this will not be considered further.) It is assumed, in addition, that optimum efficiencies for thermocells, as is the case for other thermoelectric devices, are obtained when the external load has a resistance approximately equal to the cell internal resistance, i.e. the cell output voltage is one half of the theoretical. (It is implied here that the internal cell impedence is mainly from the electrical resistance of the electrolyte rather than electrode polarization; see section VI-E.)

Based on the above simplifications, efficiencies have been estimated for cells operating at assigned electrode temperatures. These calculations are discussed in the Appendix, section D. Final results are listed in table V.

In general, it can be seen from the results that the efficiencies increase with an increase in the hot-electrode temperature as a consequence of the higher Carnot efficiency. They also increase with a reduction in total pressure due to the pressure effect on cell voltage. Note, however, for the silver chloride system that the trend reverses at a temperature of 1300°C and 0.40 atmospheres pressure. This behavior is characteristic of all molten-salt systems and results from the substantial quantity of salt

Table V

Estimated Efficiencies for Several Thermocells at Various Temperatures and Pressures

Silver Chloride-Chlorine Thermocell (base temp. 500°C)

Pressure	Temperature 900°C	1000°C	1100°C
1.000 atm	2.2 per cent	3.2 per cent	3.6 per cent
0.621	2.4	3.3	3.8
0.290	2.7	3.8	4.25 (2.8×10^{-4})
0.120	2.9 (2.7×10^{-4})(a)	4.05 (3.3×10^{-4})	

	1300°C	1527°C
1.000	4.1	2.7
0.70	4.3	
0.40	4.5 (2.6×10^{-4})	
0.20	4.3	

Boron Oxide-Oxygen Thermocell (base temp. 527°C)

	1800°C
1.00	3.7
0.50	3.9
0.20	4.25 (1.46×10^{-4})

Lithium Fluoride-Fluorine Thermocell (base temp. 877°C)

	1423°C
1.00	10.5
0.50	11.4 (1.86×10^{-3})
0.20	8.5

(a) The number in parenthesis indicates the figure of merit of a solid-state thermoelectric generator having the same efficiency.

vaporized at the hot electrode with its consequent degradation of heat. Note that high vapor pressure of itself is not a serious limitation, but rather, high vapor pressure coupled with the extremely high heats of vaporization characteristic of molten salts (about 45 to 50 Kcal/gmole). At higher temperatures, the reversal becomes more pronounced, yielding again for the silver chloride system an efficiency of only 2.7 per cent at one atmosphere pressure and a temperature of 1527°C; 20°C below the boiling point. Thus, it appears that the highest efficiency obtainable for this thermocell is in the vicinity of 5 per cent and occurs with a hot-electrode temperature of about 1300°C and a total cell pressure of about 0.4 atmospheres. Because of their higher vapor pressures and lower Seebeck coefficients, the other cells studied experimentally (lithium chloride--chlorine, sodium chloride-chlorine and potassium chloride-chlorine) have even lower efficiencies and operating temperatures.

In an effort to explore the feasibility of other systems, efficiencies were estimated for two hypothetical cells by assuming Pitzer's equation to hold and by assuming the entropies of transfer to be zero. The results of these calculations are shown also in table V. The boron oxide-oxygen thermocell was considered because of the span and absolute temperature of its operating region. But, its efficiency is low, owing to a decrease in the number of moles of gas reacted per electron transferred. On the other hand, the lithium fluoride-fluorine cell appears to have possible efficiencies higher than 10 per cent, an increase due mainly to a high electrical conductivity. Of course, the main practical limitation on this system is the corrosiveness of the electrolyte.

The feasibility of the molten-salt thermocell as an electrical generator is determined by the proposed application. The calculations mentioned above show that efficiency is definitely a limitation unless

there exists a particular application where a thermocell could feasibly extract energy, as a topping device, from high temperature heat and still exhaust this heat at the maximum temperature tolerated by conventional energy conversion systems. Tentatively, it appears that even in this application the cells studied experimentally in this work are limited by high vapor pressures to a relatively low efficiency range. One factor highly favoring thermocell systems, however, is the absence of moving parts, a definite advantage at high temperatures. Another asset in comparison with solid-state couples is the absence of deterioration and aging at high temperatures. On the other hand, the thermocell system which appears to have most promise, the lithium fluoride-fluorine cell, is severely hampered by the lack of materials of construction suitable to contain the melt.

F. Discussion of the Complex Cl_3^- Ion

In the derivation of equation (28), it was assumed that the active ion is Cl^-, the monatomin chloride ion. It has been suggested to the author that the complex ion Cl_3^- may also be present. However, the data show no evidence of this ion being present in appreciable concentrations. The low temperature data for the silver chloride-chlorine cell are very helpful in demonstrating this since dissociation and vapor pressure effects are negligible for this system up to 1000°C. For these conditions, equation (28) simplifies to

$$E = \frac{1}{\mathcal{F}} \left[\int_{T_1}^{T_3} \Delta S^\circ dT + \frac{R}{2} (T_1 - T_3) \ln \pi \right] \tag{70}$$

If Cl_3^- were an active species, the entropy change of equation (70) would involve that of the reaction

$$Cl_3^- \longrightarrow 3/2\ Cl_2 + e^- \tag{71}$$

which is the sum of the reaction

$$Cl^- \longrightarrow 1/2\ Cl_2 + e^- \qquad (72)$$

and the reaction

$$Cl_3^- \longrightarrow Cl^- + Cl_2 \qquad (73)$$

Since the entropy change for reaction (72) is undoubtedly positive, that for reaction (71) will be greater than that for (72). However, the concentration of Cl_3^- is pressure sensitive, and if reaction (71) occurred to an appreciable extent, its influence would change with pressure causing a decrease in ΔS^o with reduced pressure. In other words, the first term of equation (70) would be pressure sensitive. Assuming a ΔS^o for reaction (73) of about 30 e.u., it is estimated from the experimental results that, if present at all, the Cl_3^- concentration in the four melts studied does not exceed one mole per cent.

VIII. CONCLUSIONS AND RECOMMENDATIONS

A. Conclusions

1. Equation (28) accurately describes the contributions of total pressure, salt vapor pressure and dissociation to cell voltage for the four thermocells studied. There is no reason to doubt that equations similar to (28) will apply to other thermocells not included in this study.

2. Due to increasing Seebeck coefficients, thermocell efficiencies were found to improve with decreasing pressure until the total pressure approached the salt vapor pressure. At this point, efficiencies became less with decreasing pressure due to the increasing importance of the irreversible heat required to vaporize the salt

3. The maximum estimated overall efficiency of any of the systems studied was 4.5 per cent. This is that of the silver chloride-chlorine thermocell at a cold electrode temperature of 500°C, a hot electrode temperature of 1300°C, and a total pressure of 0.4 atmospheres. Of all conceivable molten-salt thermocells, the lithium fluoride-fluorine cell appears to have highest efficiencies. The maximum estimated for this system is 11.4 per cent.

4. Actual transported entropies were found to be nearly equal to the partial molal entropies calculated from Pitzer's equation for the chloride ions in molten lithium chloride, sodium chloride, and potassium chloride. In the silver chloride melt, the transported entropy of chloride ion was found to be less by 3.7 e.u. than the partial molal entropy similarly calculated. Due to the unknown magnitude of the entropy of transfer, it is not possible to comment on the validity of Pitzer's equation.

5. The standard half cell reaction entropy ΔS° was found to vary with temperature for all systems. The variation corresponded to a ΔC_p for

the half cell reaction of approximately -3.0 e.u.

6. Reducing the chlorine partial pressure by the addition of an inert gas proved to have the same quantitative effect as reducing the total pressur when operating with pure chlorine.

7. It is estimated from experimental data that the tri-chloride ion Cl_3^- does not exist in any of the melts studied in concentrations greater than one mole per cent.

B. Recommendations

1. Fused salt thermal conductivities are uncertain. Hence, calculated cell efficiencies are only approximate. It is recommended that an experimental program be instituted for the measurement of this property.

2. If, on the basis of present information, the thermocell appears feasible for energy conversion, studies of actual efficiency should be carried out on a small scale using a calorimetric technique.

3. In the event that suitable container materials become available, the lithium fluoride-fluorine thermocell should be studied experimentally.

IX. APPENDIX

A. Apparatus

1. Cell Configuration

A scale drawing of the cell and surrounding furnace is shown in figure 5, section IV. The outer cell container consisted of a 2-1/4" O.D. x 2" I.D. refractory tube 24 inches long and closed at one end. (Fused silica tubes fabricated by Syncor Products Co., Malden, Massachusetts were used for most of the investigations.) Suspended inside was another 1-1/8" O.D. x 7/8" I.D. open-end tube also 24" long. These tubes were secured at the top by a "teflon" plug-"viton" "O"-ring fitting which held the smaller tube about 2 inches above the floor of the large tube. The melt level in the inside tube was depressed with respect to that at the annulus by means of a variable hydrostatic head in the external vent system (see figure 22). The low temperature electrode was placed about 1 inch above the bottom of the inside tube, and it was submerged to a depth of about 1 to 2 inches in the melt. The high temperature electrode was placed in the annulus at an elevation of about 5 or 6 inches above the low temperature electrode, and it was also suspended about 1 to 2 inches below the melt surface. Thermocouples made of platinum versus 90 per cent platinum-10 per cent rhodium wire, 0.020 inches in diameter, ceramically insulated, and protected by 6 mm vycor tubes, were placed adjacent to each electrode.

2. Description of Vacuum Seal Compression Fitting

One of the major difficulties encountered in cell construction was the design of a fitting to seal the refractory tubes, the electrodes, thermocouples, and vent tubes so that the unit was gas tight under moderate vacuum. Since the seal was only about 7 inches out of the furnace, it was necessary that it also be resistant to moderately high temperature. The resultant design is that shown in figures 19 and 20. It consisted of

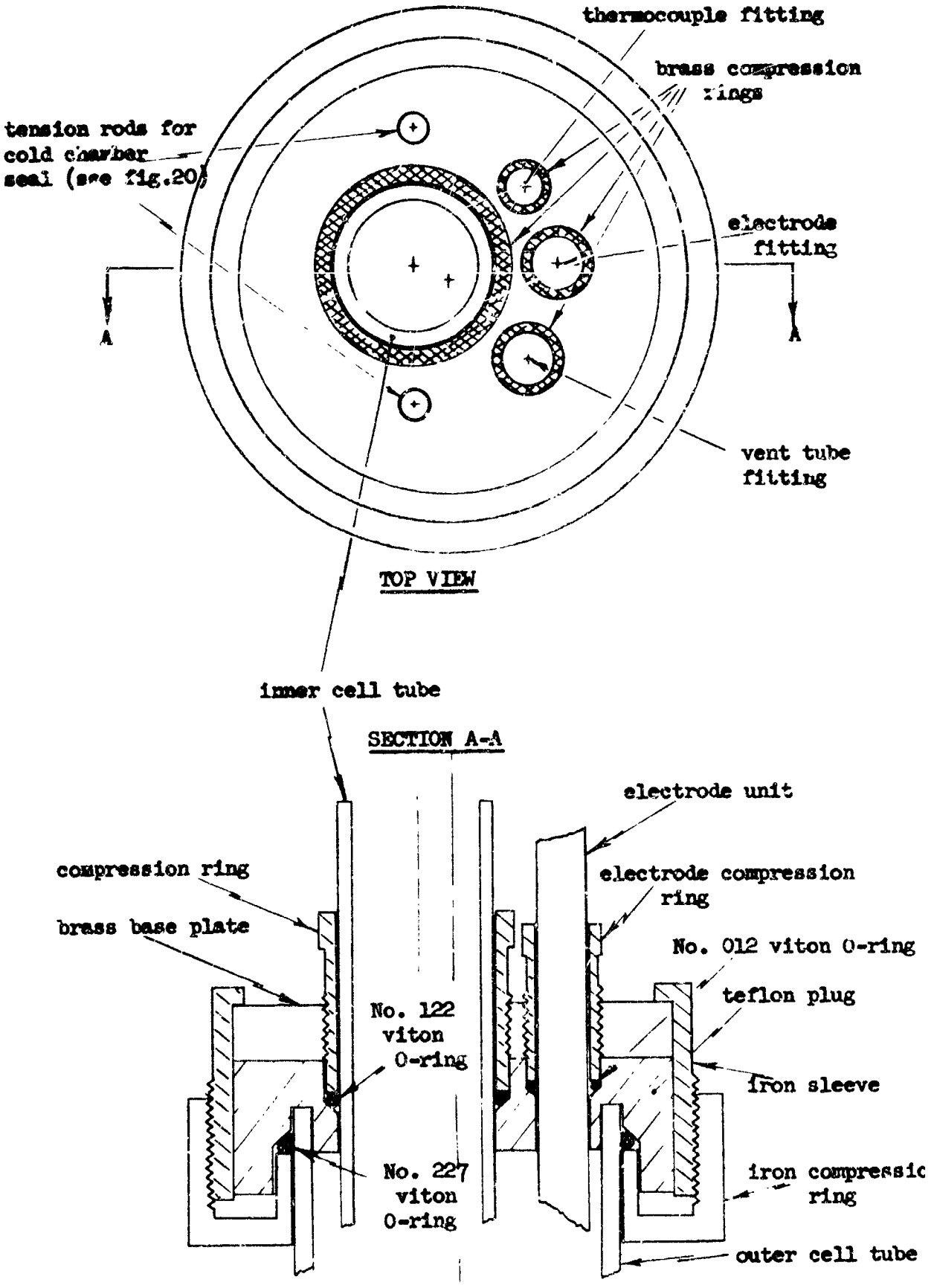

Figure 19. Detailed drawing of cell vacuum seal unit (actual size).

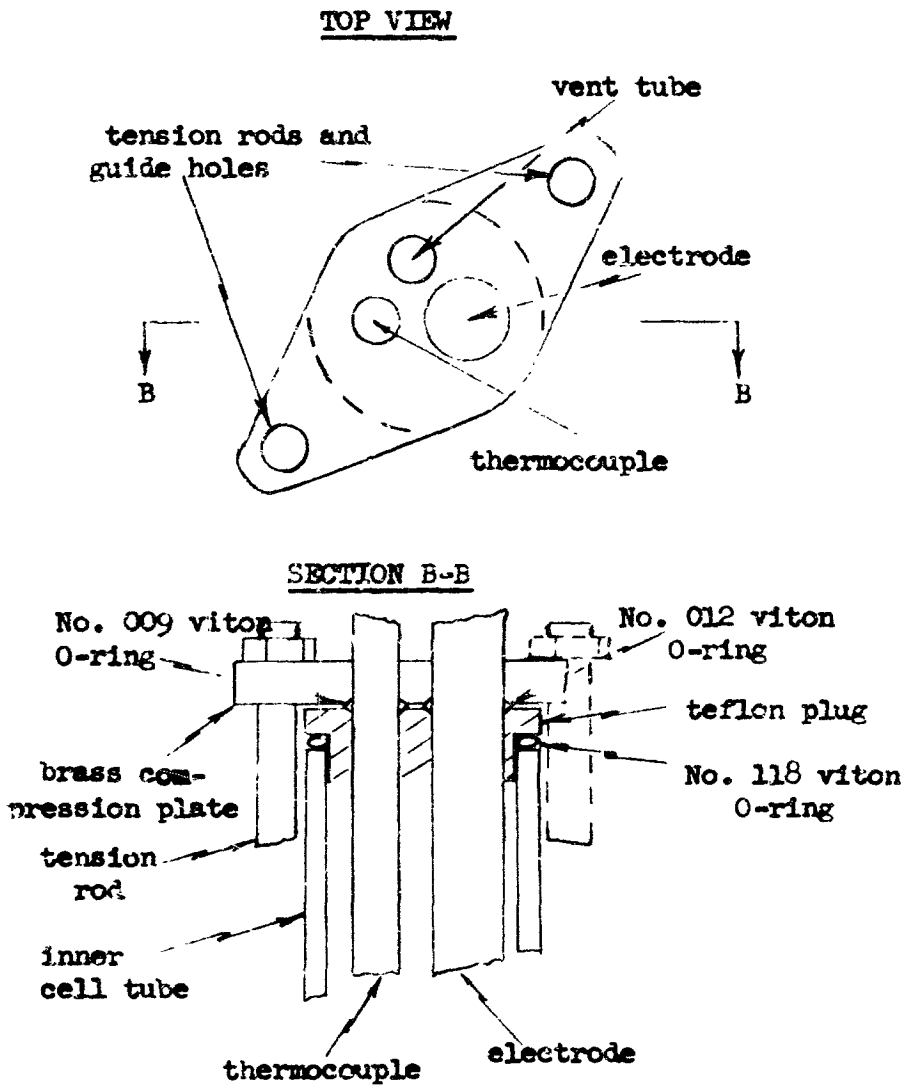

Figure 20. Detailed drawing of vacuum seal unit for cold electrode chamber (actual size).

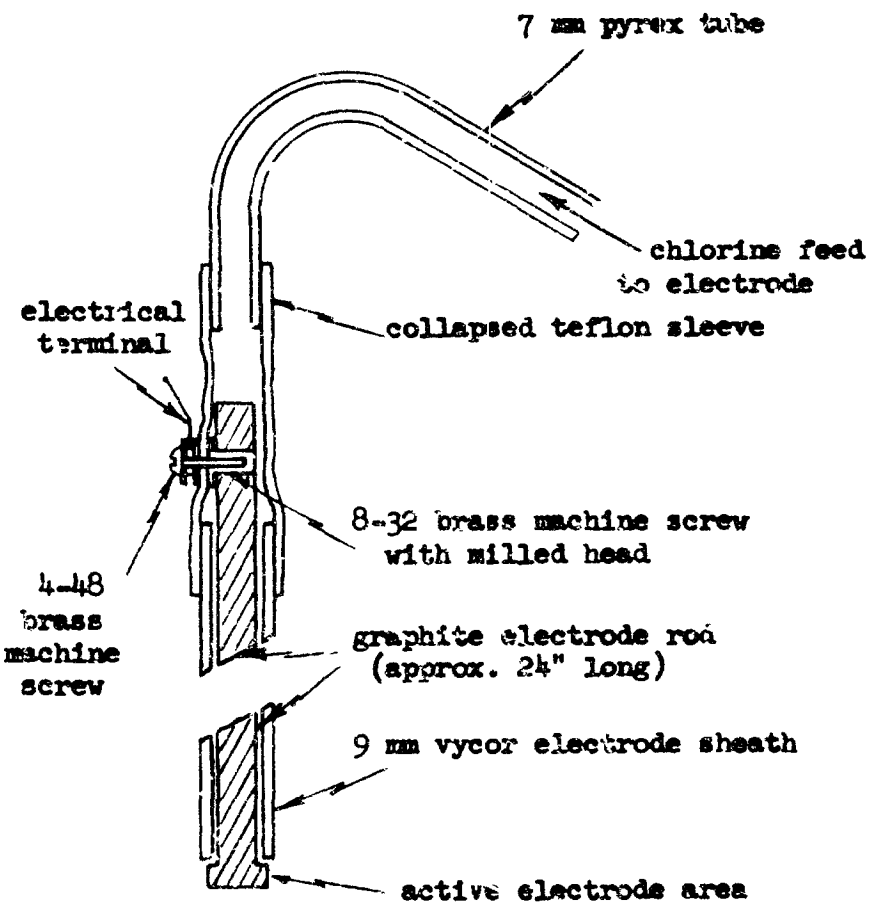

Figure 21. Detailed sketch of electrode (actual size)

a teflon plug against which viton O-rings were compressed by metal fittings. As shown in figure 19, the plug was secured to the outside of the large tube by a 2-1/4" O-ring. This was compressed by an iron ring which screwed onto the iron sleeve enclosing the teflon plug. With this arrangement also, the brass base plate was held in place. The iron fittings were tightened by spanner wrenches designed to fit holes drilled around the circumference of the sleeve and the compression ring. The small refractory tube and the electrodes and thermocouples extending into the cell annulus were sealed by viton O-rings seating against the teflon plug. These O-rings were compressed by brass rings threaded so as to screw into the base plate. They were tightened by special wrences custom made to fit into the compression ring grooves. The low temperature electrode and thermocouple were held inside the small refractory tube by another teflon plug and O-ring combination. This is shown in figure 20.

Tension rods attached to the base plate were passed through a small brass compression plate. The rods were threaded at the top so that the plate could be tightened down against the top of the 1-1/8 inch tube. The figure shows how a seal was made on the electrode, thermocouple, and vent tube when this plate compressed various O-rings between itself and a small teflon plug. This same pressure seeled the plug to the refractory tube through another O-ring.

The fitting thus constructed performed perfectly, and there was no noticeable leakage at pressures down to a centimeter of mercury. Such a configuration also made it possible to change electrodes in minutes.

3. Furnace Details (see figure 5)

The furnace shell consisted of a 7" I.D. "transite" tube, 20" long with a 5/16" wall. Circular transite plates of slightly larger diameter were clamped a both ends of the furnace by iron rods. The top plate had a

hole in the center large enough to admit the cell. The furnace tube was made from two Norton No. 17488 refractory furnace cores stacked one on top of the other and clamped between the furnace end plates. Before insertion, the composite core was firmly clamped and wrapped with Kanthal A-1 resistance heating wire. The wire, 0.072" O.D. and 0.169 ohms per foot, was pre-coiled by winding tightly on a 1-5/8" O.D. pipe rotated in the lathe. Thus prepared, the wire could be slipped into grooves on the outside of the core. The wires were tied off at each end of the core in such a way that double Kanthal leads extended outward at each end and in the center for connection to the power input terminals. The center lead acted as the common ground for both power sources, and it was made by taking a loop in the wire and twisting it before winding. When wound, the loop extended outward to be used as a terminal connection. Wound in this manner, the center furnace coils were not interrupted by tie-off knots.

After wrapping, the composite core was secured with a special clamp to the base plate of the furnace and sufficient Alundum RA 1162 cement applied to completely cover the heating coils. This was permitted to dry overnight. Because of the low strength of the uncured cement, it was necessary to exercise care in placing the furnace shell and top plate into position. However, once the nuts were tightened on the furnace rods, the core was held securely under compression between the furnace end plates.

The Kanthal leads were connected to the terminals in the shell during assembly before the top plate was installed. Two holes were made in the top plate above the annulus between the furnace shell and the core through which Alundum type K 163 bubble insulation was added. This made a compact two-zone tube furnace, and the cell unit could be lowered into or removed from the furnace without disturbing it in any way. Two control thermocouples of platinum versus 90 per cent platinum-10 per cent rhodium wire, 0.020

inches in diameter, extended into the furnace from the bottom; one extending to a position opposite the high temperature windings and the other opposite the low temperature windings. With the cell in position, the control thermocouples were situated in the annulus between the outside of the cell container and the inside of the furnace core. Before lowering the cell into position, a three inch base of bubble insulation was placed in the bottom of the furnace. The large outside cell tube then extended seven inches above the top of the furnace. The furnace was supported on metal legs about four inches above the laboratory bench, adjacent to the hood. Four gas lines extended to the cell from the hood to supply the electrodes and to vent the two cell compartments. Electrical power was supplied from two controllers (Barber-Colman No. 407 P Capacitrol-Silicon Control Rectifier combination) mounted on a laboratory cart and connected by flexible cable to the furnace terminals. The thermocouples were connected to the controllers by about eight feet of compensating wire.

4. Auxiliary Gas-Feed and Vent System

The purpose of this system was first to supply a pure stream of chlorine to the electrode at a controlled rate and second to maintain a steady hydrostatic head difference in the vent lines to regulate the relative liquid heights in the cell compartments.

The gas feed system was designed to accomodate either pure chlorine or pure argon by the turn of a stopcock (see figure 22). The gases (Matheson chlorine and Matheson lamp grade argon) passed from the cylinders through pressure reducing valves to drying columns (1 cm I.D. x 24" long) packed with anhydrous magnesium perchlorate ("Anhydrone").

The electrode feed gas (either chlorine or argon) then passed through a stopcock to the feed line. Two gas streams were separated at a "T" connection and each flowed through a stopcock, teflon needle valve (Fisher, Cat.

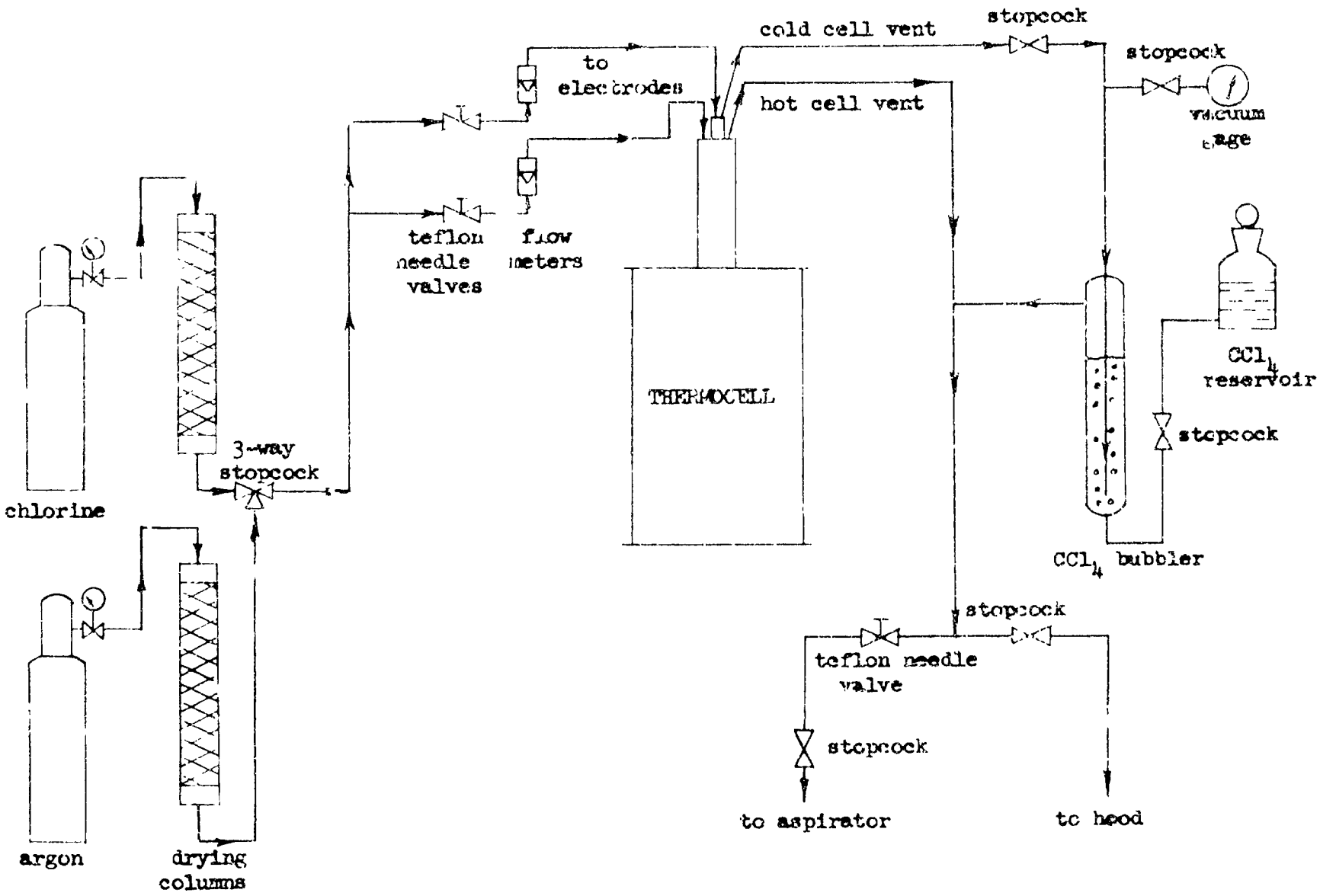

Figure 22. Schematic flow diagram showing gas feed and vent system.

No. 14-630-5), and flowmeter (Fisher-Porter 08F-1/2-08-4/36) respectively. Connections from the flowmeter outlets were made directly to the electrodes as they were installed in the cell. All gas lines were of welded "pyrex" throughout except at points where flexibility was desired such as in the lines leading to the cell. These were made by connecting a number of short lengths of glass tubing with short lengths of flexible teflon tubing. "Tygon" tubing was then slipped over the teflon, extending also onto the glass, thus assuring a gas-tight joint. This prevented any air leakage into the feed lines while the cell was operated under reduced pressure.

The gas, after flowing past the electrodes, rose inside the respective cell compartments and exited through the vent tubes. These were connected by tygon tubing to the vent train inside the hood. Tygon, which is attacked by chlorine but which is much easier to use than teflon for flexible leak-free connections was satisfactory here since the gas had already passed through the cell and subsequent contamination was not harmful. However, it was necessary occasionally to replace this tubing. Otherwise all connections in the vent system were of welded pyrex. Stopcocks generally contained teflon plugs. Those containing pyrex plugs were lubricated satisfactorily with Kooker "fluorolube" stopcock lubricant.

The vent line from the low temperature cell compartment passed through a stopcock and then through a bubbler containing carbon tetrachloride. This line was also connected to a calibrated Ashcroft type 1012 vacuum gage used to determine the cell pressure. The vent from the annulus of the cell also passed through a stopcock and then joined the stream from the bubbler before being expelled. Thus, the pressure of the high temperature electrode chamber corresponded to that at the liquid surface in the bubbler, and the pressure of the low temperature electrode chamber corresponded to that at the base of the bubbler. The pressure difference could be

varied by changing the level of carbon tetrachloride in the bubbler which was connected through another stopcock to a CCl_4 reservoir. This permitted excellent control of the liquid level difference in the thermocell. During atmospheric pressure runs, the combined exit gas stream was exhausted near the hood vent. During reduced pressure runs, it was expelled via a teflon needle valve through the water aspirator pump. By throttling the gas through the two feed needle valves and the exit needle valve at a controlled rate, steady vacuum was maintained in the system.

5. Details of Electrode Construction

For meaningful results, it was necessary that the electrodes be designed so that only a small surface was exposed to the electrolyte. To meet this criterion, the electrodes were constructed as shown in figure 21. They were of National Carbon grade AGSX graphite rods 3/8" O.D. x 24" long. The rods were machined carefully to a diameter small enough to slide easily into a 9 mm vycor sheath with just a small button, 1/8" thick and 5/16" in diameter exposed to the melt. Liquid was prevented from contacting the upper carbon rod by the passage of chlorine through the annulus. Thus, only a small isothermal electrode area was exposed to reaction regardless of its submerged depth in the fused salt.

To make a leak-free electrical connection to the electrode, a hole was drilled and tapped in the side near the top of the graphite rod to accomodate a No. 8-32 brass machine screw. The head was milled flat and a hole drilled and tapped inside this screw to accomodate a No. 4-48 machine screw. The vycor sheath was placed over the electrode so that the bottom button and a small length of rod at the top were exposed. The large machine screw was installed, and a length of expanded teflon tubing (Pennsylvania Fluorocarbon Co., 1/4" E-0.030" flexible expanded natural TFE) was heated; consequently contracting so as to make a tight

seal between it and the vycor sheath. The other end of the teflon sleeve was sealed to a glass inlet tube. The teflon entirely covered the exposed graphite and the screw. A small hole was then drilled through the teflon so that the No. 4-48 screw could be tightened against the flat head of the larger screw. By thus tightening the soldered lead wire and a washer against the teflon and the teflon against the large screw, a secure gas-tight seal was obtained which performed satisfactorily throughout the experiments. The only difficulty encountered with the electrodes was an occasional fracture of the graphite rod where it had been drilled.

B. Development of Final Data

This section is devoted to the direct comparison of equation (28) with experimental results. Equation (28) is simplified to the form shown below in order to expedite numerical calculation.

$$E = 0.0430 \left[\int_{T_o}^{T} \frac{2\Delta S^o}{R} dT + T_o \ln \pi' - T \ln\left(\left[\frac{n-1}{n+1}\right]\pi'\right)\right] \qquad (74)$$

In equation (74), 0.0430 is the quantity $R/2\mathcal{F}$ and has the units of millivolts per centigrade degree. The other terms are explained in section III.

To make the desired comparison, a temperature T and a total pressure corresponding to an experimental determination were selected. Then from known values of T_o, n, and π' (1,4,27,8); the last two terms of equation (74) were calculated. This procedure was repeated at several values of T for all of the pressures of interest. Then the value of the integral $\int_{T_o}^{T} \frac{2\Delta S^o}{R} dT$ was chosen to give the best agreement between the calculated and the experimental voltages.

The results of a trial calculation for the NaCl-Cl_2 cell are shown in Table VI. Table VII gives a tabulated comparison of final results for all of the cells studied.

The experimental voltages used for this calculation were read from figures 9 through 12.

Table VI

Comparison of E_{exp} with E_{calc} for the NaCl-Cl_2 Thermocell

Temperature Chosen..... 1000°C (1273°K)

Reference Temperature..... 900°C (1173°K)

Equilibrium Constant(8)..... 0.01

Sodium Chloride Vapor Pressure(1)..... 0.012 atmospheres

Total Pressure	$\int_{T_o}^{T} \frac{2\Delta S^\circ}{R} dT$	1173 ln π	π'	n	-1273 ln$(\frac{n-1}{n+1})\pi'$	E_{calc}	E_{exp}	ΔE
1.00 atm	1092 equivalent to 47.0 mv	-2	0.988	199	26	48.0 mv	48.5 mv	-0.5 mv
0.822		-233	0.810	180	283	49.1	49.4	-0.3
0.655		-500	[illegible]	160	579	50.5	50.5	-0.0
0.487		-849	0.475	138	966	52.0	51.5	-0.5
0.321		-1341	[illegible]309	111	1518	54.6	54.2	0.4
0.158		-2180	0.146	[illegible]6.4	2490	60.4	57.5	2.9

Table VII

Tabulation of Experimental versus Calculated Voltages

(all voltages in millivolts)

Sodium Chloride-Chlorine Thermocell

(Reference Temperature....900°C)

Temperature:	1000°C			1100°C			1150°C		
Pressure	E_{calc}	E_{exp}	ΔE	E_{calc}	E_{exp}	ΔE	E_{calc}	E_{exp}	ΔE
1.000 atm	48.0	48.5	-0.5	97.0	97.8	-0.8	122.5	123.3	-0.8
0.822	49.1	49.4	-0.3	100.5	99.3	1.2	125.9	125.5	0.4
0.655	50.5	50.5	0.0	102.8	101.5	1.3	130.0	128.4	1.6
0.487	52.0	51.5	0.5	107.0	105.3	1.7	136.2	134.9	1.3
0.321	54.6	54.2	0.4	114.0	113.0	1.0	147.1	146.6	0.5
0.158	60.4	57.5	2.9	132.0	125.3	6.7	174.1	168.7	5.4
$\int_{T_o}^{T} \frac{2\Delta S^o}{R} dT$	1092 (47.0 mv)			2167 (93.3 mv)			2702 (116.3 mv)		

	1200°C			1250°C			1300°C		
1.000	149.0	150.0	-1.0	177.0	178.5	-1.5	-----	209.4	----
0.822	153.7	154.0	-0.3	184.2	184.0	0.2			
0.655	160.3	157.8	2.5	194.6	190.2	4.4			
0.487	170.7	167.5	3.2	212.0	203.8	8.2			
0.321	191.0	185.0	6.0	258.0	-----	---			
0.158	282.0	-----	---						
$\int_{T_o}^{T} \frac{2\Delta S^o}{R} dT$	3182 (137.0 mv)			3648 (157.0 mv)			4091 (176.0 mv)		

Table VII (continued)

Potassium Chloride-Chlorine Thermocell

(Reference Temperature....850°C)

Temperature:	980°C			1060°C			1150°C		
Pressure	E_{calc}	E_{exp}	ΔE	E_{calc}	E_{exp}	ΔE	E_{calc}	E_{exp}	ΔE
1.000	62.6	63.3	-0.7	102.2	102.6	-0.4	148.0	148.5	-0.5
0.823	63.9	64.3	-0.4	109.2	104.5	-0.3	152.5	152.5	0.0
0.657	65.3	65.6	-0.3	107.2	107.4	-0.2	158.0	157.5	0.5
0.490	67.4	67.4	0.0	111.4	110.1	1.3	166.8	164.3	2.5
0.323	70.5	70.4	-0.1	118.2	115.8	2.4	183.5	176.2	7.3
0.160	77.1	78.3	-1.2	134.4	133.8	0.6	242.0	236.4	5.6
0.076	88.0	87.0	1.0	169.3	160.5	8.8	330.0	-----	---
$\int_{T_o}^{T} \frac{2\Delta S^o}{R} dT$	1430 (61.5 mv)			2306 (99.3 mv)			3221 (138.5 mv)		

	1250°C	
1.000	206	206
0.823	216	214
0.657	230.5	225
0.490	261	245
0.323	364	---
$\int_{T_o}^{T} \frac{2\Delta S^o}{R} dT$	4149 (178.5 mv)	

Lithium Chloride-Chlorine Thermocell

(Reference Temperature....700°C)

(Pressure...1.0 atmosphere)

Temperature:	800°C	900°C	1000°C	1100°C	1200°C	1260°C
E_{exp}	54.6	109.7	162.8	215.5	275.0	318.0
$\int_{T_o}^{T} \frac{2\Delta S^o}{R} dT$	1270 (54.5mv)	2530 (109mv)	3724 (160mv)	4830 (208mv)	5885 (253mv)	6425 (276mv)

Table VII (continued)

Silver Chloride-Chlorine Thermocell

(Reference Temperature.....500°C)

Temperature:	600°C			700°C			800°C		
Pressure	E_{calc}	E_{exp}	ΔE	E_{calc}	E_{exp}	ΔE	E_{calc}	E_{exp}	ΔE
1.000	68.0	67.5	0.5	135.5	134.5	1.0	200.6	199.4	1.2
0.787	69.1	69.0	0.1	137.4	136.8	0.6	203.5	202.5	1.0
0.621	70.1	70.2	-0.1	139.5	140.1	-0.6	206.8	206.5	0.3
0.455	71.4	72.0	-0.6	152.2	143.7	-1.4	210.8	212.5	-1.7
0.290	73.3	75.0	-1.7	146.0	148.6	-2.6	216.4	220.0	-3.6
0.120	77.2	77.3	-0.1	153.8	154.4	-0.6	228.0	230.5	-2.5
0.016	85.8	81.8	4.0	171.0	163.0	8.0	254.0	-----	---
$\int_{T_o}^{T} \frac{2\Delta S^o}{R} dT$	1580 (68.0 mv)			3150 (135.5 mv)			4665 (200.6 mv)		

	900°C			1000°C			1100°C		
1.000	263.0	262.0	1.0	324.2	323.5	0.7	385	385.0	0.0
0.787	267.0	265.6	1.4	330.0	327.8	2.2	391	389.3	1.7
0.621	271.0	270.0	1.0	334.4	332.3	2.1	398	393.5	4.5
0.455	276.5	278.2	-1.7	342.2	341.5	0.7	407	405.0	2.0
0.290	284.5	289.4	-4.9	352.0	357.0	-5.0	420	425.0	-5.0
0.120	300.0	303.0	-3.0	373.0	372.3	0.7	449	446.5	2.5
$\int_{T_o}^{T} \frac{2\Delta S^o}{R} dT$	6110 (263 mv)			7532 (324 mv)			8890 (382 mv)		

	1200°C			1300°C		
1.000	445	446	-1.0	-----	515	---
0.787	453.5	451	2.5			
0.621	462	457	5.0			
0.455	475	471	4.0			
0.290	493	496.5	-3.5			
$\int_{T}^{T} \frac{2\Delta S^o}{R} dT$	10,190 (438 mv)			11,600 (499 mv)		

C. Calculation of Entropy Change for the Chlorine Half Cell Reaction

The standard entropy change for the reaction

$$Cl^- \longrightarrow 1/2\ Cl_2 + e^- \qquad (75)$$

on a graphite electrode is equal to

$$\Delta S^\circ = 1/2\ S^\circ_{Cl_2} + \bar{\bar{S}}_{e,g} - \bar{\bar{S}}_{Cl^-} \qquad (76)$$

where $S^\circ_{Cl_2}$ is the standard state entropy for diatomic chlorine at one atmosphere pressure, $\bar{\bar{S}}_{e,g}$ is the transported entropy (equal to the sum of $\bar{S}_{e,g}$ plus $S^*_{e,g}$) of the electron in pure graphite and $\bar{\bar{S}}_{Cl^-}$, the corresponding term for the chloride ion in the pure fused salt. However, since the quantity $\bar{\bar{S}}_{Cl^-}$ is not known, equation (76) will be rewritten as

$$\Delta S' = \Delta S^\circ + S^*_{Cl^-} = 1/2\ S^\circ_{Cl_2} + \bar{\bar{S}}_{e,g} - \bar{S}_{Cl^-} \qquad (77)$$

The determination of $\Delta S'$ is outlined in table VIII. The first column lists the temperature in $^\circ C$. The second shows values of S_{MX}, the molal entropy of the particular fused salt at the temperature given (values taken from Kelley(15) and Glassner(9)). The third column lists the translational entropy correction term of Pitzer(24), and the fourth is the partial molal entropy of Cl^- as determined from equation (35). The next column lists the corresponding chloride entropies taken from Evans, et. al.(8). The entropy of transfer for the electron in graphite is tabulated in column 6 and is estimated to be about 0.20 e.u.* From these values substituted into equation (77), $\Delta S'$ can be calculated. The result is shown in column 7. The equivalent Seebeck coefficient and experimental values for the Seebeck coefficient and ΔS° make up columns 8, 9, and 10. $S^*_{Cl^-}$ calculated as the difference between $\Delta S'$ and ΔS° is listed in the final column.

---

*Note: The value $\bar{\bar{S}}_{e,g}$ was estimated from that of an electron in copper (-0.13 e.u. at 1000°K) reported by Tyrrell(32) from an article by Temkin and Khoroshin (Zhur. Fiz Khim., 26, 500 (1952)). The thermoelectric potential for the copper-graphite thermocouple at 1000°K (reference 37) indicates that the transported entropy of the electron in graphite minus that of the electron in copper is equal to

Table VIII

Comparison of Calculated and experimental Entropies

1 Temperature	2 S_{MX}	3 $3/2\ R\ \ln M_{Cl}/M_M$	4 $\bar{S}_{Cl}$	5 $1/2\ S^o_{Cl_2}$	6 $\bar{S}_{e,g}$	7 $\Delta S'_{calc}$	8 dE/dT_{calc}	9 dE/dT_{exp}	10 ΔS^o_{exp}	11 $S^*_{Cl^-}$
				Silver Chloride-Chlorine Cell						
527°C	41.16	-3.30	18.93	30.88	0.20	11.95	0.517	0.575	15.60	-3.65
627	43.04	"	19.87	31.40	"	11.53	0.499	0.570	15.46	-3.93
727	44.73	"	20.72	31.87	"	11.15	0.482	0.540	14.78	-3.63
				Sodium Chloride-Chlorine Cell						
827°C	41.14	1.28	21.21	32.30	0.20	11.09	0.479	-----	-----	-----
927	42.54	"	21.91	32.69	"	10.78	0.465	0.480	11.08	-0.30
1027	43.82	"	22.55	33.05	"	10.50	0.454	0.470	10.83	-0.33
1127	45.00	"	23.14	33.39	"	10.25	0.443	0.455	10.50	-0.25
1227	46.11	"	23.70	33.70	"	10.00	0.432	0.415	9.58	0.42
1327	47.14	"	24.21	34.00	"	9.79	0.423	-----	----	----
1427	48.11	"	24.70	34.27	"	9.57	0.414	-----	----	----
				Potassium Chloride-Chlorine Cell						
827	43.12	-0.28	21.42	32.30	0.20	10.88	0.471	-----	-----	-----
927	44.52	"	22.12	32.69	"	10.57	0.456	0.475	10.96	-0.39
1027	45.79	"	22.76	33.05	"	10.29	0.444	0.470	10.83	-0.54
1127	46.98	"	23.35	33.39	"	10.04	0.434	0.435	10.03	-0.01
1227	48.08	"	23.90	33.70	"	9.80	0.423	0.420	9.70	0.10
				Lithium Chloride-Chlorine Cell						
827	33.60	6.67	20.15	32.20	0.20	12.25	0.525	0.545	12.58	-0.43

D. Estimated Thermocell Efficiencies

These efficiency calculations are based on the assumptions made in section VIII-B, i.e. (1) the contribution of the solid conductor to the efficiency or inefficiency is insignificant compared to that of the electrolyte, (2) the cell output voltage is one-half of the theoretical, and (3) polarization effects are negligible in comparison to ohmic losses.

From an energy balance, the efficiency ϵ of the cell is given by

$$\epsilon = w/q_H \tag{78}$$

where w is the rate at which useful work is supplied to the external load, and q_H is the heat transfer rate to the high temperature electrode. In accordance with the above assumptions, w can be written as

$$w = EI/2 \tag{79}$$

with I defined by

$$I = \frac{E\sigma A}{2L} \tag{80}$$

where

E = open-circuit cell voltage
A = cross-sectional area of the electrolyte
L = length of the conducting path in the electrolyte
σ = electrical conductivity of the electrolyte

and E/2 is the internal voltage drop of the cell as implied in the second assumption above.

The term q_H is made up of three separate quantities; q_c, the heat conducted away from the hot electrode due to the temperature gradient in the electrolyte; q_r, the heat absorbed at the hot electrode by the cell reaction; and q_v, the heat absorbed due to the evaporation of salt which is continually carried away from the hot electrode by the circulating chlorine. Equation (78) can now be written in terms of these symbols as

$$\epsilon = \frac{EI/2}{q_c + q_r + q_v} \tag{81}$$

It should be mentioned here that the expression for q_H is complicated

by several other variables. For example, the heat generated in the electrolyte by ohmic losses alters the temperature gradient between electrodes. Likewise, heat is given up as salt condenses out of the chlorine-salt vapor mixture flowing from the hot electrode chamber. A similar effect is introduced if the electrode gas dissociates.

It can be shown(10, 14) that the effect of ohmic losses is to alter the temperature profile such that q_c may be approximated by assuming a linear profile and then subtracting from the resulting heat flux a quantity equal to half the ohmic power loss. In other words,

$$q_c = \frac{k A (T_H - T_C)}{L} - \frac{I^2 L}{2 \sigma A} \tag{82}$$

The effect of salt condensation and recombination of gas (monotomic to diatomic) in the return line also tends to reduce the quantity q_c. However, quantitative evaluation of these terms yields a second order differential equation which is not amenable to routine solution methods. For this reason, equation (82) will be used to define q_c. Therefore, the final calculated efficiency will be smaller than would have been the case had vaporization and dissociation effects been included. This will provide a safety factor to compensate for assumptions (1) and (3) discussed in the beginning of this section.

The heat absorbed by the hot electrode reaction q_r is defined by the following:

$$q_r = \frac{I T_H \Delta S_H}{\mu \mathcal{F}} \tag{83}$$

where ΔS_H is the entropy change for the process occurring at the hot electrode. ΔS_H which is related to the Seebeck coefficient α, i.e. the slope of the E versus temperature curve at T_H can be determined by differentiating equation (28), or where data are available, by direct measurement from the graph.

q_v, the heat effect due to salt vaporization is defined by equation (84) below.

$$q_v = \frac{\Delta H_v I}{\mu \mathcal{F}} \left(\frac{p^*_{MX}}{\pi - p^*_{MX}} \right) \tag{84}$$

where p^*_{MX} is the melt vapor pressure and ΔH_v is the heat of vaporization.

Equation (81) is more easily evaluated if numerator and denominator are divided by I. By doing this and then combining equations (82) and (80), the following equations result:

$$\frac{q_c}{I} = \frac{2 k (T_H - T_C)}{E \sigma} - \frac{E}{4} \tag{85}$$

$$\frac{q_r}{I} = \frac{T_H \Delta S_H}{\mu \mathcal{F}} \tag{86}$$

$$\frac{q_v}{I} = \frac{\Delta H_v}{\mu \mathcal{F}} \left(\frac{p^*_{MX}}{\pi - p^*_{MX}} \right) \tag{87}$$

In terms of quantities which can be calculated, the expression for the efficiency now becomes:

$$\epsilon = \frac{\frac{1}{2} E}{\frac{q_c}{I} + \frac{q_r}{I} + \frac{q_v}{I}} \tag{88}$$

Equation (88) was used to calculate the efficiencies listed in Table IX. Results are shown here for the silver chloride-chlorine cell and the hypothetical cells boron oxide-oxygen and lithium fluoride-fluorine. Experimental results were used for voltages of the silver chloride-chlorine cell while those of the remaining cells were estimated using equations (28) and (35).

Table IX

Estimation of Thermocell Efficiencies

Table IX-A: Silver Chloride-Chlorine

T_C = 500°C (773°K) ΔH_v = 48 Kcal/gmole (b)

k = 0.00837 Watt/C°cm (a) σ = 5 $ohm^{-1}cm^{-1}$ (c)

T_H = 900°C (1173°K); p^*_{AgCl} = 0.008 atm (d)

π	E	q_c/I	q_r/I	q_v/I	ϵ
1.000 atm	262 mv	4044 mv	728 mv	----	2.2 per cent
0.621	270	4392	739	----	2.4
0.290	289	4568	822	----	2.7
0.120	303	4344	855	----	2.9

(2.9 per cent efficiency is equivalent to a figure of merit of 2.7×10^{-4})

T_H = 1100°C (1373°K); p^*_{AgCl} = 0.0145 atm (d)

π	E	q_c/I	q_r/I	q_v/I	ϵ
1.000 atm	385 mv	5124 mv	352 mv	15 mv	3.2 per cent
0.621	393	5012	865	25	3.3
0.290	425	4624	920	55	3.8
0.120	447	4388	1000	123	4.05

(4.05 per cent efficiency is equivalent to a figure of merit of 3.3×10^{-4})

T_H = 1200°C (1473°K); p^*_{AgCl} = 0.046, atm (d)

π	E	q_c/I	q_r/I	q_v/I	ϵ
1.000 atm	445 mv	5139 mv	915 mv	51 mv	3.6 per cent
0.621	457	5006	972	84	3.8
0.290	497	4586	1060	200	4.25
0.200	528	4308	1106	666	435

(4.35 per cent efficiency is equivalent to a figure of merit of 2.9×10^{-4})

T_H = 1300°C (1573°K); p^*_{AgCl} = 0.136 atm (d)

π	E	q_c/I	q_r/I	q_v/I	ϵ
1.000 atm	510 mv	5128 mv	923 mv	164 mv	4.1 per cent
0.70	527	4938	952	251	4.3
0.40	560	4632	1003	536	4.5
0.20	634	4061	1099	2210	4.3

(4.5 per cent efficiency is equivalent to a figure of merit of 2.6×10^{-4})

Table IX-A (Continued)

$T_H = 1527^\circ C$ (1800°K); $p^*_{AgCl} = 0.906$ atm (d)

π	E	q_c/I	q_r/I	q_v/I	ϵ
1.000 atm	814 mv	4006 mv	1183 mv	10040 mv	2.7 per cent

Table IX-B: Boron Oxide-Oxygen

$T_C = 527^\circ C$ (800°K) $\quad \Delta H_v = 48$ Kcal/gmole (b)

$k = 0.00837$ Watt/C°cm (a) $\quad \sigma = 5$ ohm^{-1}cm^{-1} (c)

$T_H = 1800^\circ C$ (2073°K); $p^*_{B_2O_3} = 0.011$ atm (d)

π	E (e)	q_c/I	q_r/I	q_v/I	ϵ
1.00 atm	521 mv	6269 mv	310 mv	6 mv	3.7 per cent
0.50	540	6065	841	12	3.9
0.20	567	5758	883	30	4.25

(4.25 per cent efficiency is equivalent to a figure of merit of 1.46×10^{-4})

Table IX-C: Lithium Fluoride-Fluorine

$T_C = 877^\circ C$ (1150°K) $\quad \Delta H_v = 48$ Kcal/gmole (b)

$k = 0.00837$ Watt/C°cm (a) $\quad \sigma = 9$ ohm^{-1}cm^{-1} (c)

$T_H = 1423^\circ C$ (1700°K); $p^*_{LiF} = 0.113$ atm (d)

π	E (e)	q_c/I	q_r/I	q_v/I	ϵ
1.00 atm	649 mv	1438 mv	1380 mv	265 mv	10.5 per cent
0.50	755	1171	1520	609	11.4
0.20	910	902	1720	2700	8.5

(11.4 per cent efficiency is equivalent to a figure of merit of 1.86×10^{-3})

Notes:

(a) Thermal conductivities were assumed to be 0.00837 Watt/C°cm for all three melts as taken from Sundheim(29). This is probably low for lithium fluoride.

(b) The heat of vaporization is reported by Bloom, et. al.(4) for silver chloride. It appears to be very nearly the same for the other molten salts(9).

(c) Electrical conductivities were taken from Mantell(18) for silver chloride, from Yim and Feinleib(36) for lithium fluoride, and it was estimated for boron oxide. Note that it is not entirely valid to use normal conductivity data since only one ion migrates in the thermocell. However, in the absence of better data, these measured values were used.

(d) Vapor pressures were taken from Bloom, et. al.(4) for silver chloride. Values for other melts were estimated from boiling point and heat of vaporization data reported by Glassner(9).

(e) Voltages for cells containing boron oxide and lithium fluoride electrolytes were estimated from equation (28). The ionic entropy for the oxide ion in boron oxide was estimated to be one fifth of the entropy of the pure melt--obviously, a questionable extrapolation of Pitzer's equation. The fluoride transported entropy was assumed equal to the value calculated from Pitzer's equation, and it is considered to be quite accurate. Entropies of transfer, of course, were assumed to be zero in both cases. Entropy and equilibrium data were taken from Glassner(9) and Stull and Sinke(27).

E. Discussion of Possible Experimental Errors

The data obtained in this work were consistently reproducable. Their precision likewise was good (fluctuations in voltage were considerably less than a millivolt and can be attributed to small variations in the temperature of the melt in contact with the electrodes). However, there are two areas of possible consistent error which should be discussed. They are (1) the possible air dilution of the chlorine feed gas to the electrodes during reduced pressure operation, and (2) possible errors associated with the observed residual voltages.

1. Air Dilution of Electrode Feed Gas

As mentioned in section A of the Appendix, special precautions were taken to make both the feed lines and the electrode fittings gas tight. Otherwise, leakage of air into the electrode feed lines during vacuum operation would dilute the chlorine causing an erroneous reading of cell voltage. That the system was indeed leak proof is illustrated by the following observations:

(a) During vacuum operation, it was possible to change the chlorine flow rate to either electrode by a factor of up to two without changing cell voltage. The only limitation here was the point at which the chlorine bubbling past the electrode became too violent and caused voltage fluctuations due to mixing in the non-isothermal electrolyte. If air were leaking into the lines, the change in chlorine feed rate without a similar change in leak rate would cause a voltage shift due to the change in diluent concentration. The lack of any such shift is evidence that leakage did not occur.

(b) The chlorine was throttled through separate needle valves placed a considerable distance down stream from the point where the two feeds separated. The lines up to the needle valves contained chlorine above

atmospheric pressure (about 5 psig) so that any inward leakage of air would have to occur in the feed lines downstream from the needle valves. It is unlikely that such leakage would occur in the separate feed lines to the same extent. Therefore, if an air leak were present in one of the lines, the cell would show an e.m.f. at zero temperature difference due to a concentration effect. A leak rate sufficient to affect results would show a voltage at zero ΔT of greater than 10 millivolts, and it would vary with chlorine feed rate and total cell pressure. Aside from much smaller residual e.m.f.'s discussed below, such an effect was never observed.

(c) Leak tests, made by placing a flow meter in series in a line connecting the vacuum pump to the gas outlet at the base of the electrode showed no leakage when the teflon throttling valves were closed.

2. Discussion of Residual Voltages

As observed in section VI, the experimental curves of cell voltage versus the temperature difference between electrodes did not always go through the origin, but often showed residual voltages of several millivolts. An analysis of the experimental arrangement leads to five possible caused of this effect. The possible causes are:

(a) Inconsistent thermocouples.

(b) Thermoelectric effects resulting from differences in composition of the graphite electrodes.

(c) Thermoelectric effects resulting from external electrode connections.

(d) Voltage effects resulting from hydrostatic pressure differences.

(e) Errors resulting from differences between actual electrode temperatures and those measured by the thermocouples.

These five effects and their possible contributions to the residual voltage are discussed individually as follows:

(a) Inconsistent thermocouples: (These are thermocouples which give

different temperature readings when immersed in the same isothermal bath.)

To check for inconsistency in the couples used here, the two isothermal electrode compartments were held steady at different temperatures and the thermocouples were read. Then, the ceramically insulated couples were interchanged from one vycor protection tube to the other and read again while in their new locations. It was found that the measured temperatures of the electrode compartments were the same regardless of which thermocouple was present, thus demonstrating that the couples gave consistent temperature readings. The same procedure was repeated more than once over the period of this investigation with identical results.

On another occasion, one of the thermocouples was placed in the same temperature environment with a National Bureau of Standards standardized couple. The temperature indicated by the test couple was in agreement (to within 1°C) with that measured by the standard. Reforming of the thermocouple bead also did not affect its accuracy. In general, the platinum versus 90 per cent platinum-10 per cent rhodium couples used were found to give consistent and accurate readings. Hence, the possibility of residual voltages arising from inconsistent thermocouples, is eleminated.

(b) Thermoelectric effects resulting from differences in composition of the graphite electrodes:

It will be remembered from the apparatus description that the top ends of the graphite electrodes projecting from the cell were nearly at room temperature, and the other ends were at the temperatures of the respective electrode compartments where they made contact with the electrolyte. Under these conditions, very small differences in elec-

trode composition will cause an e.m.f. just as if the electrodes were of different materials. In other words, inhomogeneous electrodes placed in a thermal gradient and electrically connected will act as a thermocouple and generate a voltage. The graphite electrodes used were of the highest purity obtainable. Even so, if they were to contain slight impurities in different amounts, an e.m.f. would be generated in the thermocell in addition to that attributable to the half cell electrode reactions. This voltage would be relatively insensitive to the difference in electrode temperatures, since it would result from the fact that there is always a temperature gradient in the electrodes, and it could account for the residual voltage observed at zero ΔT. In order to determine whether such a voltage was present, the hot ends of the electrodes were short-circuited with a metal wire and this "junction" placed in the empty furnace. The ends of the electrodes projecting from the furnace remained cold. At hot junction temperatures greater than 800°C, voltages of less than 0.3 mv were generated; adequately demonstrating that the electrodes were sufficiently homogeneous.

(c) Thermoelectric effects resulting from external electrode connections:

Even though the top ends of the electrodes which project from the furnace are nearly at room temperature, they can still differ in temperature by several degrees. Thus, it is possible that a thermocouple e.m.f. could develope at the copper-graphite junctions where the two electrodes are connected to the external circuit. However, estimation of the voltage for a copper-graphite electrode from values tabulated in a standard reference(37) shows that this effect is insignificant. As a further check, the two electrodes were connected at the "hot" ends with a metal wire. Then, with both electrodes at room temperature, one

of the copper-graphite junctions was heated. The resulting e.m.f. was negligible as expected.

(d) Voltage effects resulting from hydrostatic pressure differences:

It is apparent that the difference in electrode-compartment pressures will influence the cell voltage due to a concentration effect. For example, if both electrodes were at the same temperature but at pressures differing by the hydrostatic head Δp, there would be a net voltage as shown by the Nernst equation below:

$$\mathcal{L}E_{\Delta p} = \frac{R\,T}{\mu\,\mathcal{F}} \ln \frac{\pi + \Delta p}{\pi} \qquad (89)$$

This voltage is small, however, except where Δp approaches π in magnitude. $\mathcal{L}E_{\Delta p}$ was negligible for most of the work reported here and was certainly so for the data reported in figure 7. Nevertheless, an increase in the residual voltage was observed experimentally as expected at total cell pressures less than half an atmosphere. The observed residual voltages of several millivolts were found to agree to within a millivolt with those calculated from equation (89)

One characteristic of $\mathcal{L}E_{\Delta p}$ which is of particular importance in this discussion is its relative insensitivity to ΔT. This can be seen from equation (89) where it is apparent that $\mathcal{L}E_{\Delta p}$ remains almost constant with ΔT when T is large. Thus, for the data reported here, because of the high temperatures involved, the residual voltage due to the hydrostatic pressure difference can be considered a constant for a particular run and hence, can be subtracted from each data point. This, correction, however, is negligible for most of the data taken, and when $\mathcal{L}E_{\Delta p}$ calculated from equation (89) is substantial, it still does not account for the total residual voltage observed. The source of the error appears to be attributable to the

factors discussed under item (e) which follows.

(e) Errors resulting from differences between actual electrode temperatures and those measured by the thermocouples:

In our experimental cell, the heat transfer situation is complicated by a number of factors. For example, heat is transferred by radiation from the furnace coils to the outer cell tube and from thence through the transparent electrolyte to the thermocouples, electrodes, and the inner cell tube. Meanwhile, these components exchange heat by conduction and radiation with the cooler parts of the cell and each other. In addition, heat is exchanged by conduction between the melt and the cell components. In light of these factors, it is quite possible that the thermocouple junctions are not at the same temperatures as the electrodes. Quantitative evaluation of this temperature discrepancy is difficult because of the complicated heat-transfer situation, but with the aid of some qualitative reasoning, it is possible to isolate its probable source.

First of all, it is important to observe, that there are essentially two sets of thermocouples in the cell, the measuring couples which indicate the temperatures of their separate junctions independently, and the electrodes which measure the temperature difference between their respective graphite-molten salt interfaces. From the experimental data, corrected for ΔE_{tp}, it appears that when the measuring couples were at the same temperatures, the so called "hot" electrode was slightly lower in temperature than the "cold" electrode. This discrepancy amounted to 8°C at around 500°C and approached zero as the temperature level of the cell increased to 900°C and above. This indicates that the electrodes for one reason or another were not at the same temperatures as their adjacent thermocouples.

the measured ΔT's yielding a curve such as that shown in Figure 6. The maximum ΔT obtainable by this cell was about 150 to 200°C because of conduction of heat from the hot to the cold zone through the melt. In other words, with a ΔT of this magnitude, all of the power supplied to the furnace came through the high temperature control unit, and any further increase in this control temperature served only to raise both the hot and the cold electrode temperatures without increasing ΔT appreciably. Therefore, after the first string of runs were made to a ΔT of 150 to 200°C, the cold electrode temperature was raised about 100°C, the hot electrode dropped to the same temperature, and another string of runs made by heating the hot electrode in 20°C steps until ΔT was again 150 to 200°C. By this method, a number of curves similar to figure 6 were obtained, each corresponding to a different cold junction temperature, but "overlapping" by about 50°C.

C. Reduced Pressure Runs

When measurements over the complete temperature range from just above the melting point to about 1300°C were made at atmospheric pressure, the procedure was repeated at various degrees of vacuum. Reduced pressure was affected by expelling the chlorine from the gas exit system through a water aspirator. Excellent pressure control was obtained by throttling the electrode feed streams and the gas to the aspirator through teflon needle valves. For vacuum data, the cell pressure was initially reduced to a -5 inches of mercury and held there for a series of runs covering the temperature range from the melting point up to nearly 1300°C. Then the pressure was reduced to a -10 inches of mercury and the procedure repeated. This was done in turn for pressures of -15, -20, -25, and in two sytems, -27 inches of mercury. Pressures were determined to within $\pm$ 0.1 inch of mercury by a vacuum gage placed in the vent line from the cold electrode. The gage was calibrated with a mercury monometer. Vacuum readings were converted to abso-

Qualitative evaluation of the various factors influencing radiation indicates that the electrode and thermocouple should not differ in temperature due to differences in view factor or emissivity. On the other hand, when the total thermal conductivity (k times cross-section area) of the electrode stem is compared with the same quantity for the thermocouple, it is found that the electrode, due to its large cross section, will conduct heat away at a rate 100 times higher than the thermocouple when they have identical temperature gradients. Hence, due to this large conductive flux, it is possible that the electrode may actually be cooler than the thermocouple adjacent to it. From the cell geometry, it is possible to limit this effect even further to the hot electrode chamber where the electrode and thermocouple experience a steep thermal gradient just above the surface of the electrolyte. (The cold electrode and thermocouple by virtue of their initial passage through the hot part of the cell do not experience much of a thermal gradient. Hence, they cannot show a significant temperature difference arising from this conduction effect.) Therefore, it is reasonable to suppose that the hot electrode can be at a lower temperature than the two thermocouples and the cold electrode when the latter are isothermal. If this is the case, the radiative heat flux increases exponentially and the relative importance of the conduction effect becomes less and less as the temperature level of the cell increases. Hence, as was observed experimentaly, the temperature discrepancy (or the residual voltage) approaches zero as the average cell temperature increases.

In order to provide a firmer basis for the above explanation, an experimental program was arranged which would yield the temperature difference between electrodes as a function of ΔT measured by the

thermocouples under conditions similar to the original runs. This was done by placing the electrodes and thermocouples in the cell in exactly the same positions as they were during a normal run. A molten salt electrolyte, however, was not placed in the cell, but instead, the cell was filled with argon and the electrodes were connected with a length of platinum wire. The thermal e.m.f. of the platinum versus graphite junctions had been carefully measured previously. Therefore, ΔT_e, the temperature difference between the electrodes, could be measured independently of ΔT, the temperature difference between the thermocouples. Since the molten salt electrolytes normally used were transparent to radiant heat, it was felt that this setup simulated the actual heat transfer situation encountered during normal operation. It was realized, of course, that due to the absence of the liquid, the heat conducted by the fluid in the cell would be much smaller than usual. This, however, would tend to accent any discrepancy which occured under normal conditions.

The results of the test program are shown in figure 23 for the experimental setup described above. The figure shows ΔT_e, the temperature difference between the electrodes as a function of ΔT, the temperature difference measured by the thermocouples. It should be observed that if ΔT_e is equal to ΔT, the point will fall on the forty-five degree line shown in the figure. It is conceivable that ΔT_e could still equal ΔT when neither electrode was at the thermocouple temperature. In this case, the difference between electrode and thermocouple temperatures would be the same in both compartments. However, considering the configuration of the cold electrode compartment, it seems unlikely that a temperature discrepancy of any size exists there, and it seems even more unlikely that such a discrepancy would be the same as that in the hot compartment.

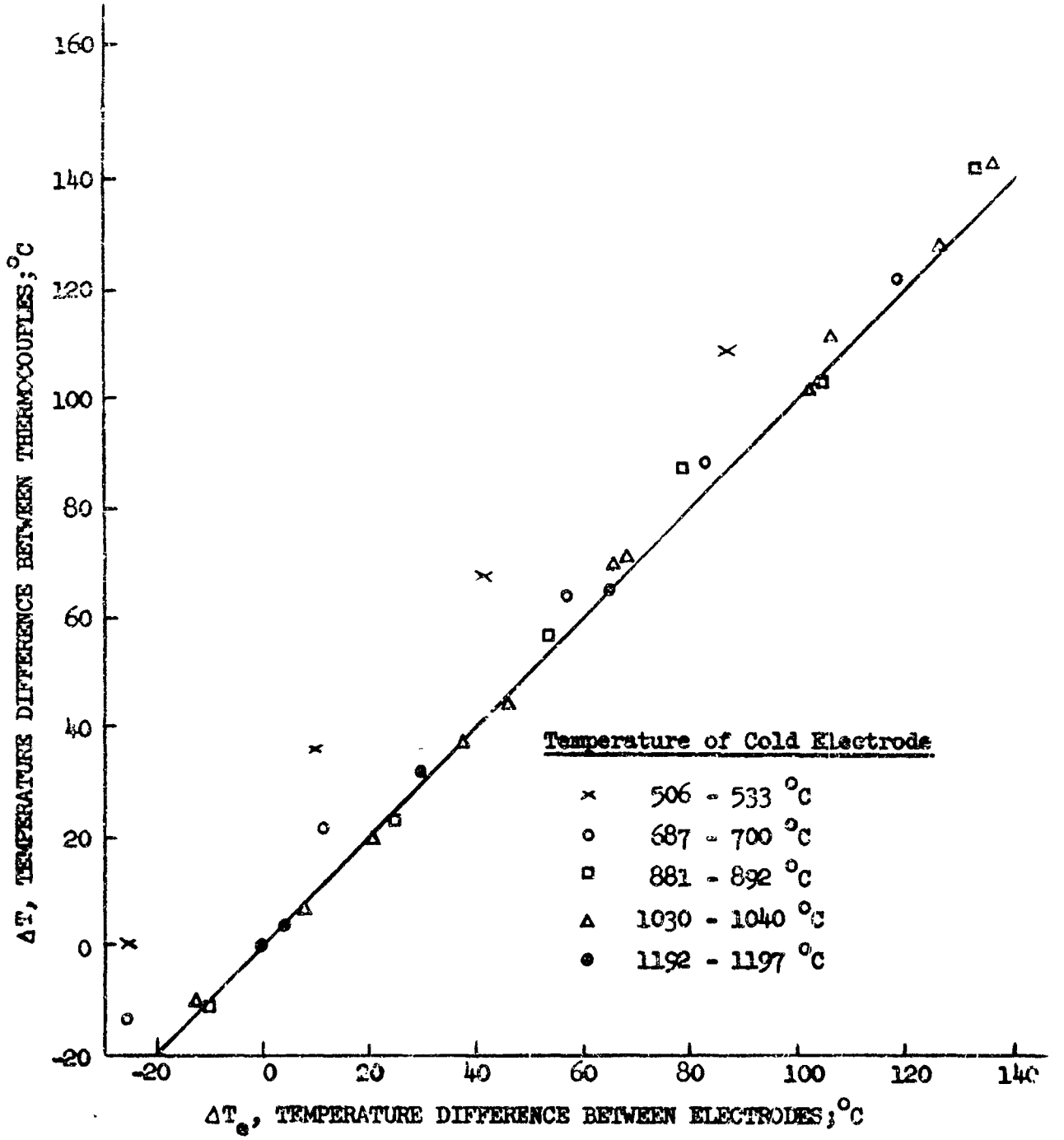

Figure 23. Temperature difference measured by electrodes versus that measured by thermocouples in empty cell.

Therefore, assuming that the temperature of the cold electrode is equal to that of the cold thermocouple, the results in figure 23 show that the hot electrode is actually colder than that of the hot thermocouple at low average cell temperatures. Further, it can be seen that this discrepancy becomes smaller as average temperature increases until at temperatures of 800°C and above, ΔT_e is very nearly equal to ΔT as read by the thermocouples. The behavior of the temperature discrepancy, even though it is larger in the absence of an electrolyte, is identical to that of the residual voltages observed during the actual thermocell experiments. These results provide strong evidence for the argument put forward above which asserts that the hot electrode and thermocouple were not at the same temperature.

The most important aspect of the above finding is that the temperature discrepancy, hence, the residual voltage, is relatively insensitive to ΔT. Therefore, this residual $\delta E_{\Delta T}$ can be treated as though it were independant of ΔT, and it can be subtracted from each data point in a given run.

Of the five considerations above, it appears that the total observed residual voltage δE is the sum of $\delta E_{\Delta p}$ discussed in item (d) and $\delta E_{\Delta T}$ discussed in item (e). Both are essentially constant with ΔT. Since the sum, therefore, is also constant with ΔT, the residual voltage determined from an experimental plot of E versus ΔT can be subtracted from each separate voltage reading to give curves which pass through the origin. Then, these curves can be superimposed (see section VI-B) to give total voltage versus temperature graphs.

F. Nomenclature

A	cross-section area of the electrolyte
E	reversible cell potential; volts
F	Gibbs free energy
$\bar{F}$	partial molal free energy; cal/g mole
$\mathcal{F}$	Faraday's constant; 96,500 coulombs/g equivalent
H	enthalpy; cal/g mole
I	current; amperes
J	transport fluxes as contained in equations (36) and (37)
k	thermal conductivity; Watt/cm ^{o}C
K	dissociation constant
K_T	half-reaction equilibrium ratio
L	coefficient used to relate fluxes and forces. Also used to denote the length of the conduction path through the electrolyte
M	coefficient of performance defined by equation (4). Also used to denote molecular weight
n	dissociation variable defined by equation (22)
p	pressure; atmospheres
p^*	vapor pressure; atmospheres
Q	used to denote heat energy
Q^*_k	heat of transfer of species "k"
q_c	rate at which heat is conducted away from the hot electrode chamber
q_H	heat transfer rate to the hot electrode
q_r	heat absorbtion rate at hot electrode due to reaction
q_v	heat absorbtion rate at hot electrode due to salt vaporization
R	gas constant; 1.987 cal/g mole ^{o}K
S	symbol used to denote entropy; entropy units (cal/g mole ^{o}C or Btu/lb mole ^{o}F)
S^o	standard state entropy
$\bar{S}$	partial molal entropy

S^* entropy of transfer

$\bar{S}$ transported entropy; $\bar{S} = \tilde{S} + S^*$

T temperature; ^oK

w rate at which work is done

W quantity of energy as work

x moles of chlorine dissociated per mole of feed

z figure of merit defined by equation (5); $^oC^{-1}$

α Seebeck coefficient, rate of change of voltage with temperature; volts/^oC

λ a multiplier less than unity which relates the entropy of transfer to the entropy of activation

δ, Δ used to denote incremental quantities

ϵ efficiency, defined as the quotient of the useful work produced divided by the heat supplied by the high temperature source

μ the number of electrochemical equivalents per gram mole

π total pressure; atmospheres

π' total pressure minus the vapor pressure of the salt; atmospheres

σ electrical conductivity; $ohm^{-1}\ cm^{-1}$

ψ electrical potential; volts

Subscripts

C denotes the low-temperature junction

i used to denote a general species. Also denotes an electrical flux or force

H denotes the high-temperature junction

M refers to the cation in a metal-halide salt

q refers to a heat flux or force

T used to denote a total quantity. Also denotes a quantity at a specific temperature

X refers to the anion in a metal-halide salt

1,2,3 used to denote the separate legs of a thermoelectric device. Also denotes quantities in zones 1, 2 and 3 in figure 3

G. Literature Citations

1. J. L. Barton and H. Bloom, J. Phys. Chem., 60, 1413 (1956)

2. A. J. deBethune, J. Electrochem. Soc., 107, 829 (1960)

3. A. J. deBethune, T. S. Licht and N. Swendeman, J. Electrochem. Soc., 106, 616 (1959)

4. H. Bloom, J. O'M. Bockris, N. E. Richards and R. G. Taylor, J. Am. Chem. Soc., 80, 2044 (1958)

4a. K. G. Denbigh, "The thermodynamics of the Steady State," Methuen (1951)

5. R. H. Detig and C. H. Archer, J. Chem. Phys., 38, 661 (1963)

6. T. B. Douglas, Trans. ASME, 79, 23 (1957)

7. E. D. Eastman, J. Am. Chem. Soc., 50, 292 (1928)

8. W. H. Evans, T. R. Munson and D. D. Wagman, J. Research, Nat'l. Bur. Stds., 55, 147 (1955)

9. A. Glassner, U. S. Atomic Energy Com. Report ANL-5750 (1959)

10. H. J. Goldschmid, "Applications of Thermoelectricity," Wiley, N.Y. (1960)

11. S. R. deGroot, "Thermodynamics of Irreversible Processes," North Holland Pub. Co. (1961)

12. H. Holtan, "Electric Potentials in Thermocouples and Thermocells," Thesis, Utrecht (1953)

13. H. Holtan, P. Mazur and S. R. deGroot, Physica, 19, 1109 (1953)

14. A. F. Joffe, "Semiconductor Thermoelements and Thermoelectric Cooling," Infosearch, London (1957)

15. K. K. Kelley, U.S. Bur. Mines Bul. 477 and 584, U.S. Gov. Printing Office, Washington, D.C. (1950) and (1960)

16. H. A. Laitinen, W. S. Ferguson and R. H. Osteryoung, J. Electrochem. Soc., 104, 516 (1957)

17. A. Lunden, Corrosion Sci., 1, 62 (1961)

18. C. L. Mantell, "Industrial Electrochemistry," 3rd Ed., McGraw-Hill, N.Y. (1950

19. I. G. Margulescu, S. Sternberg, L. Medintev and C. Mustetea, Electrochim. Acta, 8, 65 (1963)

20. D. L. Maricle and D. N. Hume, J. Electrochem. Soc., 107, 354 (1960)

21. P. Mazure, J. Phys. Chem., 58, 700 (1954)

22. A. R. Nichols and C. T. Langford, J. Electrochem. Soc., 109, 56 (1962)

23. J. H. Perry, "Chem. Eng. Handbook," 3rd Ed., McGraw-Hill, N.Y. (1950)

24. K. S. Pitzer, J. Phys. Chem., 65, 147 (1961)

25. L. Poincare, Ann. Chim. Phys., (6) 21, 289 (1890)

26. S. Senderoff and R. I. Bretz, J. Electrochem. Soc., 109, 56 (1962)

27. D. R. Stull and G. C. Sinke, "Advances in Chemistry-Series No. 18," Am. Chem. Soc. (1956)

28. B. R. Sundheim and J. Rosenstreich, J. Phys. Chem., 63, 419 (1959)

29. B. R. Sundheim, "Molten Salts as Thermoelectric Materials," in "Thermoelectric Materials and Devices," ed. by [illegible] Cadoff and E. Miller, Materials Technology Series (1960)

30. A. G. Turnbull, Australian J. App. Science, 12, 324 (1961)

31. A. G. Turnbull, Australian J. App. Science, 12, 30 (1961)

32. H. J. V. Tyrrell, "Heat and Mass Transfer in Liquids," Butterworth (1961)

33. E. R. Van Artsdalen, "The Structure of Electrolytic Solutions," W. J. Hamer, ed., p 411, Wiley (1959)

34. E. R. Van Artsdalen and I. S. Yaffe, Journ. Phys. Chem., 59, 118 (1955)

35. I. S. Yaffe and E. R. Van Artsdalen, Journ. Phys. Chem., 60, 1125 (1956)

36. E. W. Yim and M. Feinleib, J. Electrochem. Soc., 104, 626 (1957)

37. "Temperature, Its Measurement and Control in Science and Industry," Reinhold (1941)

E. Biographical Note

The author, Gail Dennis Ulrich, was born on October 29, 1935 in Devils Slide, Utah. He attended the Morgan County, Utah public schools.

He obtained the B. S. degree in Chemical Engineering in June, 1959 and the M. S. in August, 1962 from the University of Utah. He entered M. I. T. in September of 1960.

He was employed by H. C. Schutt and Associates, Boston, Massachusetts, during the summer of 1961 and part time until December 1962.